Electrochemical Properties of Natural Graphite in the Electrolyte Solutions Containing Propylene Carbonate and Nonflammable Organo-Fluorine Compounds for Lithium-Ion Batteries

2010

Takashi Achiha

Aichi Institute of Technology

Contents

Chapter 1

Introduction

Chapter 2

Electrochemical behavior of natural graphite fluorinated by F_2 in propylene carbonate-containing solvents

Chapter 3

Electrochemical behavior of natural graphite fluorinated by ClF_3 and NF_3 in propylene carbonate-containing solvents

Chapter 4

Electrochemical behavior of plasma-fluorinated natural graphite in propylene carbonate-containing solvents

Chapter 5

Thermal stability and electrochemical properties of nonflammable fluoro-carbonates for lithium-ion battery

Chapter 6

Thermal stability and electrochemical properties of fluorine-containing ethers and ester as nonflammable solvents for lithium-ion batteries

Chapter 7

Chapter 1

Introduction

1-1 Lithium-ion secondary battery

Since lithium-ion secondary (rechargeable) battery was put to practical use by Sony Co. Ltd. in 1991 its diffusion has been quite rapid. Now it is widely used as electric power sources of many kinds of electric devices [1]. In the near future, it will become very important electric power sources for not only mobile devices but also more powerful ones. Lithium-ion secondary batteries use lithium-containing transition metal-oxide cathodes ($LiCoO_2$, $LiCo_{X-1}Ni_XO_2$ etc.), carbon anodes (natural graphite, synthetic graphite etc.), organic solvents and polymer separator. During charging process, lithium-ions are inserted into carbon anode to form lithium intercalated compounds, and return to transition metal-oxide lattice during discharge process as shown in Fig. 1. The electrode reactions during charge-discharge cycling are as follows.

$$\text{Cathode reaction: } LiCoO_2 \underset{\text{Discharge}}{\overset{\text{Charge}}{\rightleftharpoons}} Li_{1-X}CoO_2 + xLi^+ + xe^- \quad (1)$$

$$\text{Anode reaction: } 6C + xLi^+ + xe^- \underset{\text{Discharge}}{\overset{\text{Charge}}{\rightleftharpoons}} Li_XC_6 \quad (2)$$

$$\text{Cell reaction: } 6C + LiCoO_2 \underset{\text{Discharge}}{\overset{\text{Charge}}{\rightleftharpoons}} Li_{1-X}CoO_2 + Li_XC_6 \quad (3)$$

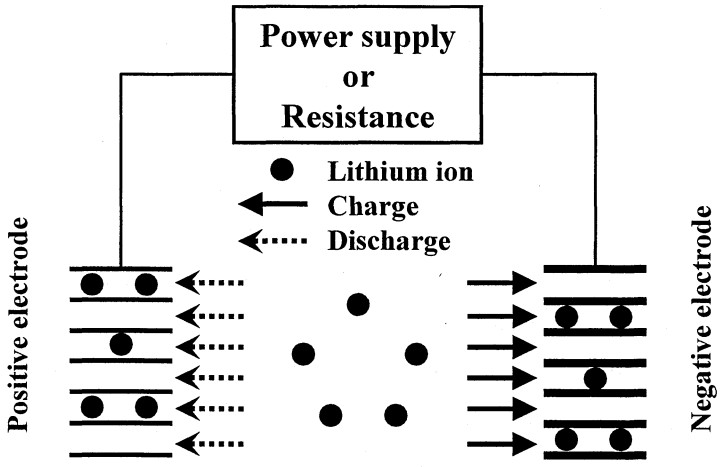

Figure 1. Charge-discharge process of lithium-ion secondary battery

Metallic lithium anode has a high discharge capacity (3860 $mAhg^{-1}$). However, continuous charge-discharge cycles cause the formation of lithium dendrites on the surface of the lithium anode. These dendrites break through the separator, and directly contact the cathode after many charge-discharge cycles, which lead to burning or explosion of the battery. In order to prevent direct contact of the lithium anode with the cathode, a graphite intercalation compound of lithium (Li-GIC) is applied to the anode material. Full intercalation of lithium into highly-crystalline graphite, such as natural graphite, yields stage 1 GIC with a composition of LiC_6, which corresponds to the theoretical discharge capacity of graphite (372 $mAhg^{-1}$). The formation of dendrites could be prevented by the use of Li-GIC. When graphite is used as anode, the electrode potential is low and constant, and irreversible capacity is small. The open-circuit voltage of a lithium-ion secondary battery (3.6-3.7 V) is several times larger than those for secondary batteries using aqueous solutions. $LiCoO_2$ provides constant and high potential of 3.9 V vs. Li/Li^+; however, the cost of $LiCoO_2$ is high, because of the insufficient supply of Co. For this reason, new cathode materials were recently developed, such as $LiCo_{X-1}Ni_XO_2$, $LiMnO_4$ etc. Mixtures of natural and synthetic graphites are mainly used as anode materials. Organic solvents incorporate two components. The first one is a high-dielectric solvent, such as ethylene carbonate (EC) or propylene carbonate (PC), which dissolves the inorganic electrolyte ($LiPF_6$, $LiClO_4$ etc.). The second one is a low-viscosity solvent, such as dimethyl carbonate (DMC), methyl ethyl carbonate (MEC) or diethyl carbonate (DEC). For high-crystalline graphite such as natural graphite, an EC-containing solvent should be used to form a stable surface film, called Solid-Electrolyte Interphase or Interface (SEI), with the electrochemical decomposition of a small amount of solvent. PC cannot be used for high-crystalline anodes, because the formation of SEI is slow and the electrochemical decomposition of solvent continues. However, PC can be used for low-crystalline carbons.

1-2 Surface modification of carbon anode materials

The crysallinity of carbon materials widely varies. Some low-crystalline carbons have high discharge capacities, but large irreversible capacities are also observed. Anode should have a small irreversible capacity, that is, high coulombic efficiency (coulombic efficiency = discharge capacity/charge capacity). If anode has a large irreversible capacity, utilization of oxide cathode is largely reduced. For this reason, graphitic materials are mainly used as anode. Graphite has a constant and low potential, a constant discharge capacity (good cycleability) and small irreversible capacity (high first coulombic efficiency). High-purity natural graphite and synthetic graphite are usually used anodes. Surface disorder of high-crystalline graphite is normally lower than that of low-crystalline carbon. For graphite with low surface disorder, EC-containing solvent should be used to form SEI with decomposition of a small amount of organic solvent. PC cannot be used for graphite because electrochemical decomposition of PC

continuously occurs. It is very convenient if PC can be used for graphite because PC has a very low melting point of -55 °C (melting point of EC: 36 °C), which enables the use of lithium-ion batteries in a wide. The molecular size of PC is larger than that of EC. Therefore, the size of lithium-ion solvated with PC molecules is larger than that solvated with EC. Since the electrochemical redox reactions take place on the surface of solid electrodes, surface structure, in particular the edge structure of carbonaceous anodes, significantly affects the electrochemical characteristics because lithium-ions are inserted from edge planes. To improve the electrochemical properties of carbonaceous anodes, some surface-modification methods have been attempted [1-5], including surface fluorination [1, 6-14], surface oxidation [15-22], metal or metal oxide coating [2, 23-29], carbon coating [30-42], polymer or silicon coating [43-51], composite electrodes [52-74]. Surface modification gives positive effects to carbonaceous anodes regarding the reversible capacities, first coulombic efficiencies, and cycleability. Methods of surface modification and their effects are summarized as follows.

1-2-1 Surface fluorination

Surface fluorination using F_2 gas, and plasma-fluorination using CF_4 gas, were applied to high-crystalline natural graphite powder samples with different particle size (average particle size: 7, 25 and 40 μm [1, 6-11]. Fluorination using F_2 is a strong oxidation reaction, and therefore, surface modification with F_2 was performed under mild conditions. Plasma-fluorination was performed at 90 °C using CF_4 gas. Surface fluorination increased BET surface areas and small mesopores with diameters less than 3 nm. Surface disorder, evaluated by Raman shifts, also increased. First coulombic efficiencies of there natural graphite samples were not change by fluorination in 1.0 mol/dm^3 $LiClO_4$ EC/DEC (1:1 vol.). Surface fluorination of natural graphite powder samples (average particle size: 5, 10 and 15 μm) with ClF_3 was also preformed under same conditions [12]. Surface fluorination of graphite samples reduced the electrochemical decomposition of PC, increasing their first coulombic efficiencies in the PC-containing electrolyte. Surface fluorination of graphitized petroleum cokes of open the closed edge surface, highly increasing first coulombic efficiencies [13, 14].

1-2-2 Surface oxidation

It was reported that mild oxidation of graphite increased discharge capacity, however, strong oxidation caused degradation of carbon materials [15]. Capacity increase due to mild oxidation is similar to the results obtained by surface fluorination. Surface oxidation of mesocarbon microbeads (MCMB) effectively removed the surface skin and significantly improved charge-discharge behavior [17]. In liquid-phase oxidation of natural graphite, ammonium peroxysulfate and nitric acid [18], H_2O_2 and $Ce(SO_4)_2$ [19, 20], nitric acid [21],

and ammonium peroxydisulfate [22] were used. Surface oxidation increased reversible capacities and first coulombic efficiencies.

1-2-3 Metal or metal-oxide coating

Coatings of metals, such as Ag, Au, Bi, In, Pb, Pd, Sn, and Zn, improves the anode characteristics of graphite [2, 23-25]. Among them, Ag, Sn and Zn were the most effective in enhancing high rate characteristics [24]. Copper coating on natural graphite increased its reversible capacity and improved cycling behavior [26]. Aluminum coating on natural graphite, using aluminum triethoxide, reduced transfer resistance [27]. A coating of tin oxide on synthetic graphite gave higher capacity than that of uncoated MCMB [28]. Nano-TiO_2 coated graphite has good cycleability in propylene carbonate-containing electrolytes [29].

1-2-4 Carbon coating

Carbon coating is one of most effective method of surface modification [30-42]. The main effect of carbon coating is large reduction of irreversible capacity, i.e., an increase in first coulombic efficiency. The main method of carbon coating is chemical vapor deposition (CVD) [31, 34-42]. Chemical vapor infiltration (CVI) is a special type of CVD, which reduces the irreversible capacity of a low-crystalline carbon having large capacity [38-42]. Another method is to mix graphite with polyvinyl chloride followed by heat treatment at 500 °C [30], or to disperse graphite in a tetrahydrofuran/acetone solution containing coal tar pitch, and then heat-treat it at 1000 °C [32, 33].

1-2-5 Polymer or silicon coating

Other methods include polymer [43-50] or Si coating [51]. Mixing poly (3-n-hexylthiophen) with graphite not only increased capacity, but also reduced irreversible capacity [43]. Coatings of gelation [44, 45, 47], polyaniline [47], cellulose [47], polypyrrole [48] and polyurea [49] on graphite significantly reduced irreversible capacities. The graphite mixed with polyacrylic acid (PAA), polymethacrylic acid (PMA) and polyvinyl alcohol (PVA) improved first coulombic efficiencies in propylene carbonate-containing electrolytes [50]. Si coating on graphite also increased reversible capacity [51].

1-2-6 Composite electrode

Various composite electrodes were prepared and examined for improving anode characteristics [52-74]. A ZrO_2/graphite composite was effective in suppressing the irreversibility of natural graphite [53]. Graphite treated with inorganic salts, such as NaCl and

Na_2CO_3, increased reversible capacity and first coulombic efficiency [54]. The PbO/carbon nanocomposite also increased capacity [55]. Many composites of graphite or carbon with metals, such as Ag [57-59], Cu [59], Sn [60-64] and Ni [64-67], have been examined. Increases in reversible capacity, decrease in irreversible capacity, and improvements in cycleability were reported. Si is an important element in making composites with graphite or carbon. Different types of Si composite, such as Si/carbon [68, 69], Si/Cu/carbon [70], Si/carbon/polyaniline [71], Si/carbon/graphite [72, 73] and Si/Ni/graphite [74] were examined as new anode materials. It was reported that these composite electrodes improved cycleability and showed high reversible capacities, between 700 and 800 $mAhg^{-1}$.

1-3 Nonflammable additives and solvents for lithium-ion secondary battery

The safety problem is one of the most important issues for the practical use of lithium-ion batteries. They use flammable organic solvents as compared to other secondary batteries that use aqueous electrolyte solutions. Overcharge and over-discharge of lithium-ion secondary battery will result in electrolyte decomposition, producing various flammable gaseous species, and increasing the inner pressure and temperature of the battery. Any of these issues will cause the exploding and firing of the battery. To increase the thermal and oxidation stability of lithium-ion batteries, alternative additives or solvents have been investigated. To improve the thermal stability of electrolytes, some nonflammable additives and solvents have been examined, including phosphorus compounds [75-80], phosphates with phenyl groups [81-84], fluorine-containing phosphorus compounds [85-89], other compounds [90-103] and organo-fluorine compounds [104-107]. These compounds improved the thermal stability of lithium-ion batteries as summarized as follows.

1-3-1 Phosphorus compounds

The trimethyl phosphate (TMP) was investigated in various solvent mixtures. TMP had good oxidation stability and poor reduction stability. P_2O_5 is formed by the oxidation of nonflammable additives and solvents as soon as the electrolyte is burned. It captures the radicals, H· and HO· in the flame zone, so that the chain reactions for combustion may be weakened or terminated [75]. The reduction decomposition of TMP solvents on natural graphite electrode may be suppressed by mixing EC and PC or EC and DEC cosolvents. Therefore, TMP was mixed by 20-30 % as one of the components of the solvent mixture. Electrochemical properties were inferior for high-crystalline graphite anode, however they can be improved by using amorphous carbon anode or mixing vinyl-containing additives [80]. Thermal stability of lithium-ion secondary batteries was improved by using TMP-containing electrolytes [75-80].

Phosphates with phenyl groups such as triphenyl phosphate (TPP), tributyl phosphate

(TBP) and cresyl diphenyl phosphate (CDP) were added to electrolyte by 3-5 wt.% as additives [81-84]. Phosphorus-based materials promote char formation, leading to protective coating of the electrode surface. The surface reaction between the lithiated graphite electrode and electrolyte will be significantly reduced. Therefore, TPP and TBP were added to electrolyte, which reduced the exothermic heat generation between fully charged anode and electrolyte [81-83]. CDP has a higher boiling point, appropriate viscosity and melting point. CDP containing electrolyte has shorter self-extinguishing time, good charge/discharge capacities and cycleability than TMP containing electrolyte [84].

Fluorine-containing phosphorus compounds: tris-(2,2,2-trifluoroethyl) phosphate (TFP), bis-(2,2,2-trifluoroethyl) methyl phosphate (BMP) and (2,2,2-trifluoroethyl) diethyl phosphate (TDP) were mixed with solvents by 20-40 % to investigate thermal stability and electrochemical behavior [85-89]. It was found that the electrolytes based on phosphates, with at least two fluorinated alkyls, demonstrate stable cell performance at room temperature, and the presence of these phosphates not only delivers higher cell safety, but also improves the cell capacity retention over a long period of testing. However, the rate capability and low temperature performance of these nonflammable electrolytes decline with increasing concentration of these phosphates, as a result of higher cell impedance. Nevertheless, compared with their nonfluorinated counterparts, fluorination introduces higher flame-retarding efficiency and lower performance impact. Among three phosphates examined, it was shown that TFP was the best candidate [85-89].

Other phosphorus compounds examined as flame retardant solvents or additives are 4-isopropyl phenyl diphenyl phosphate (IPPP) [90, 91], diphenyloctyl phosphate (DPOF) [92, 93], hexamethyl phosphoramide (HMPA) [94], dimethyl methyl phosphonate (DMMP) [95], dimethyl (2-methoxyethoxy) methyl phosphonate (DMMEMP) [96], tri-(β-chloromethyl) phosphate (TCEP) [97], aromatic phosphorus-containing esters [98] and trimethyl phosphate (TEP) [99]. It was shown that these phosphorus compounds improved thermal stability of lithium-ion batteries. In addition, cyclohexyl benzene [97], hexamethoxycyclotriphosphazene [100], lithium difluoro (oxalato) borate (LiDFOB) [101] fluorinated phophazenes [102], and vinyl tris-(methoxydiethoxy) silane (VTMS) [103] were also studied.

1-3-2 Organo-fluorine compounds

Several papers were quite recently published for the effect of organo-fluorine compounds on the electrochemical oxidation stability and charge/discharge behavior [104-107]. They are new type candidates as nonflammable solvents for lithium-ion batteries because decrease in HOMO levels gives high oxidation stability to fluorine compounds. It was reported in these papers that fluoro-esters [104], allyl tris-(2,2,2-trifluoroethyl) carbonate (ATFEC) [105], 2-trifluoromethyl-3-methoxyperfluoropentane (TMMP) [106], and fluoro-carbonates [107] gave the positive effects to oxidation stability of electrolyte solutions and battery

performance.

1-4 Purpose of the present study

High improvement in the battery performances such as low temperature characteristics, thermal stability and high rate charge/discharge is urgently requested. Because EC-based solvents should be used for graphite anode, currently used lithium-ion batteries have difficulty for the use at low temperatures. Since electrode characteristics of carbon materials are governed by crystallinity, surface structure and surface chemical species, surface modification of graphite is one of the good methods to use PC for graphite anode. In the present study, surface fluorination was applied to natural graphite samples. High safety is one of the most important issues for the application of lithium-ion batteries to hybrid cars and electric vehicles because lithium-ion batteries use flammable organic solvents. To avoid firing and/or explosion of lithium-ion batteries, nonflammable solvents should be developed. Organo-fluorine compounds are new candidates since fluorine substitution of organic compounds reduce HOMO level, i.e. increases oxidation stability. However, fluorine substitution simultaneously decreases LUMO level, which elevates reduction potentials of organic compounds. In the present study, thermal and electrochemical oxidation stability of organo-fluorine compound-mixed electrolyte solutions was evaluated, and charge/discharge characteristics of natural graphite were investigated using fluorine compound-mixed electrolyte solutions.

1-5 Scope of the present study

Chapter 1 describes the principle of lithium-ion secondary batteries, and summarizes the effects of surface modification and nonflammable solvents on the electrode characteristics of carbonaceous anodes. The purpose of the present study and an outline of each chapter are also added.

Chapter 2 presents the results of surface structure changes and charge/discharge behavior of natural graphite fluorinated by F_2 in propylene carbonate-containing solvents

Chapter 3 deals with the surface structure changes and electrochemical behavior of natural graphite of fluorinated by ClF_3 and NF_3 in propylene carbonate-containing solvents.

Chapter 4 describes the charge/discharge properties and surface structure of plasma-fluorinated natural graphite in propylene carbonate-containing solvents.

Chapter 5 deals with thermal stability and electrochemical properties of nonflammable fluoro-carbonates for lithium-ion battery.

Chapter 6 presents the thermal stability and electrochemical behavior of nonflammable fluoro-ethers and esters for lithium-ion battery.

Chapter 7 summarizes the results obtained in the present study.

References

[1] T. Nakajima, and H. Groult (eds.), "Fluorinated Materials for Energy Conversion", Elsevier Amsterdam, 2005.

[2] T. Takamura, Bul. Chem. Soc. Jpn., 75, 3491 (2002).

[3] Y. P. Wu, E. Rahm, and R. Holze, Electrochim. Acta, 47, 3491 (2002).

[4] Y. P. Wu, E. Rahm, and R. Holze, J. Power Sources, 114, 228 (2003).

[5] L. J. Ning, Y. P. Wu, S. B. Fang, E. Rahm, and R. Holze, J. Power Sources, 133, 229 (2004).

[6] T. Nakajima, M. Koh, R.N. Singh, and M. Shimada, Electrochim. Acta, 44, 2879 (1999).

[7] V. Gupta, T. Nakajima, Y. Ohzawa, and H. Iwata, J. Fluorine Chem.,112, 233 (2001).

[8] T. Nakajima, V. Gupta, Y. Ohzawa, H. Iwata, A. Tressaud, and E. Durand, J. Fluorine Chem.,114, 209 (2002).

[9] T. Nakajima, V. Gupta, M. Koh, R. N. Singh A. Tressaud, and E. Durand, J. Power Sources, 104, 108 (2002).

[10] T. Nakajima, V. Gupta, M. Koh, R. N. Singh A. Tressaud, and E. Durand, Mol. Cryst. Liq. Cryst., 388, [517]/103 (2002).

[11] H. Groult, T. Nakajima, L. Perrigaud, Y. Ohzawa, H. Yashiro, S. Komaba, and N. Kumagai, J. Fluorine Chem.,126, 1111 (2006).

[12] K. Matsumoto, J. Li, Y. Ohzawa, T. Nakajima, Z. Mazej, and B. Žemva, J. Fluorine Chem.,127, 1383 (2006).

[13] K. Naga, T. Nakajima, S. Aimura, Y. Ohzawa, B. Žemva, Z. Mazej, H. Groult, and A. Yoshida, J. Power Sources, 167, 192 (2007).

[14] T. Nakajima, S. Shibata, K. Naga, Y. Ohzawa, A. Tressaud, E. Durand, H. Groult, and F. Warmont, J. Power Sources, 168, 265 (2007).

[15] E. Peled, C. Menachem, D. Bat-Tow, A. Melman, and A. Melman, J. Electrochem. Soc., 143, L4 (1996)

[16] J. S. Xue, and J. R. Dahn, J. Electrochem. Soc., 142, 3668 (1995).

[17] M. Hara, A. Satoh, N. tamaki, and T. Ohsaki, Tanso, 165, 261 (1994).

[18] Y. Ein-Eli, and V. R. Koch, J. Electrochem. Soc., 144, 2968 (1997).

[19] Y. Wu C. Jiang, C. Wan, and E. Tsuchida, J. Mater. Chem., 11, 1233 (2002).

[20] Y. P. Wu C. Jiang, C. Wan, and R. Holze, Electrochem. Commum., 4, 483 (2002).

[21] Y. P. Wu C. Jiang, C. Wan, and R. Holze, J. Power Sources, 111, 329 (2002).

[22] Y. Wu C. Jiang, C. Wan, and R. Holze, J. Appl. Electrochem., 32, 1011 (2002).

[23] R. Takagi, T. Okubo, K. Sekine, and T. Takamura, Deniki Kagaku, 65, 333 (1997).

[24] T. Takamura, K. Sumiya, J. Suzuki, C. Yamada, and K. Sekine, J. Power Sources, 81/82, 368 (1999).

[25] J. Gao, H. P. Zhang, L. J. Fu, T. Zhang, Y. P. Wu, T. Takamura H, Q. Wu, and R. Holze, Electrochim. Acta, 52, 5417 (2007).

[26] Y. Wu, C. Jiang, C. Wan, and E. Tsuchida, Electrochem. Commun., 2, 626 (2000).
[27] S.-S. Kim, Y. Kadoma, H, Ikuta, Y. Uchimoto, and M. Wakihara, Electrochem. Solid-State Lett., 4, A109 (2001).
[28] J. K. Lee, D. H. Ryu, J. B. Ju, Y. G. Shul, B. W. Cho, and D. Park, J. Power Sources, 107, 90 (2002).
[29] J. Gao, L. J. Fu, H. P. Zhang, L. C. Yang, and Y. P. Wu, Electrochim. Acta, 53, 2376 (2008).
[30] T. Tsumura, A. Katanosaka, I. Souma, T. Ono, Y. Aihara, J Kuratomi, and M. Inagaki, Solid State Ionics, 135, 209 (2000).
[31] H. Wang, and M. Yoshino, J. Power Sources, 93, 123 (2001).
[32] S. Soon, H. Kim, and S. M. Oh, J. Power Sources, 94, 68 (2001).
[33] J.-H. Lee, H.-Y Lee, S.-M. Oh, S.-J. Lee, K.-Y. Lee, and S.-M. Lee, J. Power Sources, 166, 250 (2007).
[34] M. Yoshino, H. Wang, K, Fukuda, Y, Hara, and Y. Adachi, J. Electrochem. Soc., 147, 1245 (2000).
[35] H. Wang, M. Yoshida, T. Abe, and Z. Ogumi, J. Electrochem. Soc., 149, A499 (2002).
[36] M. Yoshino, H. Wang, K, Fukuda, T. Ueno, N. Dimov, and Z. Ogumi, J. Electrochem. Soc., 149, A1598 (2002).
[37] Y.-S. Han, and J.-Y. Lee, Electrochim. Acta, 48, 1073 (2003).
[38] Y. Ohzawa, M. Mitani, T. Suzuki, V. Gupta, and T. Nakajima, J. Power Sources, 122, 153 (2003).
[39] Y. Ohzawa, Y. Yamanaka, K. Naga, and T. Nakajima, J. Power Sources, 146, 125 (2005).
[40] Y. Ohzawa, K. Mizuno, and T. Nakajima, Carbon, 46, 562 (2008).
[41] Y. Ohzawa, and T. Nakajima, Carbon, 46, 565 (2008).
[42] Y. Ohzawa, R, Minamikawa, T. Okada, and T. Nakajima, Carbon, 46, 1628 (2008).
[43] S. Kuwabata, N. Tsumura, S. Goda, C. R. Martin, and H. Yoneyama, J. Electrochem. Soc., 145, 1415 (1998).
[44] M. Gaberscek, M. Bele, J. Drofenik, R. Dominko, and S. Pejovnik, Electrochem. Solid-State Lett., 3, 171 (2000).
[45] J. Drofenik, M. Gaberscek, R. Dominko, M. Bele, and S. Pejovnik, J. Power Sources, 94, 97 (2001).
[46] M. Bele, M. Gaberscek, R. Dominko, J. Drofenik, K, Zupan, P. Koma, K. Kocevar, I. Musevic, and S. Pejovnik. Carbon, 40, 1117 (2002).
[47] M. Gaberscek, M. Bele, J. Drofenik, R. Dominko, and S. Pejovnik, J. Power Sources, 97/98, 67 (2001).
[48] B. Veeraraghavan, J. Paul, B. Haran, and B. Popov, J. Power Sources, 109, 377 (2002).
[49] Y. F. Zhou, S. Xie, and C. H. Chen, Electrochim. Acta, 50, 4728 (2003).
[50] S. Komaba, T. Ozeki, and K. Okushi, J. Power Sources, 189, 197 (2009).

[51] M. Holzapfel, H. Buqa, F. Krumeich, P. Novak, F. M. Petrat, and C. Veit, Electrochem. Solid-State Lett., 8, A516 (2005).
[52] I. R. M. Kottegoda, Y. Kadoma, H. Ikuta, Y. Uchimoto, and M. Wakihara, Electrochem. Solid-State Lett., 5, A275 (2002).
[53] I. R. M. Kottegoda, Y. Kadoma, H. Ikuta, Y. Uchimoto, and M. Wakihara, J. Electrochem. Soc., 152, 1595 (2005).
[54] S. Komaba, M. Watanabe, H. Groult, N. Kumagai and K. Okahara, Electrochem. Solid-State Lett., 9, A130 (2006).
[55] S. H. Ng, J. Wang, K. Konstantinov, D. Wexler, J. Chen, and H. K. Liu, J. Electrochem. Soc., 153, A787 (2006).
[56] H. Huang, E. M. Kelder, and J. Schoonman, J. Power Sources, 97/98, 114 (2001).
[57] K. Nishimura, H. Honbo, S. Takeuchi, T. Horiba, M. Oda, M. Koseki, Y. Muranaka, Y. Kozono, and H. Miyadera, J. Power Sources, 68, 436 (1997).
[58] Y. P. Wu, C. Jiang, C. Wang, and R. Holze, J. Power Sources, 112, 255 (2002).
[59] Y. P. Wu, C. Jiang, C. Wang, and R. Holze, Carbon , 41, 437 (2003).
[60] J. Y. Lee, R. Zhang, and Z. Liu, J. Power Sources, 90, 70 (2000).
[61] Y. S. Jung. K. T. Lee, J. H. Ryu, D. Im, and S. M. Oh. J. Electrochem. Soc., 152, A1452 (2005).
[62] A. Caballero, J. Morales, and L. Sanchez, Electrochem. Solid-State Lett., 8, A464 (2005).
[63] K. Wang, X. He, J. Ren, C. Jiang, and C. Wan, Electrochem. Solid-State Lett., 9, A320 (2006).
[64] L.-Y. Hsiao, T. Fang, and J.-G. Duh, Electrochem. Solid-State Lett., 9, A232 (2006).
[65] P. Yu, J. A. Ritter, R. E. White, and B. N. Popov, J. Electrochem. Soc., 147, 1280 (2000).
[66] P. Yu, J. A. Ritter, R. E. White, and B. N. Popov, J. Electrochem. Soc., 147, 2081 (2000).
[67] L. Shi, Q. Wang, H. Li, Z. Wang, X. Huang, and L. Chen, J. Power Sources, 102, 60 (2001).
[68] W.-R. Liu, J.-H. Wang, H.-C. Wu, D.-T. Shieh, M.-H. Yang, and N.-L. Wu, J. Electrochem. Soc., 152, A1719 (2005).
[69] Z. P. Guo, E. Milin, J. Z. Wang, J. Chen, and H. K. Liu, J. Electrochem. Soc., 152, A2211 (2005).
[70] B.-C. Kim, H. Uono, T. Satou, T. Fuse, T. Ishihara, M. Ue, and M. Senna, J. Electrochem. Soc., 152, A523 (2005).
[71] Y. Liu, T. Matsumra, N. Imanishi, A. Hiroya, T. Ichikawa, and Y. Takeda, Electrochem. Solid-State Lett., 8, A599 (2005).
[72] X. Yang, Z. Wen, X. Xu, B. Lin, and Z. Lin, J. Electrochem. Soc., 153, A1341 (2006).
[73] H. Uono, B.-C. Kim, T. Fuse, M. Ue, and J. Yamaki, J. Electrochem. Soc., 153, A1708

(2006).
[74] M.-S. Park, S. Rajendran, Y.-M. Kang, K.-S. Han, Y.-S. Han, and J.-Y. Lee, J. Power Sources, 158, 650 (2001).
[75] O. P. Korobeinichev, S. B. Ilyin. Chen, V. M. Shvartsberg, and A. A. Chernov, Combust. Flame 121, 593 (2000).
[76] X. Wang, E. Yasukawa, and S. Kasuya, J. Electrochem. Soc., 148, A1058 (2001).
[77] X. Wang, E. Yasukawa, and S. Kasuya, J. Electrochem. Soc., 148, A1066 (2001).
[78] K. Xu, M. S. Ding, S. Zhang, J. L. Allen, and T. R. Jow, J. Electrochem. Soc., 149, A622 (2002).
[79] X. L. Yao, S. Xie, C. H. Chn, Q. S. Wang, J. H. Sun, Y. L. Li, and S. X. Lu, J. Power Sources, 144, 170 (2005).
[80] X. Wang, C. Yamada, H. Naito, G. Segami, and K. Kibe, J. Electrochem. Soc., 153, A135 (2006).
[81] Y. E. Hyung, D. R. Vissers, and K. Amine, J. Power Sources, 119, 383 (2003).
[82] E.-G. Shim, T.-H. Nam, J.-G. Kim, H.-S. Kim, and S.-I Moon, J. Power Sources, 172, 919 (2007).
[83] T.-H. Nam, E-G. Shim, J-G. Kim, H.-S. Kim, and S.-I Moon, J. Electrochem. Soc., 154, A957 (2007).
[84] D. Zhou, W. Li, C. Tan, X. Zuo, and Y. Huang, J. Power Sources, 184, 589 (2008).
[85] K. Xu, S. Zhang, J. L. Allen, and T. R. Jow, J. Electrochem. Soc., 149, A1079 (2002).
[86] K. Xu, M. S. Ding, S. Zhang, J. L. Allen, and T. R. Jow, J. Electrochem. Soc., 150, A161 (2003).
[87] K. Xu, S. Zhang, J. L. Allen, and T. R. Jow, J. Electrochem. Soc., 150, A170 (2003).
[88] S. S. Zhang, K. Xu, and T. R. Jow, J. Power Sources, 113, 166 (2003).
[89] D. H. Doughty, E. P. Roth, C. C. Crafts, G. Nagasubramanian, G. Henriksen, and K. Amine, J. Power Sources, 146, 116 (2005).
[90] Q. Wang, J. Sun, X. Yao, and C. Chen, Electrochem. Solid-State Lett., 8, A467 (2005).
[91] Q. Wang, J. Sun, and C. Chen, J. Power Sources, 162, 1363 (2006).
[92] E.-G. Shim, T.-H. Nam, J.-G. Kim, H.-S. Kim, and S.-I. Moon, J. Power Sources, 175, 533 (2008).
[93] T.-H. Nam, E.-G. Shim, J.-G. Kim, H.-S. Kim, and S.-I. Moon, J. Power Sources, 180, 561 (2008).
[94] S. Izquierdo-Gonzales, W. Li, and B. L. Lucht, J. Power Sources, 135, 291 (2004).
[95] H. F. Xiang, Q. Y. Jin, C. H. Chen, X. W. Ge, S. Guo, and J. H. Sun, J. Power Sources, 174, 335 (2007).
[96] L. Wu, Z. Song, L. Liu, X Guo, L. Kong, H. Zhan, Y. Zhou, and Z. Li, J. Power Sources, 188, 570 (2009).
[97] Y.-B. He, Q. Liu, Z.-Y. Tang, Y.-H. Chen, and Q.-S. Song, Electrochim. Acta, 52, 3534 (2007).

[98] B. K. Mandal, A. K. Padhi, Z. Shi, S. Chakraborty, and R. Filler, J. Power Sources, 161, 1341 (2006).

[99] B. S. Lalia, T. Fujita, N. Yoshimoto, M. Egashira, and M. Morita, J. Power Sources, 186, 211 (2009).

[100] C. W. Lee, R. Venkatachalapathy, and J. Prakash, Electrochem. Solid-State Lett., 3, 63 (2000).

[101] A. Chen, Y. Qin, J. Liu, and K. Amine, Electrochem. Solid-State Lett., 12, A69 (2009)

[102] T. Tsujikawa, K. Yabuta, T. Matsushita, T. Matsushima, K. Hayashi, and M. Arakawa, J. Power Sources, 189, 429 (2009).

[103] H. P. Zhang, Q. Xia, B. Wang, L. C. Yang, Y. P. Wu, D. L. Sun, C. L. Gan, H. J. Luo, A. W. Bebeda, and T. v. Ree, Electrochem. Commun., 11, 526 (2009).

[104] K. A. Smith, M. C. Smart, G. K. S. Prakash, and B. V. Ratnakumar, ECS Trans., 11, 91 (2008).

[105] S. Chen, Z. Wang, H. Zhao, H. Qiao, H. Luan, and L. Chen., J. Power Sources, 187, 229 (2009).

[106] K. Naoi, E. Iwama, N. Ogihara, Y. Nakamura, H. Segawa, and Y. Ino, J. Electrochem. Soc., 156, A272 (2009).

[107] T. Achiha, T. Nakajima, Y. Ohzawa, M. Koh, A. Yamauchi, M. Kagawa, and H. Aoyama, J. Electrochem. Soc., 156, A483 (2009).

Chapter 2

Electrochemical behavior of natural graphite fluorinated by F_2 in propylene carbonate-containing solvents

2-1 Introduction

Graphitic materials such as natural and synthetic graphites are mainly used as anodes materials of lithium-ion batteries because of their low potentials, low irreversible capacities (high first coulombic efficiencies), constant reversible capacities and good cycleability. It is known that ethylene carbonate (EC)-based solvents should be used for graphite anodes for quick formation of surface film (Solid Electrolyte Interface: SEI) with decomposition of a small amount of solvent [1]. Because EC has a high melting point of 36 °C, the use of propylene carbonate (PC) is preferable due to its low melting point, -55 °C. Unfortunately PC cannot be used for high-crystallinity graphite because of continuous decomposition of PC. However, PC can be used for low-crystalline carbons with high disorder. This suggests that high-crystalline graphite is useable in PC-containing solvents if surface disordering is made by surface modification. Recently some methods of surface modification were applied to improve electrode characteristics of carbonaceous anodes for lithium-ion batteries [2-4]. They are carbon coating [5-16], metal or metal oxide coating [17-23], surface oxidation [24-32], surface fluorination [33-42] and polymer or Si coating [43-51]. These methods gave positive effects to reversible capacities, first coulombic efficiencies (irreversible capacities), cycleability and so on. Among them, surface fluorination is an effective method to increase the surface disorder of graphite [33-42]. Surface fluorination of natural graphite powder samples (average particle sizes: 7, 25 and 40 μm; surface areas: 4.8, 3.4 and 2.7 m^2/g) by F_2 increased *R* values calculated from peak intensity ratios of D-band to G-band of Raman shifts, indicating the increase in surface disorder [33-35, 37]. Plasma-fluorination of the same natural graphite samples with CF_4 also increased surface disorder [36]. Simultaneously the fluorination highly increased their surface areas. First coulombic efficiencies of these natural graphite samples were not changed by fluorination in 1.0 mol/dm^3 $LiClO_4$ - ethylene carbonate (EC) / diethyl carbonate (DEC) (1:1 vol.) probably because the large increase in surface areas facilitated the decomposition of EC leading to reduction of first coulombic efficiencies [33-37]. Surface fluorination of heat-treated petroleum cokes by F_2 destroyed and opened the closed edge planes which were formed during the heat-treatment at 2300-2800 °C, increasing surface disorder of petroleum cokes [39-41]. Surface areas of heat-treated petroleum cokes were nearly the same or only slightly increased after fluorination. These

surface structure changes led to increase in their first coulombic efficiencies in EC-based solvents [39-41]. Fluorination of carbon materials with F_2 is an electrophilic reaction [52-54], yielding surface fluorinated layers. Plasma-fluorination is a radical reaction by chemically active species such as CF_3, however, giving surface fluorinated layers because the sample temperature was low (90 °C) [36]. Fluorination reactions of petroleum cokes made by ClF_3 and NF_3 at 200-500 °C are radical reactions by chemically active species such as F, Cl, ClF_2 and NF_2, having surface etching effect [42]. No increase in surface disorder of petroleum cokes was observed after the fluorination. Main effect of surface fluorination by ClF_3 and NF_3 was increase in first charge capacities of heat-treated petroleum cokes [42]. However, surface disorder was increased by fluorination with ClF_3 when natural graphite samples with high surface areas were used probably because natural graphite has the higher crystallinity than heat-treated petroleum cokes [38]. First coulombic efficiencies of natural graphites with average particle sizes of 10 μm and 15 μm increased in 1.0 mol/dm^3 $LiClO_4$ - EC/DEC/PC (1:1:1 vol.) at 150 mA/g [38]. Importance of high rate characteristics is increasing due to the application to electric vehicle. Therefore charge/discharge characteristics are often examined at high current densities. From the results hitherto obtained on the surface fluorination of graphitic materials, F_2 is a suitable fluorinating agent for increasing the surface disorder of graphite, yielding surface fluorinated layers. In the present study, high crystalline natural graphites were fluorinated by F_2 to prepare surface-disordered graphites which are usable in PC-based solvents, and charge/discharge behavior of surface-disordered graphites were examined in PC-containing solvent. If surface-modified graphitic materials can be used as anodes in PC-containing solvents, lithium-ion secondary batteries are operated in a wide range of temperatures.

2-2 Experimental

2-2-1 Surface fluorination and characterization of natural graphite samples

Starting materials were natural graphite powder samples with average particle sizes of 5 μm, 10 μm and 15 μm (abbreviated to NG5 μm, NG10 μm and NG15 μm; d_{002} = 0.3355, 0.3354 and 0.3355 nm; purity: >99.95 %), supplied by SEC Carbon Co., Ltd. Surface fluorination of natural graphite sample was performed by F_2 ($3x10^4$ Pa) at 200 °C and 300 °C for 2 minutes using a nickel fluorination reactor. Surface fluorinated natural graphite samples were characterized by X-ray diffractometry (SHIMADZU, XRD-6100), X-ray photoelectron spectroscopy (XPS) (SHIMADZU, ESCA 1000 with Mg Kα radiation), IR absorption spectroscopy (KBr method) (SHIMADZU, FTIR-8600PC), surface area and meso-pore size distribution measurements using nitrogen gas (SHIMADZU, Tri Star 3000) and Raman spectroscopy (JASCO, NRS-1000 with Nd:YVO4 laser, 532 nm).

2-2-2Electrochemical measurements for surface-fluorinated natural graphite samples

Beaker type three electrode-cell with natural graphite sample as a working electrode and metallic lithium as counter and reference electrodes was used for cyclic voltammetry and galvanostatic charge/discharge experiments. Electrolyte solution was 1.0 mol/dm^3 $LiClO_4$ - EC/DEC/PC (1:1:1 vol.) (Kishida Chemicals, Co. Ltd., H_2O: 2-5 ppm). For comparison, electrode behavior of non-fluorinated graphite samples was checked in 1.0 mol/dm^3 $LiClO_4$ - EC/DEC (1:1 vol.). Natural graphite electrode was prepared as follows. Natural graphite sample was dispersed in N-methyl-2-pyrrolidone (NMP) containing 12 wt.% poly vinylidene fluoride (PVdF) and pasted on copper plate. The electrode was dried at 120 °C under vacuum overnight using a rotary pump. After drying, the electrode contained 80 wt.% natural graphite sample and 20 wt.% PVdF. Potential scan for cyclic voltammetry was made at 1.0 mV/s (HOKUTO DENKO, HSV-100). Charge/discharge experiments were performed at current densities of 60 and 150 mA/g between 0 and 3.0 V relative to Li/Li^+ in a glove box filled with Ar at 25 °C (HOKUTO DENKO, HJ1001 SM8A).

2-3 Results and Discussion

2-3-1 Surface structure change of natural graphite samples by fluorination with F_2

X-ray diffraction patterns of natural graphite samples were almost the same before and after surface fluorination. Diffraction peaks were only slightly broadened. Figures 1-3 show typical XPS spectra of original and surface-fluorinated natural graphite samples. Table I summarizes binding energies of C1s, O1s and F1s electrons, and surface composition calculated from peak areas of XPS spectra. F1s peaks were located at 687.8-688.0 eV corresponding to C-F covalent bond. In consistence with F1s spectra, small shifted C1s peaks were observed at 288.8-289.3 eV. These binding energies of F1s and C1s electrons are slightly smaller than those observed for graphite fluoride, $(CF)_n$ (F1s: 689-690 eV, C1s: 289-290 eV). This would be due to smaller charging effect of surface-fluorinated graphite samples with high electric conductivity than that of insulating $(CF)_n$. Surface fluorine concentrations were in the range of 11.1-15.3 at.% and 17.7-20.5 at.% for natural graphite samples fluorinated at 200 °C and 300 °C, respectively, increase with increasing fluorination temperature. However, there is no large difference in surface fluorine concentrations among three graphite samples. Surface fluorine concentrations were higher than those observed for the same natural graphite samples fluorinated by ClF_3 [38]. The difference in the surface fluorine concentrations is ascribed to difference in the reaction mechanisms of F_2 and ClF_3 with carbon materials. The reaction of F_2 with a carbon is an electrophilic reaction, in which $F^{\delta+}$ attacks carbon atom with higher electron density ($C^{\delta-}$) and $F^{\delta-}$ is bonded to another carbon with lower electron density ($C^{\delta+}$), mainly giving solid fluorinated layers [52-54]. Fluorination reaction proceeds with

carbon-carbon bond breaking and C-F bond formation. Simultaneously sp^2 bond of carbon is changed to sp^3 bond. On the other hand, the reaction of ClF_3 with a carbon material is a radical reaction with atomic and radical species such as F, Cl and ClF_2, in which surface etching of carbon occurs, mainly yielding gaseous fluorocarbons [38, 42]. Surface oxygen was reduced by fluorination as given in Table I. Weak O1s peaks were observed in the range of 532.2-532.9 eV indicating the existence of COH group together with small shoulders at 530.2-530.9 eV and 534.1-535.0 eV corresponding to CO group and adsorbed water, respectively as shown in Figs. 1-3. Weak C1s peaks showing C-O bonds were located at 285.8-286.3 eV for both original and surface-fluorinated samples (Figs. 1-3). Very weak shoulders observed at 291.5-291.8 eV are satellite peaks. The surface oxygen of high purity natural graphite powder (≈ 7 μm) was 6 at.% when Shimadzu ESCA 1000 spectrometer was used as in the present study [39]. However, it was 1.5-2.0 at.% when Ulvac Phi Model 5500 spectrometer was used [33]. The difference in the surface oxygen concentrations may be due to the difference in the vacuum levels of the spectrometers. This suggests that the actual concentrations of surface oxygen are lower than those listed in Table I. Figure 4 shows IR absorption spectra of natural graphite samples fluorinated at 300 °C. Broad and weak absorptions are observed at around 1080 cm^{-1} in all samples. Highly fluorinated graphite ($C_{1.4}F$–$C_{2.9}F(HF)_{0.65}$) showed some strong absorptions between 1080 and 1230 cm^{-1} corresponding to stretching vibration of covalent C-F bonds [55]. These absorptions are observed in highly fluorinated graphite in which sp^2 and sp^3 carbons coexist [55, 56]. Broad absorptions centered at 1080 cm^{-1} in Fig. 4 seem to consist of several absorptions between 1000 and 1200 cm^{-1}. Another absorption at around 1554 cm^{-1} is attributed to vibration of graphene layers (IR active A_{2u} mode) [55].

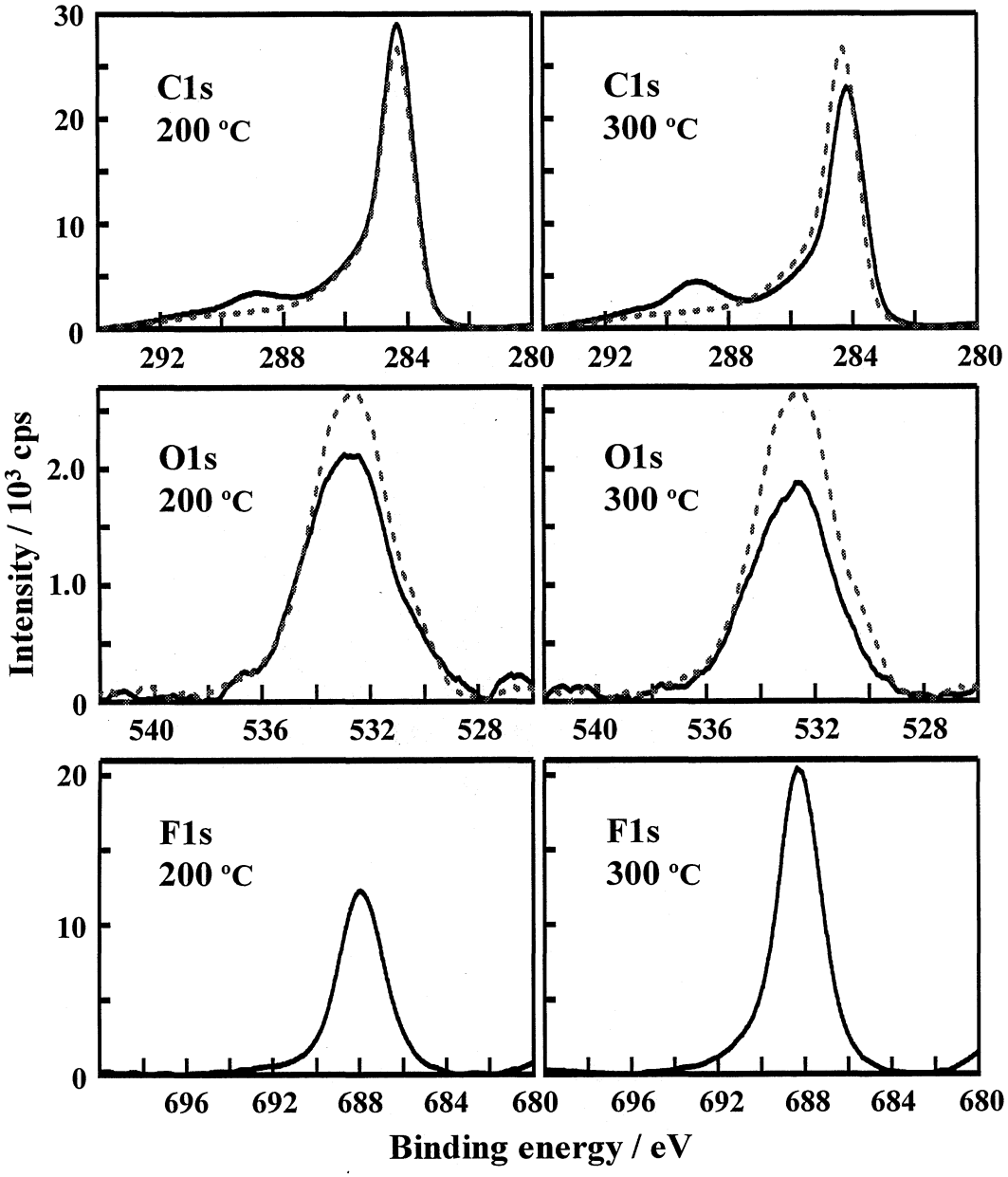

Figure 1. XPS spectra of NG5 μm and surface-fluorinated NG5 μm.
- - - - - : NG5 μm, ———: NG5 μm fluorinated at 200 and 300 °C.

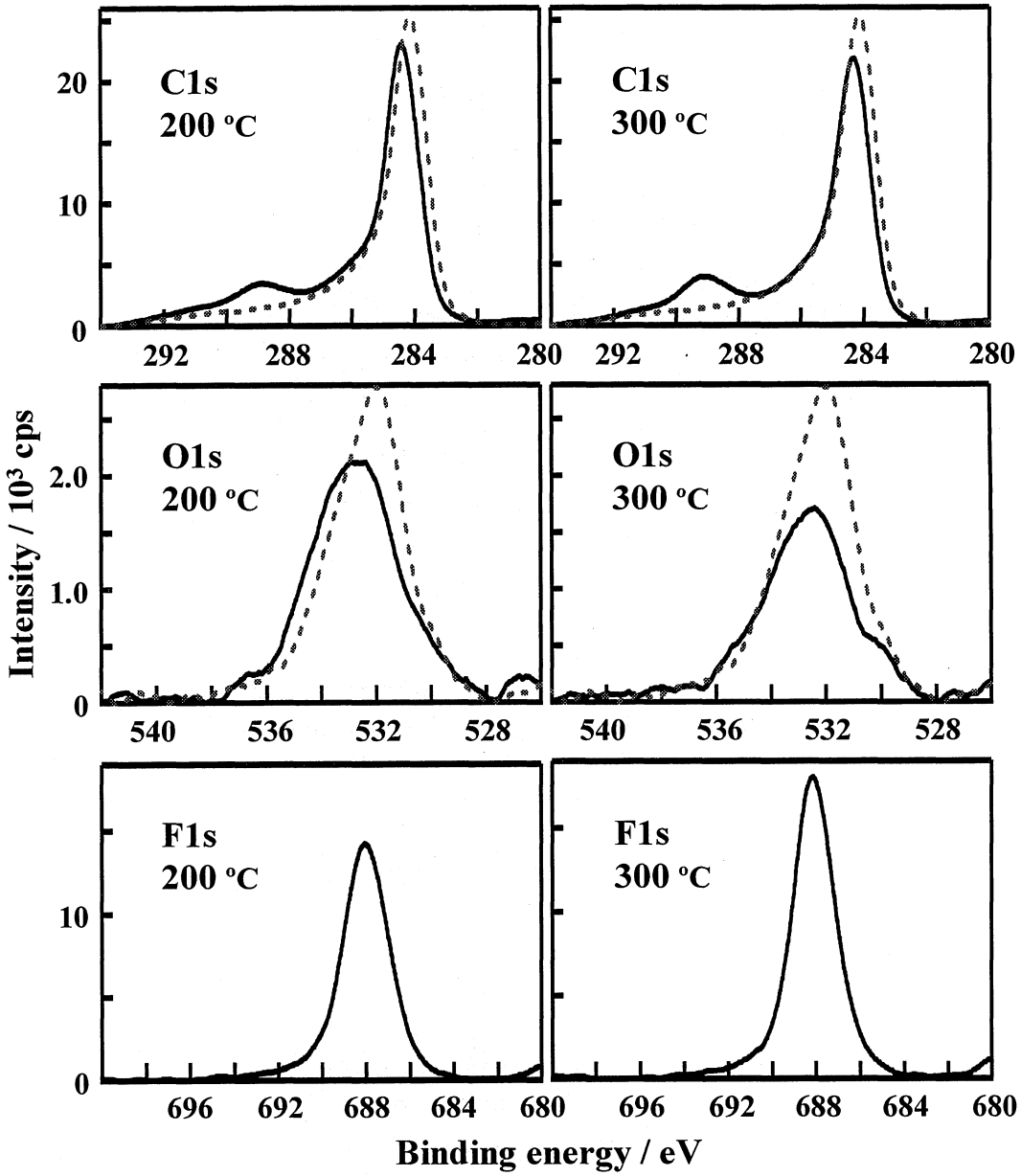

Figure 2. XPS spectra of NG10 μm and surface-fluorinated NG10 μm.
- - - - - : NG10 μm, ———: NG10 μm fluorinated at 200 and 300 °C.

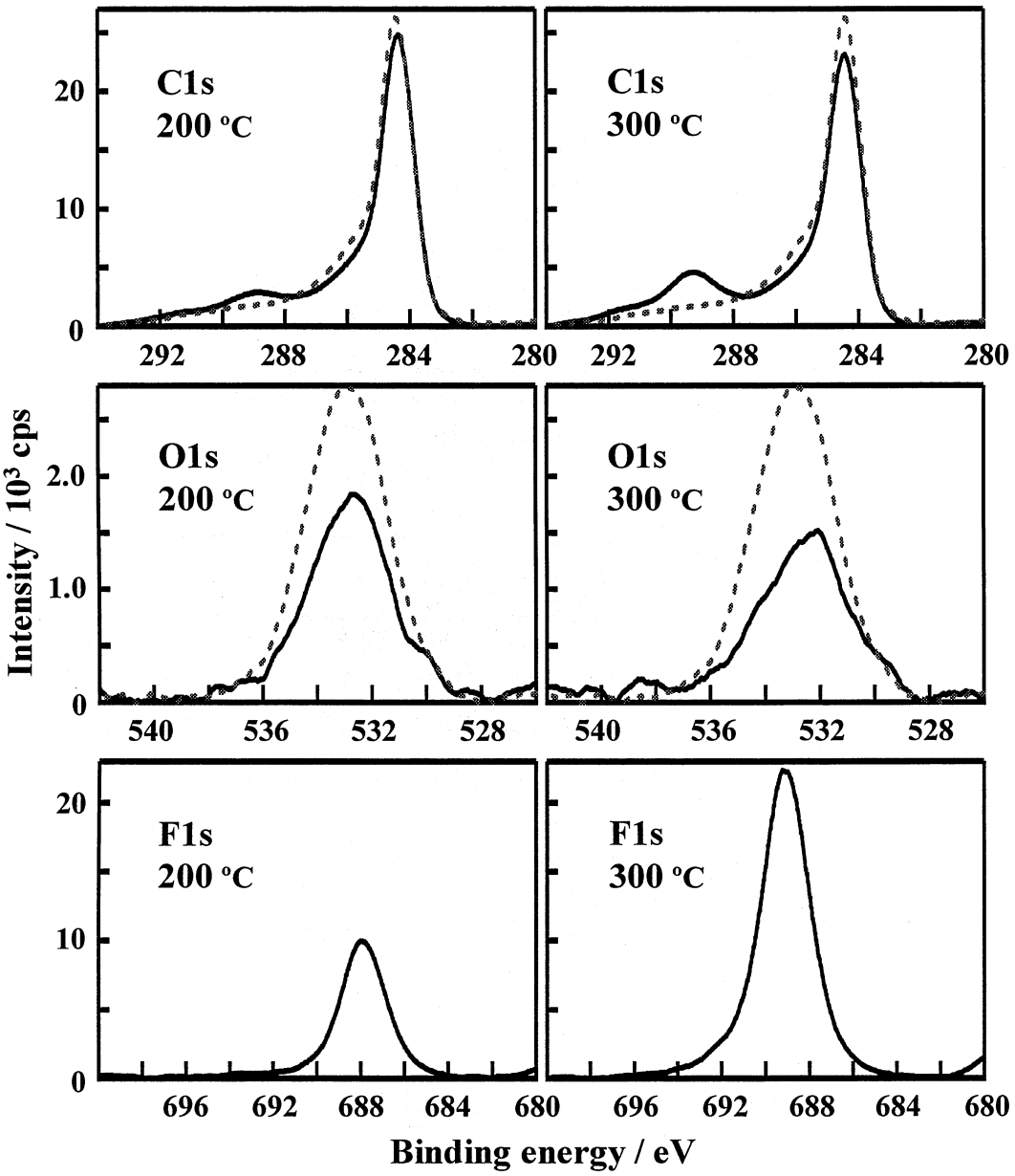

Figure 3. XPS spectra of NG15 μm and surface-fluorinated NG15 μm.
- - - - - : NG15 μm, ———: NG15 μm fluorinated at 200 and 300 °C.

Table I. Binding energies and surface composition
of original and surface-fluorinated natural graphite samples, obtained by XPS.

Graphite Sample		Fluorination temperature							
		Original		200 °C			300 °C		
		C	O	C	O	F	C	O	F
NG5 μm	Binding energy (eV)	284.3 286.3 291.6	530.6 532.7 534.7	284.3 285.8 288.8 291.7	530.4 532.8 534.8	687.8	284.2 286.0 289.0 291.8	530.9 532.8 534.8	688.0
	Surface composition (at.%)	93.6	6.4	84.2	4.2	11.6	77.3	3.7	19.0
NG10 μm	Binding energy (eV)	284.2 286.0 291.6	530.4 532.2 534.1	284.4 286.0 288.9 291.7	530.2 532.9 535.0	687.9	284.3 285.9 289.0 291.8	530.3 532.6 534.8	688.0
	Surface composition (at.%)	93.5	6.5	81.1	3.6	15.3	78.4	3.9	17.7
NG15 μm	Binding energy (eV)	284.4 286.1 291.5	530.8 532.9 535.0	284.4 286.0 288.9 291.8	530.4 532.7 534.8	687.9	284.5 286.1 289.3 291.7	530.5 532.5 534.5	688.0
	Surface composition (at.%)	93.3	6.7	84.8	4.1	11.1	76.2	3.3	20.5

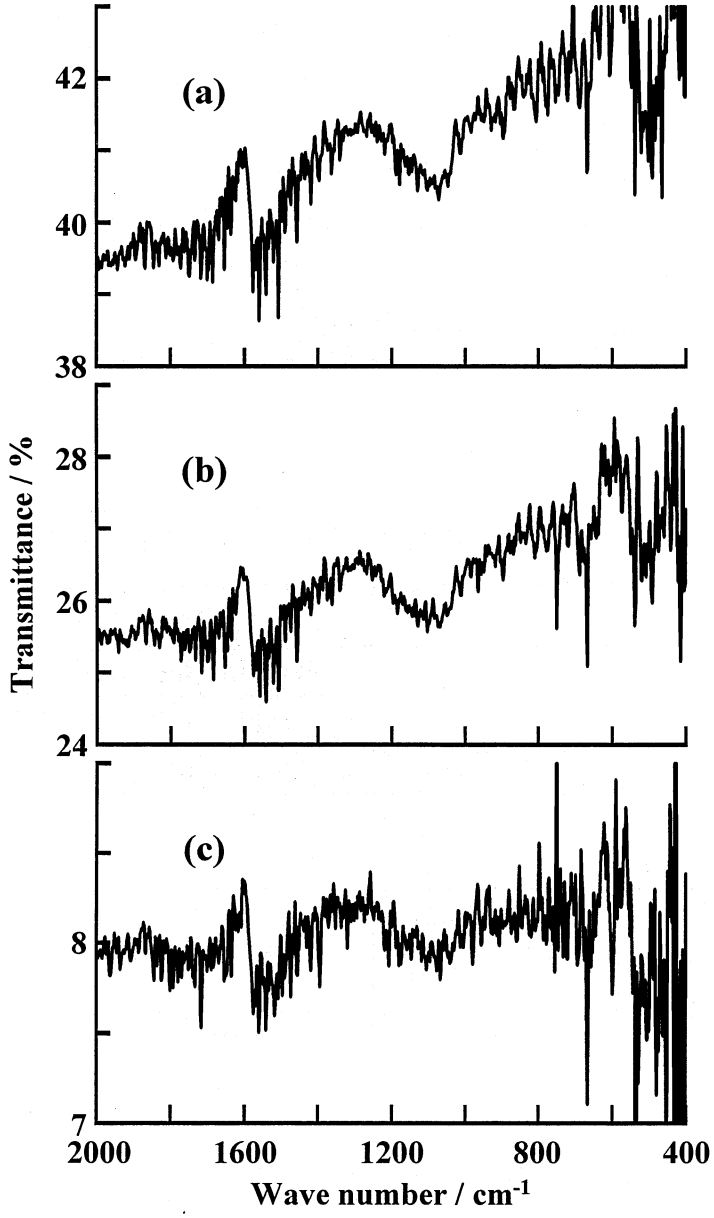

Figure 4. IR absorption spectra of (a) NG5 μm, (b) NG10 μm and (c) NG15 μm fluorinated at 300 °C.

Surface area and total pore volume of non-fluorinated sample decreased with increasing particle size as given in Table II. Surface areas and pore volumes were both increased by surface fluorination causing carbon-carbon bond breaking and formation of covalent C-F bonds. Increase in the surface area and pore volume was the largest in NG5 μm among three natural graphite samples, particularly in NG5 μm fluorinated at 300 °C probably because surface fluorinated layers were thick. However, the increase in the surface areas and pore volumes was small in NG10 μm and NG15 μm. Increase of surface areas may be correlated with meso-pore size distributions shown in Fig. 5, in which meso-pores with diameters of 1.7 and 2.3 nm increased in all surface-fluorinated samples due to carbon-carbon bond breaking caused by fluorination. These results are very different from those obtained for the same natural graphite samples fluorinated by ClF_3 [38]. Surface areas and pore volumes were reduced by the fluorination with ClF_3 due to the radical reaction having surface etching effect.

Table II. Surface areas and total meso-pore volumes
of original and surface-fluorinated natural graphite samples.

		Fluorination temperature		
Sample		**Original**	**200 °C**	**300 °C**
NG5 μm	**Surface area**	**13.9**	**16.2**	**19.3**
NG10 μm	**(m^2g^{-1})**	**9.2**	**9.9**	**10.8**
NG15 μm		**6.9**	**7.3**	**7.7**
NG5 μm	**Pore volume**	**0.047**	**0.049**	**0.059**
NG10 μm	**(cm^3g^{-1})**	**0.035**	**0.036**	**0.038**
NG15 μm		**0.026**	**0.028**	**0.029**

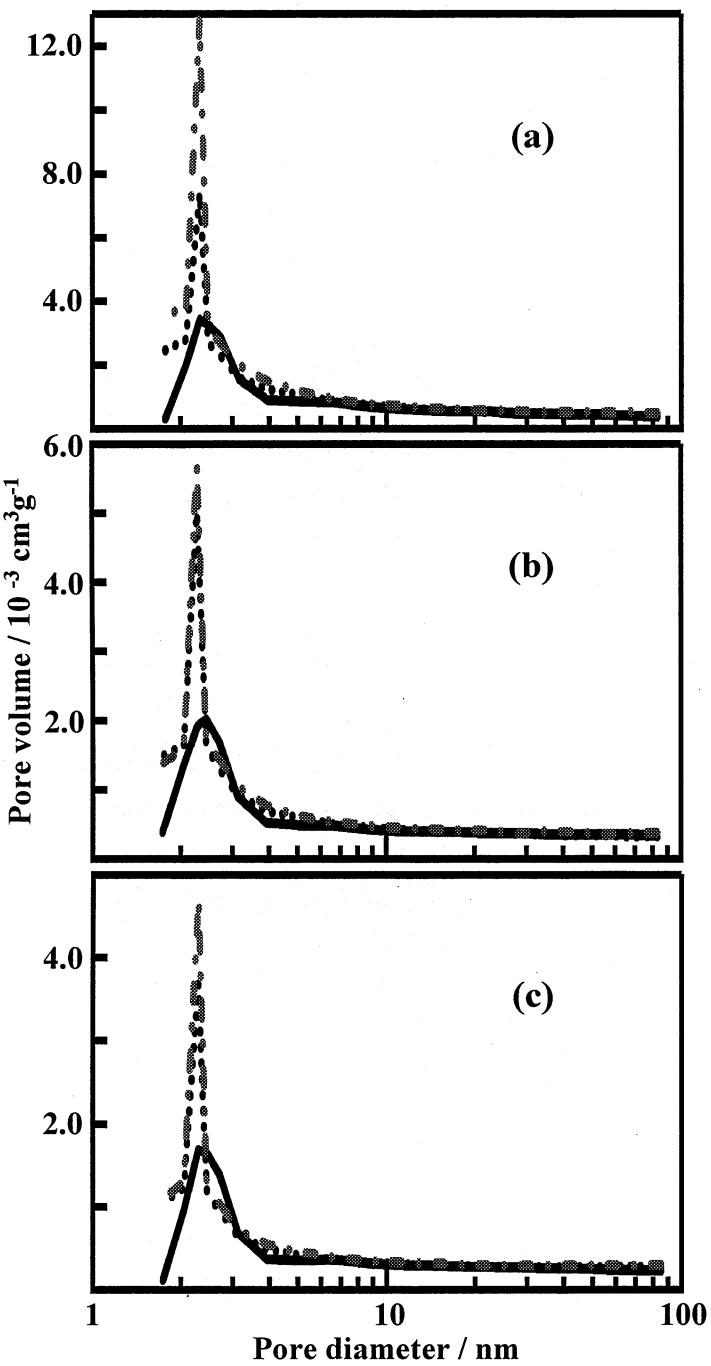

Figure 5. Meso-pore size distribution of original and surface-fluorinated natural graphite samples. (a) NG5 μm, (b) NG10 μm, (c) NG15 μm.
———: original, ·····: fluorinated at 200 °C, — · — · —: fluorinated at 300 °C.

R value calculated from peak intensity ratio of D-band to G-band in Raman spectrum expresses the degree of surface disorder of a carbon material. In addition to D-band, weak D'-band at 1620 cm^{-1} is normally observed in Raman spectrum. *R* values were therefore calculated after separating D'-band from G-band. Figure 6 shows Raman spectra of non-fluorinated graphite samples and those fluorinated at 200 °C and 300 °C. D-band intensity was increased by surface fluorination while G-band intensity was reduced. Intensity of two Raman shifts changed in the similar manner also in NG5 μm and NG10 μm. *R* values increased with increasing fluorination temperature and particle size of graphite, i.e. from NG5 μm to NG15 μm as given in Table III. The increase in *R* values by fluorination using F_2 is larger than that obtained for the same natural graphite samples fluorinated by ClF_3 [38]. This is also attributed to the reaction mechanism of F_2 with a carbon. As already discussed, the reaction of F_2 with a carbon is an electrophilic reaction, easily forming surface fluorinated layers with C-F covalent bonds. Carbon-carbon bond breaking and change of sp^2 bond of carbon to the sp^3 would have brought about the high surface disordering of natural graphite samples.

Table III. *R* values ($=I_D/I_G$) of Raman spectra
of original and surface-fluorinated natural graphite samples.

	Fluorination temperature		
Sample	**Original**	**200 °C**	**300 °C**
NG5 μm	**0.23**	**0.23**	**0.26**
NG10 μm	**0.23**	**0.31**	**0.41**
NG15 μm	**0.25**	**0.38**	**0.53**

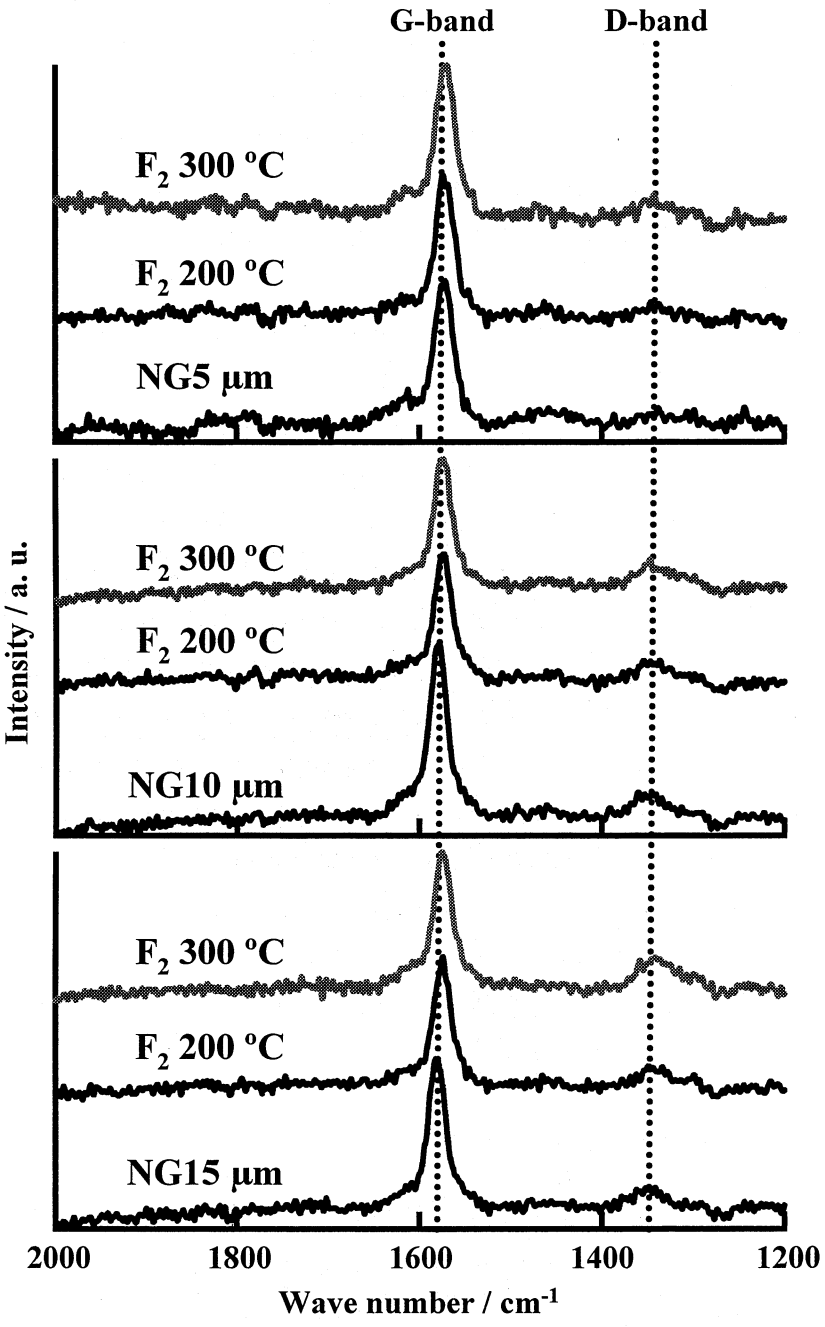

Figure 6. Raman spectra of original and surface-fluorinated natural graphite samples.

2-3-2 Electrochemical properties of surface-fluorinated natural graphite samples

Table IV shows first coulombic efficiencies for non-fluorinated natural graphite samples in 1.0 mol/dm^3 $LiClO_4$ - EC/DEC and - EC/DEC/PC solutions. In EC/DEC solution, three natural graphite samples exhibited higher first coulombic efficiencies than 80 %. First coulombic efficiency increased with increasing particle size, i.e. with decreasing surface area, indicating that decomposition of EC is reduced with decreasing surface area. The result shows that SEI is quickly formed by decomposition of a small amount of EC. On the contrary, first coulombic efficiency decreased with decreasing surface area, i.e. from NG5 μm to NG15 μm in EC/DEC/PC mixture as given in Table IV. It means that decomposition of PC increased with decreasing surface area. The area of edge plane, where desolvation of PC and reduction of PC and Li^+ ion, followed by Li insertion, may mainly occur, decreases with decreasing total surface area, i.e. from NG5 μm to NG15 μm. In addition, the ratio of edge plane to total surface area is close to 50 % in case of fine graphite powder such as NG5 μm, however, decreasing with increasing particle size, i.e. decreasing total surface area. Since charge/discharge cycling was made at a constant current density (constant current per 1g of graphite), actual current density increases with decreasing area of edge plane, that is, from NG5 μm to NG15 μm. Since SEI formation on high crystalline graphite is more difficult in PC-based solvent than in EC-based one, decomposition of PC would be accelerated with decrease in the area of edge plane, that is, with increase in actual current density. Exfoliation of surface region of natural graphite might occur, facilitating the electrochemical decomposition of PC. In the case of NG5 μm, first coulombic efficiencies were high in both EC/DEC and EC/DEC/PC solutions (81.4 and 81.8 %, respectively as given in Table IV). NG5 μm has the largest surface area, i.e. the largest area of edge plane, among three natural graphite samples. Additionally edge plane has the higher surface disorder than basal plane. These structural factors may facilitate the smooth formation of SEI on NG5 μm even in EC/DEC/PC.

Table IV. First coulombic efficiencies for non-fluorinated natural graphite samples in 1.0 mol/dm^3 $LiClO_4$ - EC/DEC and - EC/DEC/PC at 60 mA/g.

Electrolyte	NG5 μm	NG10 μm	NG15 μm (%)
EC/DEC	81.4	82.2	85.4
EC/DEC/PC	81.8	66.2	51.8

It was found that surface fluorination effectively improved electrode characteristics of NG10 μm and NG15 μm with relatively larger particle sizes. Figure 7 shows cyclic voltammograms obtained for non-fluorinated graphite samples and those fluorinated at 200 °C and 300 °C. Reduction current at 1st cycle indicating the decomposition of PC

increased with increasing particle size as shown in Figs. 7(a), Figs. 8(a) and 8(d). This is consistent with the results given in Table IV. However, reduction peaks at 1st cycle for NG10 μm and NG15 μm, shown in Figs. 8(b) and 8(e), were highly reduced by surface fluorination. The NG10 μm and NG15 μm fluorinated at 300 °C showed the similar potential-current curves to those obtained at 200 °C while NG5 μm fluorinated at 300 °C had a large reduction peak at around 0.5 V and another one at around 1.85 V vs. Li/Li^+ indicating the reduction of fluorine atoms bonded to basal plane of graphite [2]. In addition, peak currents of oxidation were also increased by surface fluorination. It means that reversibility of Li^+ intercalation and deintercalation into and from natural graphites was improved by fluorination.

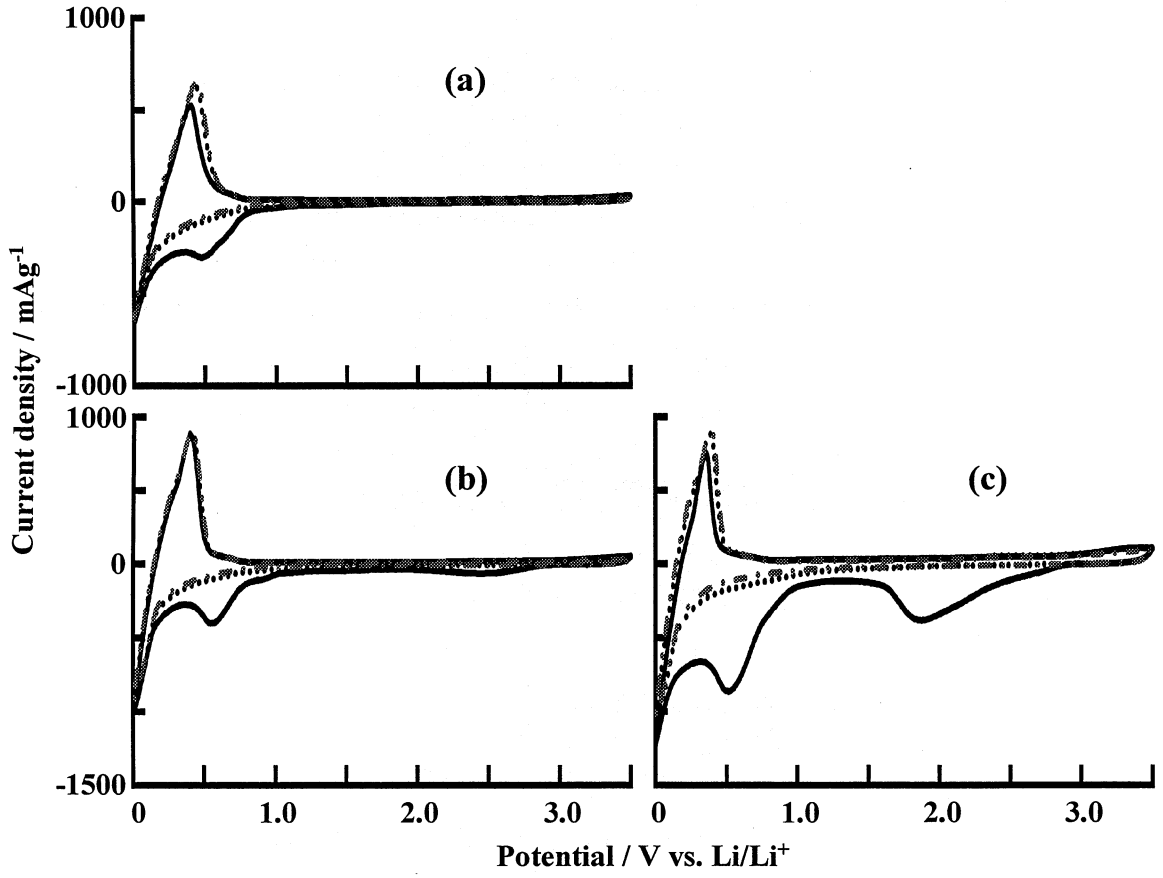

Figure 7. Cyclic voltammograms for original and surface-fluorinated natural graphite samples in 1.0 mol/dm^3 $LiClO_4$ - EC/DEC/PC at 1 mV/s.
(a) NG5 μm, (b) NG5 μm fluorinated at 200 °C, (c) NG5 μm fluorinated at 300 °C.
———: 1st cycle, ·····: 2nd cycle, — · — · —: 10th cycle.

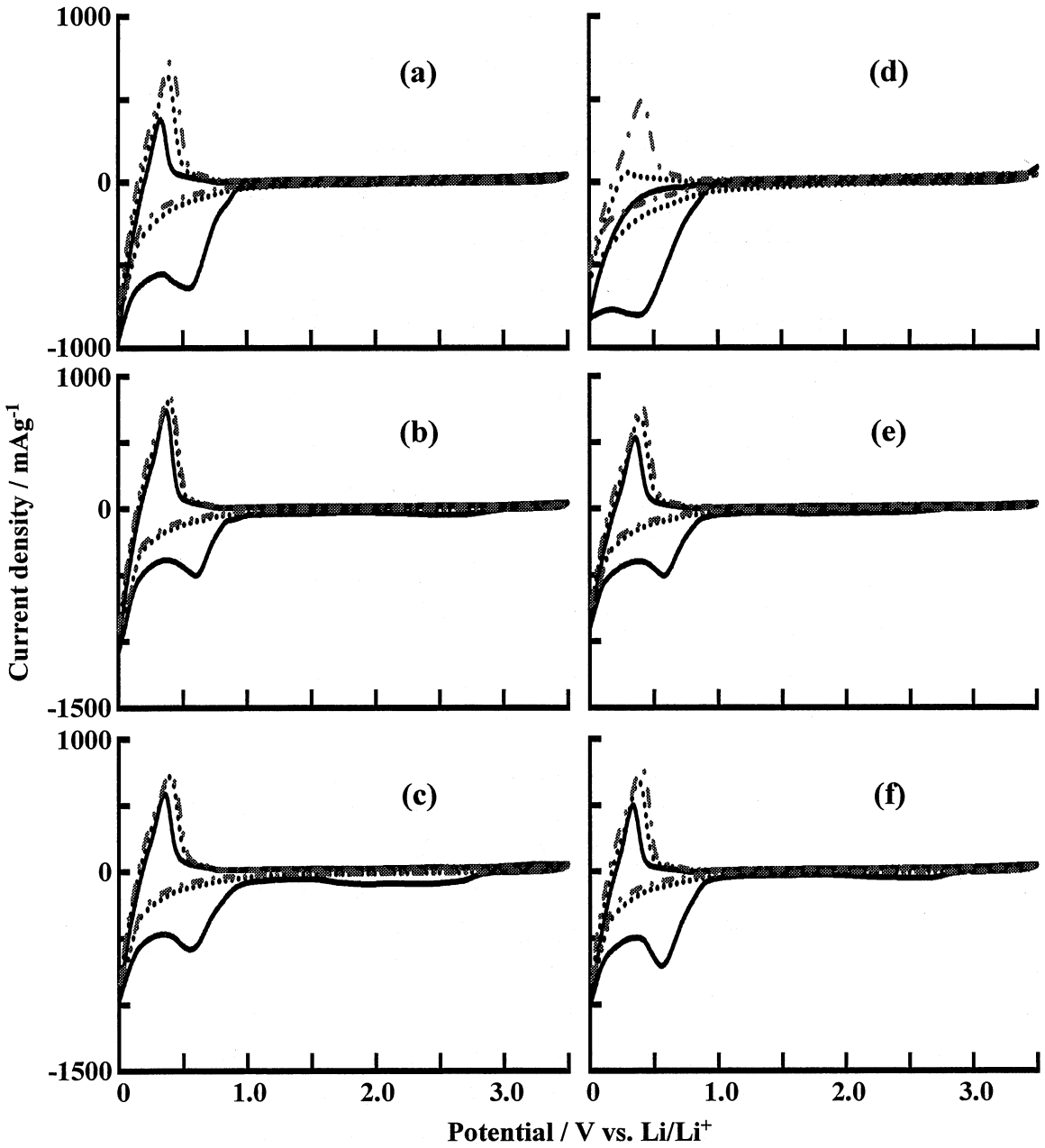

Figure 8. Cyclic voltammograms for original and surface-fluorinated natural graphite samples in 1 mol/dm^3 $LiClO_4$ - EC/DEC/PC at 1 mV/s.
(a) NG10 μm, (b) NG10 μm fluorinated at 200 °C, (c) NG10 μm fluorinated at 300 °C.
(d) NG15 μm, (e) NG15 μm fluorinated at 200 °C, (f) NG15 μm fluorinated at 300 °C.
———: 1st cycle, ·····: 2nd cycle, — · — · —: 10th cycle.

Figure 9 demonstrates first charge/discharge curves, charge capacities and coulombic efficiencies for original and surface-fluorinated natural graphite samples, obtained at 60 mA/g. Table V summarizes first charge/discharge capacities and first coulombic efficiencies at 60 and 150 mA/g. Surface fluorination was not effective for further improvement of electrochemical properties of NG5 μm. Charge/discharge behavior of NG5 μm fluorinated at 200 °C was nearly the same as that for non-fluorinated sample. A large reduction potential for fluorine and PC was observed for NG5 μm fluorinated at 300 °C as shown in Fig. 9(a), which shows that fluorination degree of NG5 μm was much higher at 300 °C than 200 °C. Therefore first coulombic efficiency was highly reduced for NG5 μm fluorinated at 300 °C. Surface fluorination effectively improved the charge/discharge characteristics of NG10 μm and NG15 μm with larger particle sizes. Large potential plateaus indicating the reduction of PC were significantly diminished by the fluorination at both 200 °C and 300 °C (Figs. 9(c) and 9(e)). As a consequence, first coulombic efficiencies for NG10 μm and NG15 μm highly increased (Figs. 9(d) and 9(f), and Table 5). The results obtained at 60 and 150 mA/g were similar to each other as given in Table V though first charge capacities and coulombic efficiencies decreased due to increase in the current density at 150 mA/g. The increments of first coulombic efficiencies were in the range of 9.9-13.2 % and 20.3-23.3 % for NG10 μm and NG15 μm, respectively, at both 60 and 150 mA/g. The charge capacities were nearly the same before and after fluorination for three natural graphite samples. The increase in first coulombic efficiencies is due to the quick formation of SEI on surface-fluorinated NG10 μm and NG15 μm with decomposition of much less amounts of PC. Surface fluorination increased surface disorder of NG10 μm and NG15 μm by carbon-carbon bond rupture as shown by R values in Table III. Surface disordering of NG10 μm and NG15 μm by fluorination increases surface defects [40], which would facilitate the smooth formation of SEI. Highly disordered surface can enable the easy accommodation of Li^+ ions solvated by PC with larger molecular size than EC and quick formation of SEI. This surface structure change may also increase the actual electrode area where desolvation of PC and reduction of PC and Li^+ ion, followed by Li insertion, occur. It corresponds to increase in the area of edge plane, leading to decrease in actual current density. Surface fluorine is reduced during electrode preparation in NMP [57]. Residual surface fluorine would also contribute to the formation of SEI by yielding LiF.

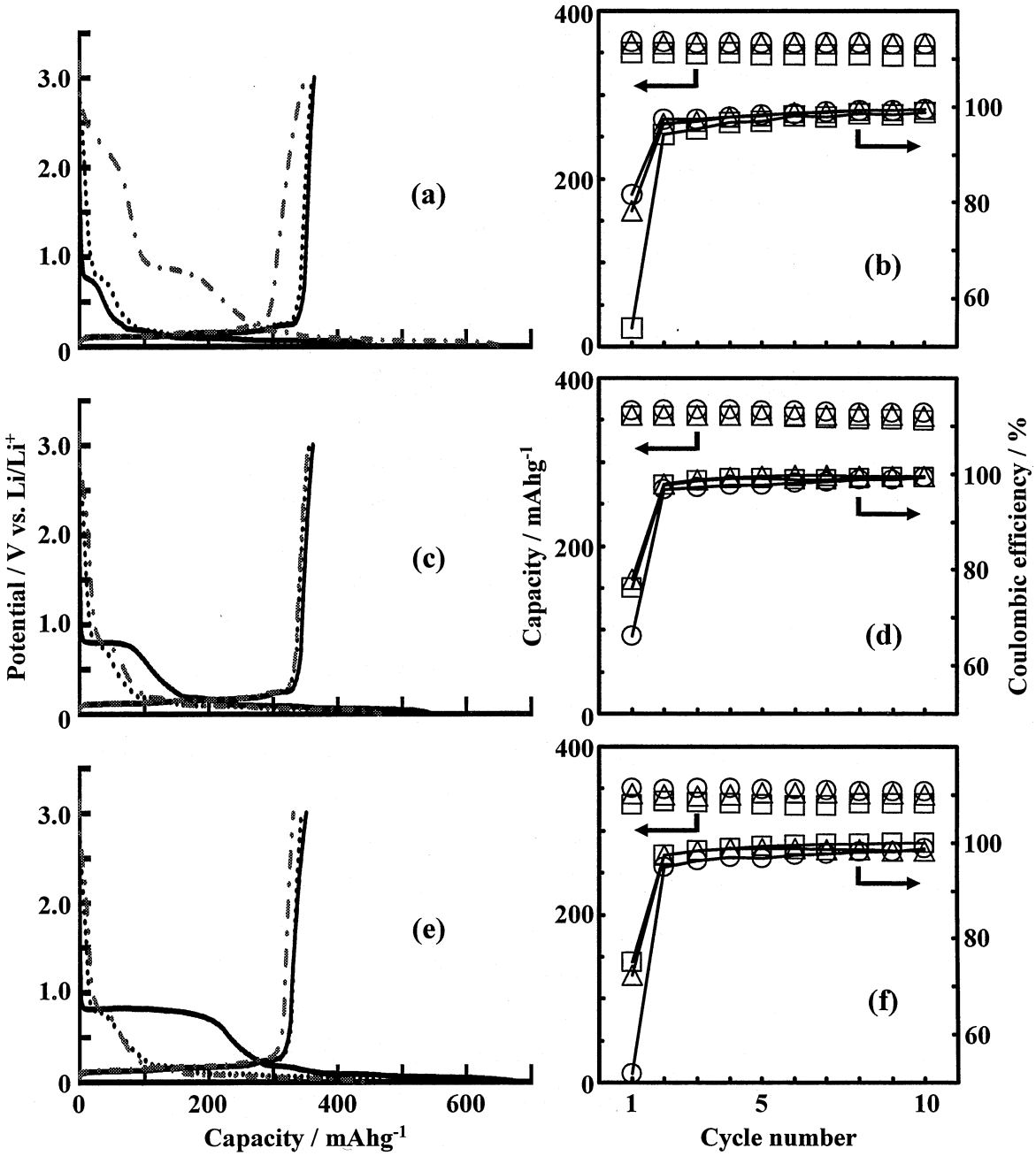

Figure 9. First charge/discharge curves, charge capacities and coulombic efficiencies for original and surface-fluorinated natural graphite samples
in 1.0 mol/dm^3 $LiClO_4$ - EC/DEC/PC at 60 mA/g.
(a), (b) NG5 μm, (c), (d) NG10 μm, (e), (f) NG15 μm.
———: original, ·····: fluorinated at 200 °C, — · — · —: fluorinated at 300 °C.
○: original, △: fluorinated at 200 °C, □: fluorinated at 300 °C.

Table V. First charge/discharge capacities and first coulombic efficiencies for original and surface-fluorinated natural graphite samples in 1.0 mol/dm^3 $LiClO_4$ - EC/DEC/PC.

Graphite sample	Current density (mA/g)	Fluorination temperature (°C)	First discharge capacity ($mAhg^{-1}$)	First charge capacity ($mAhg^{-1}$)	First coulombic efficiency (%)
NG5 μm	60	Original	445	364	81.8
		200 °C	461	361	78.4
		300 °C	650	351	53.9
	150	Original	432	340	78.7
		200 °C	452	358	79.2
		300 °C	605	326	53.9
NG10 μm	60	Original	546	362	66.2
		200 °C	456	356	78.0
		300 °C	466	354	76.1
	150	Original	540	317	58.7
		200 °C	459	323	70.3
		300 °C	455	327	71.9
NG15 μm	60	Original	678	351	51.8
		200 °C	475	343	72.3
		300 °C	441	331	75.1
	150	Original	675	295	43.7
		200 °C	442	292	66.0
		300 °C	464	297	64.0

2-4 Conclusions

Natural graphite powder samples with average particle sizes of 5 μm, 10 μm and 15 μm (NG5 μm, NG10 μm and NG15 μm) were fluorinated by F_2 ($3x10^4$ Pa) at 200 °C and 300 °C for 2 min. in order to prepare natural graphite with high surface disorder, and electrochemical behavior of surface-fluorinated samples were examined in 1.0 mol/dm^3 $LiClO_4$ - EC/DEC/PC (1:1:1 vol.). NG5 μm exhibited good electrode behavior without surface fluorination as obtained in 1.0 mol/dm^3 $LiClO_4$ - EC/DEC (1:1 vol.). Surface fluorine concentrations were in the range of 11.1-15.3 at.% and 17.7-20.5 at.% for natural graphite samples fluorinated at 200 °C and 300 °C, respectively, increasing with increasing fluorination temperature. Increase in surface areas and total pore volumes by surface fluorination were smaller for NG10 μm and NG15 μm than for NG5 μm. However, surface disorder was highly increased in NG10 μm and NG15 μm by fluorination, but less in NG5 μm. Cyclic voltammetry study indicated that

decomposition of PC increased with increasing particle size of natural graphite, i.e. with decreasing the area of edge plane. Surface fluorination highly reduced the electrochemical decomposition of PC on NG10 μm and NG15 μm. Due to decrease in the decomposition of PC, first coulombic efficiencies for NG10 μm and NG15 μm increased by 9.9-13.2 % and 20.3-23.3 %, respectively. The increase in first columbic efficiencies is attributed to the increase in surface disorder providing a large amount of surface defects and probably actual electrode area by surface fluorination. Surface fluorine would also contribute to SEI formation by giving LiF.

References

[1] R. Fong, U. von Sacken and J.R. Dahn, J. Electrochem. Soc., 137, 2009 (1990).

[2] T. Nakajima and H. Groult (eds.), "Fluorinated Materials for Energy Conversion", Elsevier, Oxford, 2005.

[3] T. Takamura, Bul. Chem. Soc. Jpn., 75, 21 (2002).

[4] L.J. Ning, Y.P. Wu, S.B. Fang, E. Rahm and R. Holze, J. Power Sources, 133, 229 (2004).

[5] H. Wang and M. Yoshio, J. Power Sources, 93, 123 (2001).

[6] S. Soon, H. Kim and S.M. Oh, J. Power Sources, 94, 68 (2001).

[7] M. Yoshio, H. Wang, K. Fukuda, Y. Hara and Y. Adachi, J. Electrochem. Soc., 147, 1245 (2000).

[8] H. Wang, M. Yoshio, T. Abe and Z. Ogumi, J. Electrochem. Soc., 149, A499 (2002).

[9] M. Yoshio, H. Wang, K. Fukuda, T. Umeno, N. Dimov and Z. Ogumi, J. Electrochem. Soc., 149, A1598 (2002).

[10] Y.-S. Han and J.-Y. Lee, Electrochim. Acta, 48, 1073 (2003).

[11] Y. Ohzawa, M. Mitani, T. Suzuki, V. Gupta and T. Nakajima, J. Power Sources, 122, 153 (2003).

[12] Y. Ohzawa, Y. Yamanaka, K. Naga and T. Nakajima, J. Power Sources, 146, 125 (2005).

[13] J.-H. Lee, H.-Y Lee, S.-M. Oh, S.-J. Lee, K.-Y. Lee, and S.-M. Lee, J. Power Sources, 166, 250 (2007).

[14] Y. Ohzawa, K. Mizuno, and T. Nakajima, Carbon, 46, 562 (2008).

[15] Y. Ohzawa, and T. Nakajima, Carbon, 46, 565 (2008).

[16] Y. Ohzawa, R, Minamikawa, T. Okada, and T. Nakajima, Carbon, 46, 1628 (2008).

[17] R. Takagi, T. Okubo, K. Sekine and T. Takamura, Electrochemistry, 65, 333 (1997).

[18] T. Takamura, K. Sumiya, J. Suzuki, C. Yamada and K. Sekine, J. Power Sources, 81/82, 368 (1999).

[19] Y. Wu, C. Jiang, C. Wan and E. Tsuchida, Electrochem. Commun., 2, 626 (2000).

[20] S.-S. Kim, Y. Kadoma, H. Ikuta, Y. Uchimoto and M. Wakihara, Electrochem. Solid-State Lett., 4, A109 (2001).

[21] J.K. Lee, D.H. Ryu, J.B. Ju, Y.G. Shul, B.W. Cho and D. Park, J. Power Sources, 107, 90 (2002).

[22] I.R.M. Kottegoda, Y. Kadoma, H. Ikuta, Y. Uchimoto and M. Wakihara, Electrochem. Solid-State Lett., 5, A275 (2002).

[23] I.R.M. Kottegoda, Y. Kadoma, H. Ikuta, Y. Uchimoto and M. Wakihara, J. Electrochem. Soc., 152, A1595 (2005).

[24] E. Peled, C. Menachem, D. Bar-Tow and A. Melman, J. Electrochem. Soc., 143, L4 (1996).

[25] J. Gao, H. P. Zhang, L. J. Fu, T. zhang, Y. P. Wu, T. Takamura H, Q. Wu, and R. Holze, Electrochim. Acta, 52, 5417 (2007).

[26] J. Gao, L. J. Fu, H. P. Zhang, L. C. Yang, and Y. P. Wu, Electrochim. Acta, 53, 2376 (2008).

[27] J. S. Xue and J. R. Dahn, J. Electrochem. Soc., 142, 3668 (1995).

[28] Y. Ein-Eli and V.R. Koch, J. Electrochem. Soc., 144, 2968 (1997).

[29] Y. Wu, C. Jiang, C. Wan and E. Tsuchida, J. Mater. Cem., 11, 1233 (2001).

[30] Y.P. Wu, C. Jiang, C. Wan and R. Holze, Electrochem. Commun., 4, 483 (2002).

[31] Y. Wu, C. Jiang, C. Wan and R. Holze, J. Power Sources, 111, 329 (2002).

[32] Y.P. Wu, C. Jiang, C. Wan and R. Holze, J. Appl. Electrochem., 32, 1011 (2002).

[33] T. Nakajima, M. Koh, R.N. Singh and M. Shimada, Electrochim. Acta, 44, 2879 (1999).

[34] V. Gupta, T. Nakajima, Y. Ohzawa and H. Iwata, J. Fluorine Chem., 112, 233 (2001).

[35] T. Nakajima, V. Gupta, Y. Ohzawa, H. Iwata, A. Tressaud and E. Durand, J. Fluorine Chem., 114, 209 (2002).

[36] T. Nakajima, V. Gupta, Y. Ohzawa, M. Koh, R.N. Singh, A. Tressaud and E. Durand, J. Power Sources, 104, 108 (2002).

[37] H. Groult, T. Nakajima, L. Perrigaud, Y. Ohzawa, H. Yashiro, S. Komaba and N. Kumagai, J. Fluorine Chem., 126, 1111 (2006).

[38] K. Matsumoto, J. Li, Y. Ohzawa, T. Nakajima, Z. Mazej and B. Žemva, J. Fluorine Chem., 127, 1383 (2006).

[39] T. Nakajima, J. Li, K. Naga, K. Yoneshima, T. Nakai and Y. Ohzawa, J. Power Sources, 133, 243 (2004).

[40] J. Li, K. Naga, Y. Ohzawa, T. Nakajima, A.P. Shames and A.I. Panich, J. Fluorine Chem., 126, 265 (2005).

[41] J. Li, Y. Ohzawa, T. Nakajima and H. Iwata, J. Fluorine Chem., 126, 1028 (2005).

[42] K. Naga, T. Nakajima, Y. Ohzawa, B. Žemva, Z. Mazej and H. Groult, J. Electrochem. Soc., 154, A347 (2007).

[43] S. Kuwabata, N. Tsumura, S. Goda, C.R. Martin and H. Yoneyama, J. Electrochem. Soc., 145, 1415 (1998).

[44] M. Gaberscek, M. Bele, J. Drofenik, R. Dominko and S. Pejovnik, Electrochem. Solid State Lett., 3, 171 (2000).

[45] J. Drofenik, M. Gaberscek, R. Dominko, M. Bele and S. Pejovnik, J. Power Sources, 94, 97 (2001).
[46] M. Bele, M. Gaberscek, R. Dominko, J. Drofenik, K. Zupan, P. Komac, K. Kocevar, I. Musevic and S. Pejovnik, Carbon, 40, 1117 (2002).
[47] M. Gaberscek, M. Bele, J. Drofenik, R. Dominko and S. Pejovnik, J. Power Sources, 97/98, 67 (2001).
[48] B. Veeraraghavan, J. Paul, B. Haran and B. Popov, J. Power Sources, 109, 377 (2002).
[49] M. Holzapfel, H. Buqa, F. Krumeich, P. Novak, F.M. Petrat and C. Veit, Electrochem. Solid-State Lett., 8, A516 (2005).
[50] Y.F. Zhou, S. Xie, and C.H. Chen, Electrochim. Acta, 50, 4728 (2003).
[51] S. Komaba, T. Ozeki, and K. Okushi J. Power Sources, 189, 197 (2009).
[52] S. Rozen and C. Gal, Tetrahedron Lett., 25, 449 (1984).
[53] S. Rozen and C. Gal, J. Fluorine Chem., 27, 143 (1985).
[54] M. Koh, H. Yumoto, H. Higashi and T. Nakajima, J. Fluorine Chem., 97, 239 (1999).
[55] T. Nakajima, V. Gupta, Y. Ohzawa, H. Groult, Z. Mazej and B. Žemva, J. Power Sources, 137, 80 (2004).
[56] Y. Sato, T. Kume, R. Hagiwara and Y. Ito, Carbon, 41, 351 (2003).
[57] K. Naga, Y. Ohzawa and T. Nakajima, Electrochim. Acta, 51, 4003 (2006).

Chapter 3

Electrochemical behavior of natural graphite fluorinated by ClF_3 and NF_3 in propylene carbonate-containing solvents

3-1 Introduction

Electrochemical properties of carbonaceous anodes for lithium-ion batteries are highly influenced by not only their crystallinity and bulk structures but also surface structures and surface chemical species. Surface modification is therefore one of useful methods to improve electrode characteristics of carbon materials [1-3]. Some methods have been attempted to modify surface structures and composition of carbonaceous anodes [4-50]. They are carbon coating [4-15], metal or metal oxide coating [16-22], polymer or Si coating [23-30], surface oxidation [31-37] and surface fluorination [38-50]. These methods effectively improve electrode characteristics of carbon materials such as reversible capacities, first coulombic efficiencies (irreversible capacities), cycleability and so on. Since carbon materials have a large variety in crystallinity and structures, a suitable method of surface modification should be chosen depending on a carbon material. Among various carbon materials, natural and synthetic graphites are mainly used as anodes of lithium-ion secondary batteries in combination with ethylene carbonate (EC) - based solvents. EC-based solvents should be used for the quick formation of protective surface film (Solid Electrolyte Interface: SEI) on graphite anode. However, the melting point of EC is high (36 °C), which limits the use of EC-based solvents in a wide range of temperatures. Since propylene carbonate (PC) has a low melting point (-55 °C), it is very convenient if PC can be used for graphitic materials. It is known that PC cannot be used for graphite with high crystallinity because of the slow SEI formation accompanying the vigorous reduction of PC but can be used for low crystalline carbon anodes, which suggests that high crystalline graphite such as natural graphite may be used in PC-containing solvents if surface disordering is achieved by surface modification. Based on this idea, we have performed surface fluorination of natural graphite powder samples to improve their charge/discharge behavior in PC-containing solvent [49-51]. Fluorination using a fluorinating gas is a strong oxidation reaction, being suitable for the surface modification of graphitic materials. Surface fluorination of natural graphite samples with average particle sizes of 5, 10 and 15 μm by F_2 increased small meso-pores and surface disorder, reducing the electrochemical decomposition of PC, i.e. increasing first coulombic efficiencies at current densities of 60 and 150 mA/g [50]. Surface treatment of the same

natural graphite samples with ClF_3 also increased first coulombic efficiencies at a high current density of 150 mA/g [49]. Plasma-fluorination using CF_4 was shown to be a good method to increase first coulombic efficiencies of the natural graphite samples [51]. This positive effect of surface fluorination was found for natural graphite samples having the larger particle sizes of 10 and 15 μm [49-51]. Fluorination mechanisms of carbon materials are different depending on fluorinating gases. Surface fluorination of carbon materials by such fluorinating agents as F_2, ClF_3 and NF_3 easily occurs in the range of 200-500 °C [38-40, 42-47, 49, 50]. F_2 is a highly reactive fluorinating gas even at room temperature because of its low dissociation energy, 154.6 kJ/mol. On the contrary, ClF_3 is a mild fluorinating agent and NF_3 is stable at room temperature while they are strong fluorinating agents at a temperature higher than ca. 200 °C. Handling of ClF_3 and NF_3 gases is therefore easier than that for F_2 gas. It is very convenient for the improvement of electrode characteristics of graphite if surface modification of graphite anodes can be effectively made by ClF_3 and NF_3. Fluorination of carbon materials by F_2 is an electrophilic reaction in which $F^{\delta+}$ attacks a carbon atom with higher electron density ($C^{\delta-}$) and $F^{\delta-}$ is successively bonded to another carbon atom with lower electron density ($C^{\delta+}$) [52-54], yielding fluorinated C-F layers with high surface disorder. On the other hand, fluorination reaction of carbon materials by NF_3 is a radical reaction with chemically active species such as F, NF_2 and so on, having surface etching effect [46, 47]. In the fluorination with ClF_3, radical reaction is also dominant though the dissociation equilibrium ($ClF_3 \leftrightarrow ClF + F_2$) exists at high temperatures above 200 °C. In fact, no surface fluorine was detected when surface fluorination of graphitized petroleum cokes was made by ClF_3 and NF_3 at 200-500 °C probably because the reaction products were gaseous fluorocarbons such as CF_4 [46, 47]. Therefore the surface disorder of graphitized petroleum cokes were nearly the same as that of original samples after surface fluorination by ClF_3 and NF_3 [47]. However, in the case of surface fluorination of natural graphite samples by ClF_3, surface-fluorinated layers were formed for those with larger particle sizes of 10 and 15 μm [49], which may be because natural graphite has the higher crystallinity than graphitized petroleum cokes, i.e. the stronger carbon skeleton against fluorination reaction. This result suggests that surface fluorination by ClF_3 and NF_3 gives surface-disordered natural graphite samples if they are fluorinated under stronger conditions than the previous case made using ClF_3 [49]. In the present study, natural graphite powder samples with average particle sizes of 5, 10 and 15 μm (NG5 μm, NG10 μm and NG15 μm) were fluorinated by ClF_3 and NF_3 gases, and charge/discharge characteristics of surface-fluorinated samples were investigated in PC-containing solvent.

3-2 Experimental

3-2-1 Surface fluorination and analyses of natural graphite samples

Natural graphite powder samples with average particle sizes of 5, 10 and 15 μm (abbreviated to NG5 μm, NG10 μm and NG15 μm; d_{002} = 0.3355, 0.3354 and 0.3355 nm, respectively; purity: >99.95 %), supplied by SEC Carbon Co., Ltd., were fluorinated by ClF_3 and NF_3 ($1x10^5$ Pa) at 200 °C and 300 °C for 5 min. using a nickel fluorination reactor. Fluorination conditions with ClF_3 were stronger in the present study than those in the previous one (pressure of ClF_3: $3x10^4$ Pa, temperatures: 200 °C and 300 °C, fluorination time: 2 min.) [49]. The amount of natural graphite was 150 mg for one batch reaction. Surface composition of surface-fluorinated samples was determined by X-ray photoelectron spectroscopy (XPS) (SHIMADZU, ESCA 1000 with Mg Kα radiation). Binding energies were determined relative to that of graphite, 284.3 eV. Surface areas and meso-pore volumes were measured by BET method using nitrogen gas (SHIMADZU, Tri Star 3000). Surface disorder was evaluated by Raman spectroscopy (JASCO, NRS-1000 with Nd:YVO4 laser, 532 nm).

3-2-2 Electrochemical measurements for natural graphite samples fluorinated by ClF_3 and NF_3

Beaker type three electrode-cell with natural graphite sample as a working electrode and metallic lithium as counter and reference electrodes was used for galvanostatic charge/discharge experiments. Electrolyte solution was 1.0 mol/dm^3 $LiClO_4$ - EC/DEC/PC (1:1:1 vol.) (Kishida Chemicals, Co. Ltd., H_2O: 2-5 ppm). Natural graphite electrode was prepared as follows. Natural graphite powder sample was dispersed in N-methyl-2-pyrrolidone (NMP) containing 12 wt.% poly vinylidene fluoride (PVdF) and slurry was pasted on a copper current collector. The electrode was dried at 120 °C under vacuum attained by a rotary pump for a half day. After drying, the electrode contained 80 wt.% natural graphite sample and 20 wt.% PVdF. Charge/discharge experiments were performed at current densities of 60 and 150 mA/g between 0 and 3.0 V relative to Li/Li^+ reference electrode in a glove box filled with Ar at 25 °C (HOKUTO DENKO, HJ1001 SM8A).

3-3 Results and Discussion

3-3-1 Surface composition and structure of natural graphite samples fluorinated by ClF_3 and NF_3

Typical XPS spectra are shown in Figure 1 (NG15 μm fluorinated by ClF_3 at 300 °C). C1s

spectrum had a strong peak showing non-fluorinated C-C bond at 284.2 eV and a shifted one indicating C-F covalent bond at 288.8 eV. F1s peak corresponding to the C1s peak shifted to 288.8 eV was observed at 687.8 eV. The existence of chlorine was negligible in all samples fluorinated by ClF_3. O1s peak was also observed at 532.3 eV indicating the existence of COH group. Table I shows surface composition of natural graphite samples fluorinated by ClF_3 and NF_3. Surface fluorine concentrations given in Table I were much lower than those observed for the same natural graphite samples fluorinated by F_2 ($3x10^4$ Pa) at 200 °C and 300 °C for 2 min. (11.1-15.3 at.% at 200 °C, 17.7-20.5 at.% at 300 °C) [50]. The difference in the surface fluorine concentrations is attributed to the reaction mechanisms. As mentioned in the Introduction, fluorination of carbon materials by ClF_3 and NF_3 is a radical reaction having surface etching effect while fluorination with F_2 is an electrophilic reaction yielding surface-fluorinated layers. Surface fluorine concentrations in Table I were somewhat lower than those observed when the same samples were fluorinated by ClF_3 under the milder conditions (ClF_3: $3x10^4$ Pa, temperatures: 200 °C and 300 °C, fluorination time: 2 min.) [49]. Surface fluorine concentrations were ~ 0 and 0.9 at.% for NG5 μm, 1.0 and 4.0 at.% for NG10 μm, and 6.6 and 12.7 at.% for NG15 μm at 200 °C and 300 °C, respectively [49]. Since high temperature fluorination reactions of carbon materials by ClF_3 and NF_3 are radical reactions having surface etching effect [46, 47, 49-51], surface etching by chemically active atoms and radicals would be stronger under the reaction conditions in the present study (ClF_3 and NF_3: $1x10^5$ Pa, temperatures: 200 °C and 300 °C, fluorination time: 5 min.). This may be the reason why surface fluorine concentrations were relatively lower than those observed in the previous study [49]. Surface fluorine was mainly detected in the samples fluorinated at 300 °C. In particular, NG10 μm and NG15 μm fluorinated by ClF_3 at 300 °C showed the higher surface fluorine concentrations (11.5 and 12.0 at.%) than others. ClF_3 is partially dissociated into ClF and F_2 at high temperatures ($ClF_3 \leftrightarrow ClF + F_2$). The dissociation rates are 1.75 %, 4.95 % and 11.95 % at 250 °C, 300 °C and 350 °C, respectively [55-57]. The data show that 5 % F_2 coexists in the fluorinating gas mixture at 300 °C. Since fluorination of carbon materials by F_2 is an electrophilic reaction giving surface-fluorinated layers, the relatively high surface fluorine concentrations (11.5 and 12.0 at.%), which were observed for NG10 μm and NG15 μm fluorinated by ClF_3 at 300 °C, might be due to the effect of coexistence of F_2. However, no surface fluorine was found for NG5 μm fluorinated by ClF_3 at 300 °C. Surface area decreases with increasing particle size of natural graphite powder. NG5 μm has the largest surface area among three natural graphite samples as given in Table II. This suggests that surface disordered part was lost as fluorocarbon gases such as CF_4 by the fluorination in the case of NG5 μm. In addition, no chlorine was detected in all samples fluorinated by ClF_3 while traces of chlorine were found in the previous study [49]. This is probably because the fluorination conditions were stronger in the present study than in the previous one. On the other hand, no surface fluorine was detected for all natural graphite samples fluorinated by NF_3 at 200 °C. Only trace amounts of surface fluorine (1.2-1.4 at.%)

were found for the same samples fluorinated at 300 °C. Dissociation of NF_3 into NF_2 and F is initiated at ca. 200 °C. The result is consistent with a fact that fluorination of graphite by NF_3 is a radical reaction. No nitrogen was also found in all samples fluorinated by NF_3. Surface oxygen concentrations were increased by surface fluorination, in particular by the fluorination using NF_3 as shown in Table I. Both ClF_3 and NF_3 have surface etching effect because of the radical reactions. Many dangling bonds or lattice defects are formed in the surface region of natural graphite by carbon-carbon bond breaking. These chemically active sites would easily react with moisture when a fluorinated sample is taken out from the reactor. This may be the reason why surface oxygen concentrations were increased by surface fluorination. However, when NG10 μm and NG15 μm were fluorinated by ClF_3 at 300 °C, surface oxygen concentrations were nearly the same before and after the fluorination. This may be due to the fluorination of chemically active sites by F_2 coexisting in ClF_3.

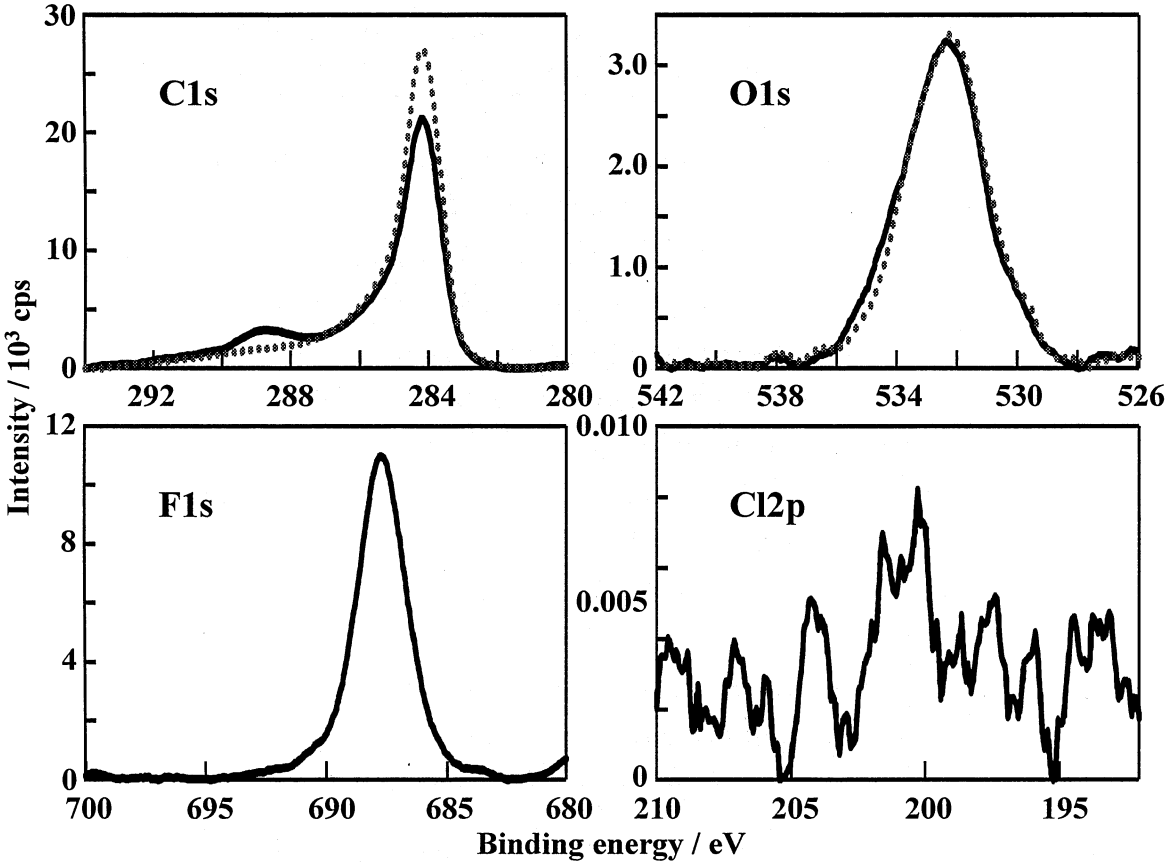

Figure 1. XPS spectra of NG15 μm fluorinated by ClF_3 at 300 °C.
———: Fluorinated by ClF_3 at 300 °C, ·····: Original.

Table I. Surface composition (at.%)
of natural graphite samples fluorinated by ClF_3 and NF_3.

ClF_3	Fluorination temperature									
	Original		200 °C				300 °C			
Sample	C	O	C	O	F	Cl	C	O	F	Cl
NG5 μm	91.9	8.1	91.7	8.3	0.0	0.0	91.6	8.4	0.0	0.0
NG10 μm	92.5	7.5	91.2	8.8	0.0	0.0	91.1	7.4	11.5	0.0
NG15 μm	93.2	6.8	90.0	7.5	2.5	0.0	81.3	6.7	12.0	0.0

NF_3	Fluorination temperature									
	Original		200 °C				300 °C			
Sample	C	O	C	O	F	N	C	O	F	N
NG5 μm	93.5	6.5	90.4	9.6	0.0	0.0	89.0	9.6	14.0	0.0
NG10 μm	91.6	8.4	89.5	10.8	1.2	0.0	88.0	10.8	1.2	0.0
NG15 μm	92.6	7.4	90.9	9.1	0.0	0.0	87.5	11.1	1.4	0.0

Surface areas and total meso-pore volumes were reduced by the fluorination with both ClF_3 and NF_3 as given in Table II. This is due to surface etching effect by the atomic and radical species generated by thermal decomposition of ClF_3 and NF_3. Decrease in the surface areas and meso-pore volumes by the fluorination using ClF_3 and NF_3 is similar to the results previously obtained for petroleum cokes [46, 47]. However, meso-pore size distributions of fluorinated samples are different from the previous data [49] as shown in Figure 2 probably because the fluorination conditions are stronger in the present study. Figure 2 shows that meso-pores with diameter of 2.0 nm were highly increased by surface fluorination while those with diameters of 2.5 and 3.0 nm were reduced. This change in meso-pore size distributions may have been caused by carbon-carbon bond breaking due to fluorination.

Table II. Surface areas and total meso-pore volumes
of natural graphite samples fluorinated by ClF_3 and NF_3.

Sample		ClF_3			NF_3		
		Fluorination temperature					
		Original	200 °C	300 °C	Original	200 °C	300 °C
NG5 μm	Surface area	13.2	11.7	11.2	13.2	13.0	11.1
NG10 μm	(m^2g^{-1})	8.5	7.3	6.5	8.5	8.2	6.6
NG15 μm		7.0	6.3	6.2	7.0	7.0	4.8
NG5 μm	Pore volume	0.062	0.031	0.030	0.062	0.047	0.045
NG10 μm	(cm^3g^{-1})	0.048	0.036	0.037	0.048	0.033	0.032
NG15 μm		0.037	0.030	0.031	0.037	0.026	0.023

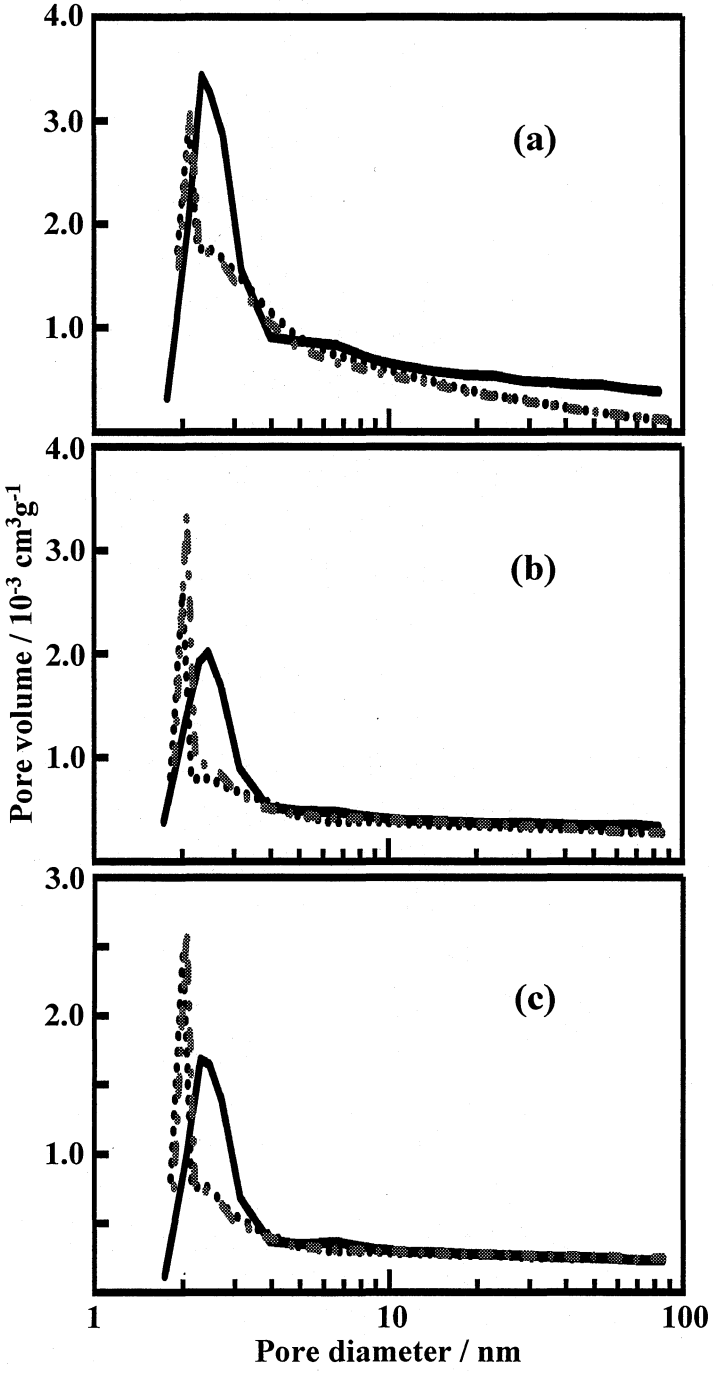

Figure 2. Meso-pore size distribution of original and surface-fluorinated natural graphite samples. (a) NG5 μm, (b) NG10 μm (c) NG15 μm.
———: Original, ·····: Fluorinated by ClF_3 at 200 °C,
— · — · —: Fluorinated by ClF_3 at 300 °C.

Raman spectrum of a carbon material gives two Raman shifts, i.e. G-band and D-band at 1580 cm^{-1} and 1360 cm^{-1}, respectively. Peak intensity ratio of D-band to G-band ($R = I_D/I_G$) shows the degree of surface disorder [58, 59]. Figure 2 shows Raman spectra of NG10 μm and those fluorinated by ClF_3 at 200 °C and 300 °C, and Table III summarizes R values of original and surface-fluorinated samples. Profile of Raman spectra was not largely changed before and after fluorination. However, peak intensity ratios, i.e. R values were increased by the fluorination as given in Table III, which shows that surface disorder of all natural graphite samples was increased by surface fluorination using ClF_3 and NF_3. The increase in R values was slightly larger for the samples fluorinated by ClF_3 at 300 °C than those fluorinated by NF_3 at the same temperature. This may be because the fluorination by ClF_3 yielded surface fluorinated layers due to coexistence of a small amount of F_2 at 300 °C. When the same natural graphite samples were fluorinated by ClF_3 under the milder conditions (ClF_3: $3x10^4$ Pa, temperatures: 200 °C and 300 °C, fluorination time: 2 min.), the increase in R values was also observed for NG10 μm and NG15 μm [49]. In the present study, R values increased for all natural graphite samples probably because of the stronger fluorination conditions. Surface disordering of natural graphite powder was thus achieved by the surface fluorination with ClF_3 and NF_3 at high temperatures. When petroleum cokes graphitized at 2300-2800 °C were fluorinated by ClF_3 and NF_3 at 200-500 °C, no surface fluorine was detected by XPS and no increase in surface disorder was found by Raman spectroscopy due to the surface etching effect [46, 47]. Since natural graphite samples have the higher crystallinity than graphitized petroleum cokes, surface disordering would have been attained by the surface fluorination using ClF_3 and NF_3.

Table III. R values ($=I_D/I_G$) of Raman spectra
of natural graphite samples fluorinated by ClF_3 and NF_3

Sample	Fluorination temperature					
	ClF_3			NF_3		
	Original	200 °C	300 °C	Original	200 °C	300 °C
NG5 μm	0.21	0.24	0.30	0.21	0.23	0.24
NG10 μm	0.22	0.28	0.34	0.22	0.24	0.29
NG15 μm	0.23	0.26	0.39	0.23	0.26	0.32

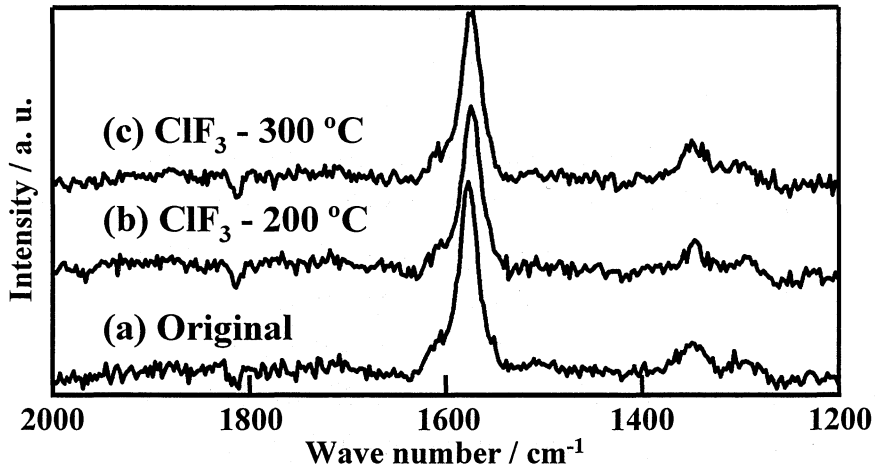

Figure 3. Raman spectra of (a) NG10 μm
and those fluorinated by ClF_3 at (b) 200 °C and (c) 300 °C.

3-3-2 Electrochemical behavior of natural graphite samples fluorinated by ClF_3 and NF_3 in PC-containing solvent

Potential plateau at ca. 0.8 V vs. Li/Li^+ indicating the decomposition of PC was lengthened with increasing average particle size of natural graphite sample, i.e. from NG5 μm to NG15 μm (Figures 4(a), 5(a) and 6(a)). It shows that decomposition of PC increased from NG5 μm to NG15 μm. As shown in Table IV, first coulombic efficiency decreased from NG5 μm to NG15 μm with increasing average particle size of natural graphite powder, i.e. with decreasing surface area. It is expected that decrease in the surface area reduces the electrochemical decomposition of PC, leading to the reduction of irreversible capacity. However, irreversible capacity increased with decreasing surface area, i.e. from NG5 μm to NG15 μm. Decrease in surface area simultaneously increases actual current density because the experiments were performed at constant current densities of 60 and 150 mA/g. The experimental results indicate that electrochemical decomposition of PC is significantly accelerated with increasing actual current density since the formation of SEI is slow on high crystalline graphite.

The effect of surface fluorination was mainly found for NG10 μm and NG15 μm at 60 mA/g and for all natural graphite samples at 150 mA/g, being small for NG5 μm. Surface fluorination reduced the electrochemical decomposition of PC for NG10 μm and NG15 μm as shown in Figures 5 and 6 in which the long potential plateaus at 0.8 V vs. Li/Li^+ were shortened for those fluorinated at both 200 °C and 300 °C though the long potential plateau was only slightly reduced in the case of NG15 μm fluorinated by NF_3 (Figure 6(d) and 6(e)). Decrease in the decomposition of PC led to decrease in the irreversible capacities, i.e. increase in first coulombic efficiencies of surface-fluorinated natural graphite samples. The potential

slopes observed between 0.8 V and 2.5 V vs. Li/Li^+ in Figures 5(c) and 6(c) may be due to reduction of surface fluorine because NG10 μm and NG15 μm fluorinated by ClF_3 at 300 °C had the higher surface fluorine concentrations than other samples. Charge capacities were not changed by surface fluorination for all natural graphite samples as shown in Figures 4-6. First coulombic efficiencies for surface-fluorinated NG5 μm samples with the largest surface area were nearly the same as that of non-fluorinated sample at 60 mA/g, but slightly increased at 150 mA/g (Table IV). There is no difference in first coulombic efficiencies between surface-fluorinated NG5 μm samples fluorinated by ClF_3 and NF_3. For NG10 μm and NG15 μm, effect of surface fluorination was observed at both 60 and 150 mA/g. Increase in first coulombic efficiencies was larger at a higher current density of 150 mA/g.

Some factors on the surface structure and composition such as surface area, meso-pore size distribution, surface disorder and surface fluorine should be considered for the increase in first coulombic efficiencies by fluorination. As shown in Table I, no surface fluorine or small amounts of fluorine were detected because radical reactions are dominant in the case of fluorination of graphite by ClF_3 and NF_3. Such small amounts of surface fluorine do not increase an irreversible capacity [49-51]. BET surface areas were reduced by surface etching effect with ClF_3 and NF_3 as given in Table II. Decrease in the surface areas would contribute to the reduction of the electrochemical decomposition of PC. On the other hand, it simultaneously increases actual current density, leading to increase in the decomposition of PC. The experimental results show that first coulombic efficiencies were increased by surface fluorination, which means that SEI was quickly formed on the surface-fluorinated graphites, suggesting that the more important factors for the effective reduction of irreversible capacity, i.e. increase in first coulombic efficiency are the change in meso-pore size distributions and increase in surface disorder by fluorination. As shown in Figure 2, surface meso-pores with diameter of 2.0 nm were increased while those with 2.5 and 3.0 nm were reduced by fluorination. The diameter of Li^+ ion solvated by four PC molecules is calculated to be 1.44 nm. The solvated Li^+ ions and electrochemically decomposed products would be well kept in surface meso-pores with diameter of 2.0 nm and the larger surface area of graphite would be covered by the decomposed products as shown in Figure 7(b). However, solvated Li^+ ions cannot be well accommodated in meso-pores with the larger diameters of 2.5 and 3.0 nm and coverage of graphite surface by the decomposed products would be less (Figure 7(a)). The fluorination also increased surface disorder of natural graphite samples (Figure 3 and Table III), which would contribute to the quick formation of SEI by keeping the decomposed products on the natural graphite surfaces as shown in Figure 7(b)-(II).

In addition, first coulombic efficiencies for NG10 μm and NG15 μm, obtained at 150 mA/g, had a large difference depending on the fluorinating agents, ClF_3 and NF_3. First coulombic efficiencies of NG10 μm and NG15 μm fluorinated by ClF_3 were larger than those of the same graphite samples fluorinated by NF_3. The difference in first coulombic efficiencies due to fluorinating agents was particularly large for NG15 μm. As mentioned in the previous

section, ClF_3 is dissociated into ClF and F_2 at high temperatures. The dissociation rates of ClF_3 are 1.75 and 4.95 % at 250 °C and 300 °C, respectively [55-57]. Because fluorination of graphite by F_2 is an electrophilic reaction yielding fluorinated graphite with high disorder and small meso-pores [50], coexistence of F_2 in ClF_3 would contribute to the formation of graphite having such surface structure. In fact, natural graphites fluorinated by ClF_3 had the larger *R* values than those fluorinated by NF_3 as given in Table III. On the other hand, NG5 μm samples fluorinated by ClF_3 and NF_3 gave the better results than NG5 μm samples fluorinated by F_2 [50]. First coulombic efficiencies for NG5 μm samples fluorinated by ClF_3 and NF_3 were nearly the same as that of original NG5 μm at 60 mA/g and slightly larger at 150 mA/g as shown in Table IV. NG5 μm having the largest surface area was highly fluorinated by F_2, particularly at 300 °C [50]. Such a large amount of surface fluorine increased irreversible capacity, i.e. decreased first coulombic efficiency by the formation of LiF.

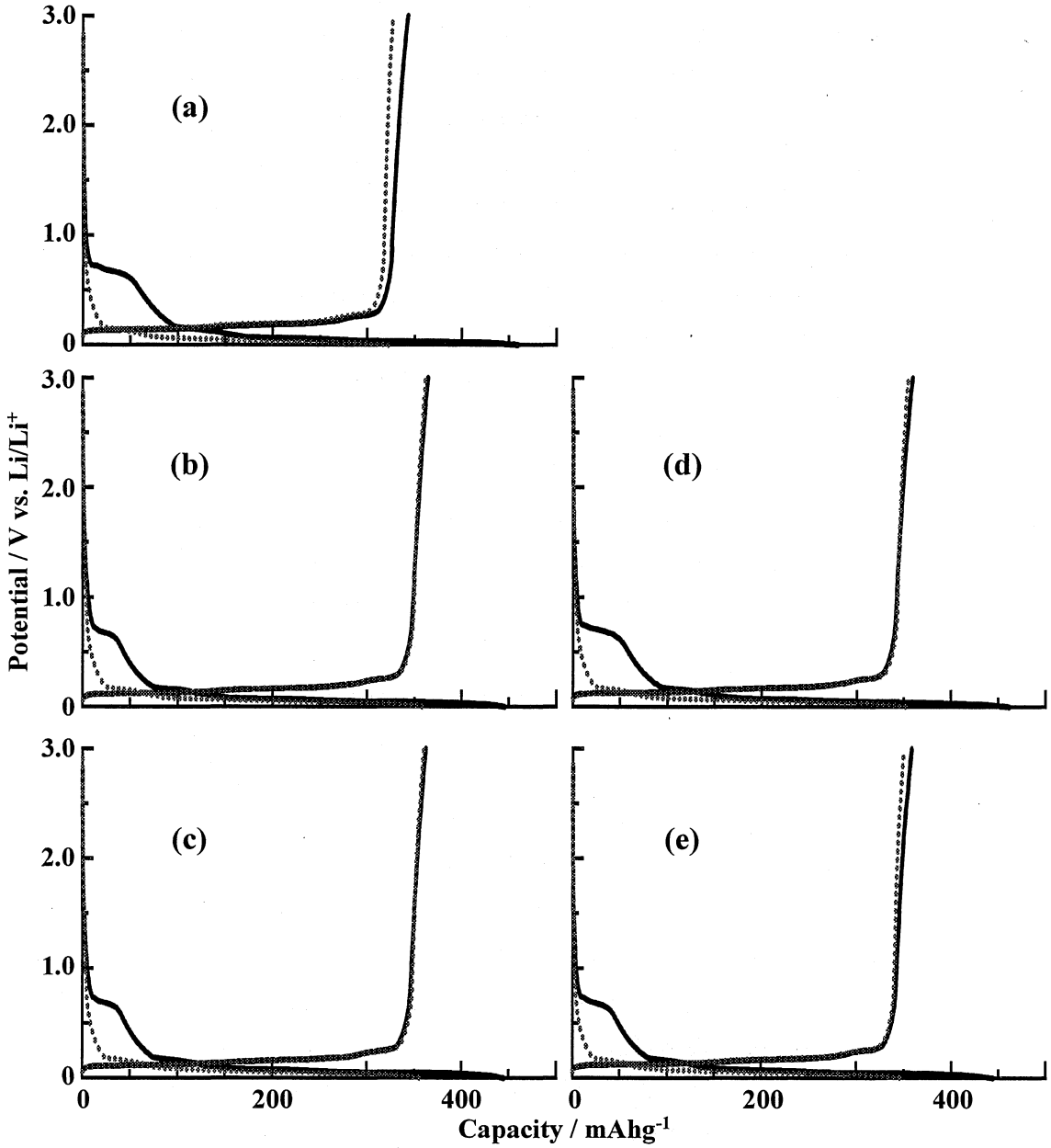

Figure 4. Charge/discharge curves for NG5 μm and those fluorinated by ClF_3 and NF_3 at 150 mA/g in 1.0 mol/dm^3 $LiClO_4$ - EC/DEC/PC (1:1:1 vol.). (a) NG5 μm, (b) NG5 μm fluorinated by ClF_3 at 200 °C, (c) NG5 μm fluorinated by ClF_3 at 300 °C, (d) NG5 μm fluorinated by NF_3 at 200 °C, (e) NG5 μm fluorinated by NF_3 at 300 °C. ———: 1st cycle, ·····: 10th cycle

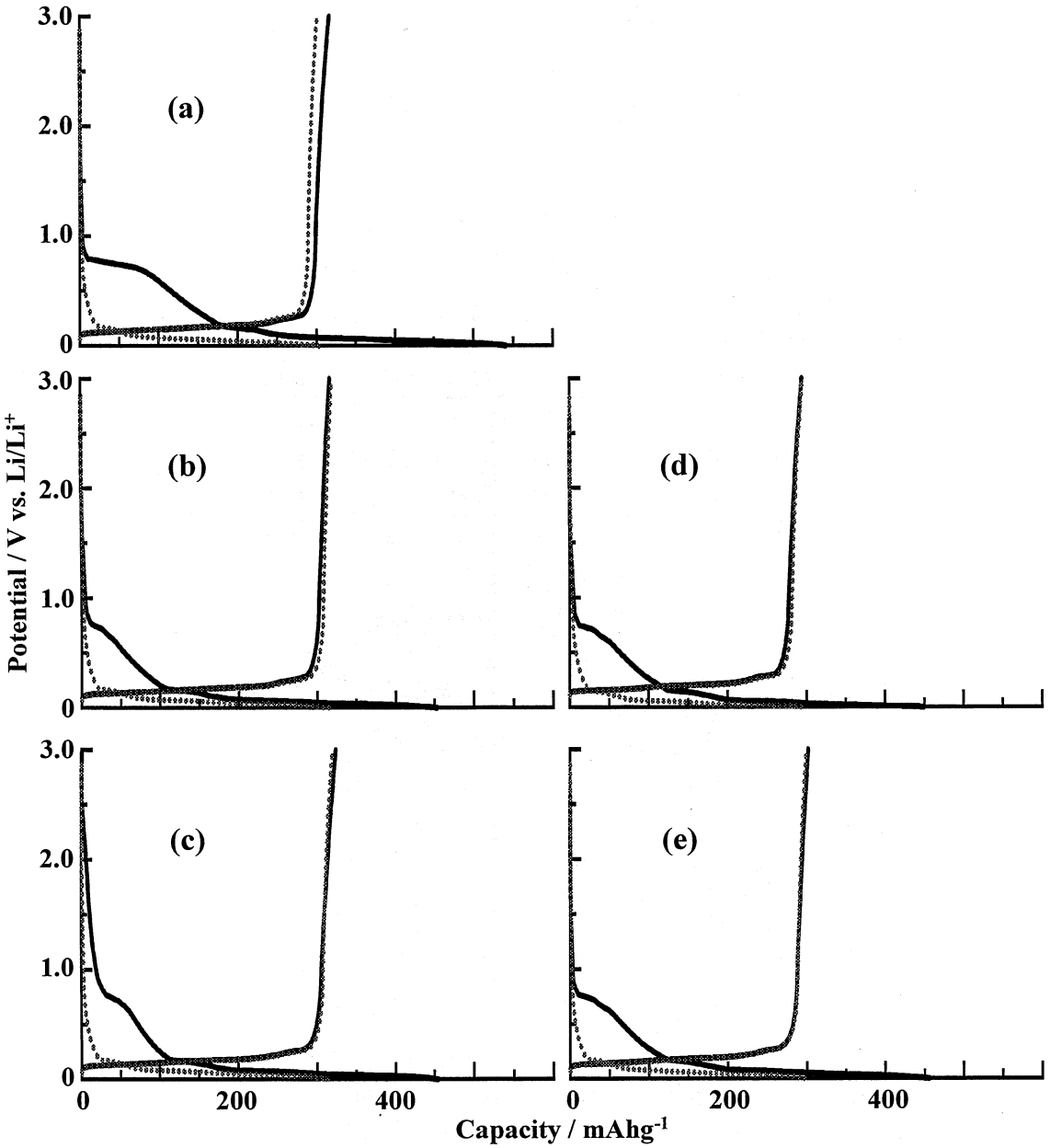

Figure 5. Charge/discharge curves for NG10 μm and those fluorinated by ClF_3 and NF_3 at 150 mA/g in 1.0 mol/dm^3 $LiClO_4$ - EC/DEC/PC (1:1:1 vol.). (a) NG10 μm, (b) NG10 μm fluorinated by ClF_3 at 200 °C, (c) NG10 μm fluorinated by ClF_3 at 300 °C, (d) NG10 μm fluorinated by NF_3 at 200 °C, (e) NG10 μm fluorinated by NF_3 at 300 °C. ———: 1st cycle, ·····: 10th cycle

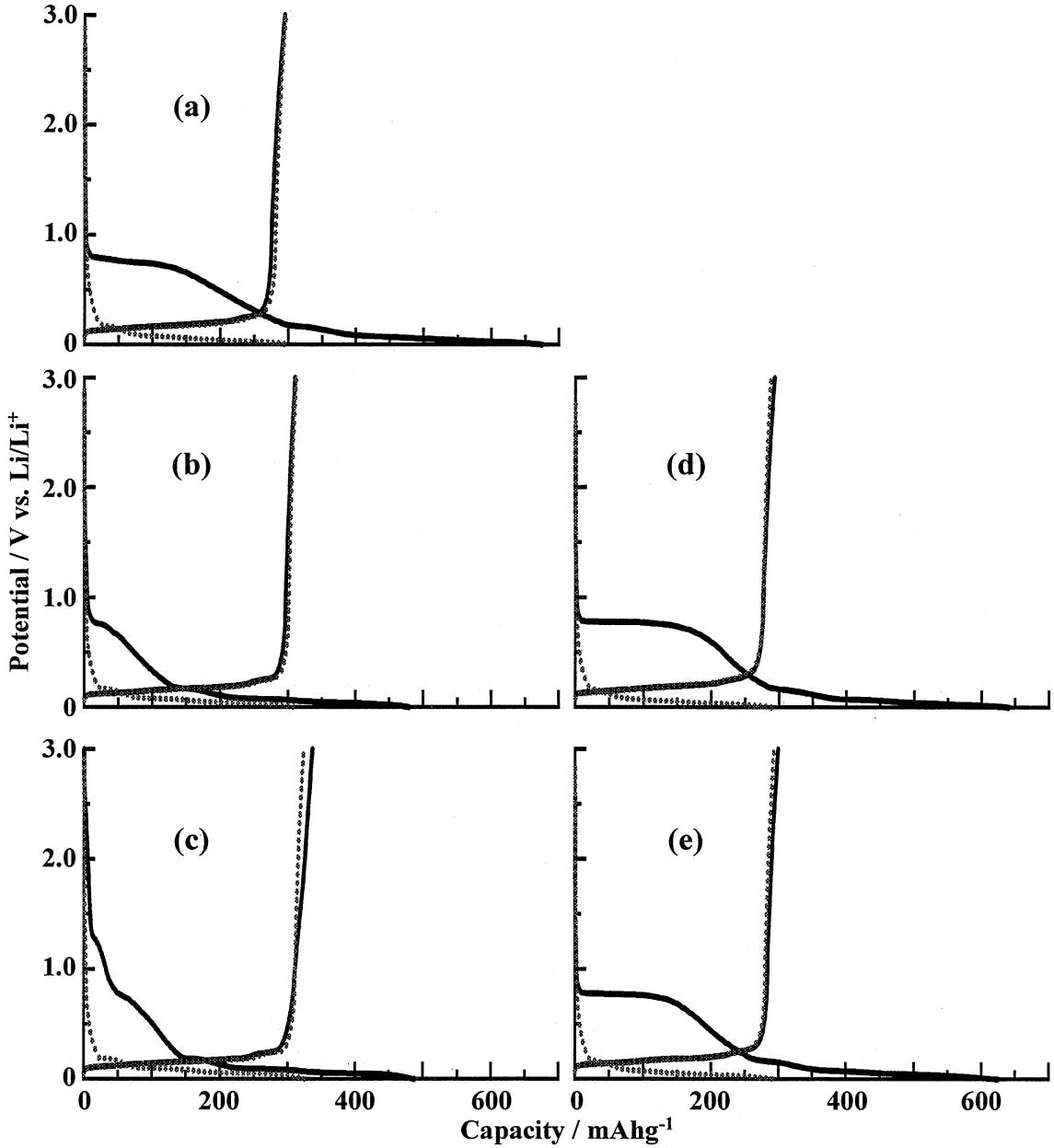

Figure 6. Charge/discharge curves for NG15 μm and those fluorinated by ClF_3 and NF_3 at 150 mA/g in 1.0 mol/dm^3 $LiClO_4$ - EC/DEC/PC (1:1:1 vol.). (a) NG15 μm, (b) NG15 μm fluorinated by ClF_3 at 200 °C, (c) NG15 μm fluorinated by ClF_3 at 300 °C, (d) NG15 μm fluorinated by NF_3 at 200 °C, (e) NG15 μm fluorinated by NF_3 at 300 °C. ———: 1st cycle, ·····: 10th cycle

Table IV. Coulombic efficiencies of natural graphite samples fluorinated by ClF_3 and NF_3 at 1st, 5th, and 10th cycle in 1.0 mol/dm^3 $LiClO_4$ - EC/DEC/PC (1:1:1 vol.).

ClF_3	Fluorination	NG5 μm			NG10 μm			NG15 μm		
Current density	temperature	1st	5th	10th	1st	5th	10th	1st	5th	10th
60 mA/g	Original	79.8	99.2	99.1	66.2	97.7	99.2	51.8	96.8	98.7
	200 °C	80.5	99.7	98.8	64.4	98.8	99.1	56.4	98.5	98.8
	300 °C	79.8	99.7	98.9	75.5	99.4	99.1	72.3	99.0	97.7
150 mA/g	Original	76.2	99.9	100.0	58.7	98.4	99.5	44.5	98.1	99.6
	200 °C	81.7	100.0	100.0	69.7	99.2	100.0	64.8	99.3	100.0
	300 °C	81.4	100.0	100.0	71.1	99.6	100.0	68.9	98.4	99.4

NF_3	Fluorination	NG5 μm			NG10 μm			NG15 μm		
Current density	temperature	1st	5th	10th	1st	5th	10th	1st	5th	10th
60 mA/g	Original	79.8	99.2	99.1	66.2	97.7	99.2	51.8	96.8	98.7
	200 °C	81.5	98.4	99.4	71.4	98.2	99.2	54.8	98.3	98.5
	300 °C	82.4	98.6	99.5	72.2	98.2	99.2	54.9	98.4	98.2
150 mA/g	Original	76.2	99.9	100.0	58.7	98.4	99.5	44.5	98.1	99.6
	200 °C	81.4	99.7	100.0	65.5	98.4	99.3	47.6	97.4	98.9
	300 °C	80.6	99.4	—	66.3	98.5	99.2	50.9	97.4	98.9

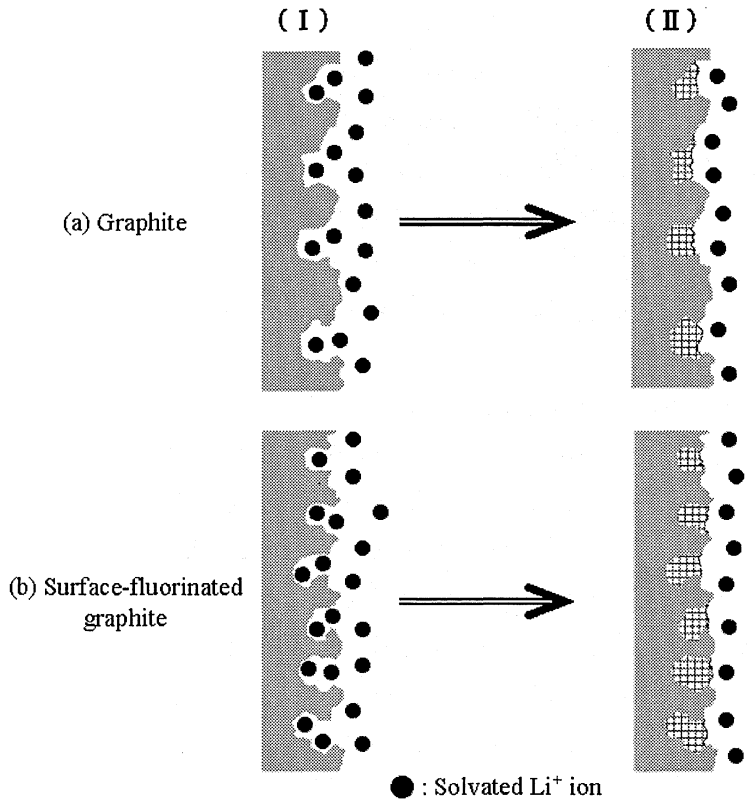

Figure 7. Schematic illustrations of SEI formation on graphite (a) and surface-fluorinated graphite (b).
(I) Just before solvent reduction, (II) initial stage of SEI formation.

3-4 Conclusion

Surface modification of natural graphite samples with average particle sizes of 5, 10 and 15 μm (NG5 μm, NG10 μm and NG15 μm, purity: > 99.95 %) was performed by ClF_3 and NF_3, and electrochemical properties of surface-fluorinated samples were investigated in propylene carbonate-containing solvent (1.0 mol/dm^3 $LiClO_4$ - EC/DEC/PC (1:1:1 vol.)). Surface fluorine concentrations were negligible or very small in most of fluorinated samples, however, being 11.5 and 12.0 at.% for NG10 μm and NG15 μm fluorinated by ClF_3 at 300 °C, respectively. Meso-pores with diameter of 2.0 nm were increased by surface fluorination while those with diameters of 2.5 and 3.0 nm were reduced. *R* values obtained from Raman spectra increased with increasing fluorination temperature and particle size of natural graphite sample, indicating increase in surface disorder by surface fluorination. These surface structure changes would have reduced the electrochemical decomposition of PC at 1st cycle, i.e. increased first coulombic efficiencies, which was more clearly observed at a high current density of 150 mA/g and mainly for NG10 μm and NG15 μm having the larger particle sizes. The increase in first coulombic efficiencies for NG10 μm and NG15 μm fluorinated by ClF_3 reached ca. 10 and 20 %, respectively.

References

[1] T. Takamura, Bul. Chem. Soc. Jpn., 75, 21 (2002).

[2] L.J. Ning, Y.P. Wu, S.B. Fang, E. Rahm and R. Holze, J. Power Sources, 133, 229 (2004).

[3] T. Nakajima and H. Groult (eds.), "Fluorinated Materials for Energy Conversion", Elsevier, Oxford, 2005.

[4] M. Yoshio, H. Wang, K. Fukuda, Y. Hara and Y. Adachi, J. Electrochem. Soc., 147, 1245 (2000).

[5] H. Wang and M. Yoshio, J. Power Sources, 93, 123 (2001).

[6] S. Soon, H. Kim and S.M. Oh, J. Power Sources, 94, 68 (2001).

[7] H. Wang, M. Yoshio, T. Abe and Z. Ogumi, J. Electrochem. Soc., 149, A499 (2002).

[8] M. Yoshio, H. Wang, K. Fukuda, T. Umeno, N. Dimov and Z. Ogumi, J. Electrochem. Soc., 149, A1598 (2002).

[9] Y.-S. Han and J.-Y. Lee, Electrochim. Acta, 48, 1073 (2003).

[10] Y. Ohzawa, Y. Yamanaka, K. Naga and T. Nakajima, J. Power Sources, 146, 125 (2005).

[11] Y. Ohzawa, M. Mitani, T. Suzuki, V. Gupta and T. Nakajima, J. Power Sources, 122, 153 (2003).

[12] J.-H. Lee, H.-Y Lee, S.-M. Oh, S.-J. Lee, K.-Y. Lee, and S.-M. Lee, J. Power Sources, 166, 250 (2007).

[13] Y. Ohzawa, K. Mizuno, and T. Nakajima, Carbon, 46, 562 (2008).

[14]Y. Ohzawa, and T. Nakajima, Carbon, 46, 565 (2008).
[15]Y. Ohzawa, R, Minamikawa, T. Okada, and T. Nakajima, Carbon, 46, 1628 (2008).
[16]R. Takagi, T. Okubo, K. Sekine and T. Takamura, Electrochemistry, 65, 333 (1997).
[17]T. Takamura, K. Sumiya, J. Suzuki, C. Yamada and K. Sekine, J. Power Sources, 81/82, 368 (1999).
[18]Y. Wu, C. Jiang, C. Wan and E. Tsuchida, Electrochem. Commun., 2, 626 (2000).
[19]S.-S. Kim, Y. Kadoma, H. Ikuta, Y. Uchimoto and M. Wakihara, Electrochem. Solid-State Lett., 4, A109 (2001).
[20]J.K. Lee, D.H. Ryu, J.B. Ju, Y.G. Shul, B.W. Cho and D. Park, J. Power Sources, 107, 90 (2002).
[21]I.R.M. Kottegoda, Y. Kadoma, H. Ikuta, Y. Uchimoto and M. Wakihara, Electrochem. Solid-State Lett., 5, A275 (2002).
[22]I.R.M. Kottegoda, Y. Kadoma, H. Ikuta, Y. Uchimoto and M. Wakihara, J. Electrochem. Soc., 152, A1595 (2005).
[23]S. Kuwabata, N. Tsumura, S. Goda, C.R. Martin and H. Yoneyama, J. Electrochem. Soc., 145, 1415 (1998).
[24]M. Gaberscek, M. Bele, J. Drofenik, R. Dominko and S. Pejovnik, Electrochem. Solid State Lett., 3, 171 (2000).
[25]J. Drofenik, M. Gaberscek, R. Dominko, M. Bele and S. Pejovnik, J. Power Sources, 94, 97 (2001).
[26]M. Bele, M. Gaberscek, R. Dominko, J. Drofenik, K. Zupan, P. Komac, K. Kocevar, I. Musevic and S. Pejovnik, Carbon, 40, 1117 (2002).
[27]M. Gaberscek, M. Bele, J. Drofenik, R. Dominko and S. Pejovnik, J. Power Sources, 97/98, 67 (2001).
[28]B. Veeraraghavan, J. Paul, B. Haran and B. Popov, J. Power Sources, 109, 377 (2002).
[29]M. Holzapfel, H. Buqa, F. Krumeich, P. Novak, F.M. Petrat and C. Veit, Electrochem. Solid-State Lett., 8, A516 (2005).
[30]Y.F. Zhou, S. Xie, and C.H. Chen, Electrochim. Acta, 50, 4728 (2003).
[31]E. Peled, C. Menachem, D. Bar-Tow and A. Melman, J. Electrochem. Soc., 143, L4 (1996).
[32]J. S. Xue and J. R. Dahn, J. Electrochem. Soc., 142, 3668 (1995).
[33]Y. Ein-Eli and V.R. Koch, J. Electrochem. Soc., 144, 2968 (1997).
[34]Y. Wu, C. Jiang, C. Wan and E. Tsuchida, J. Mater. Chem., 11, 1233 (2001).
[35]Y.P. Wu, C. Jiang, C. Wan and R. Holze, Electrochem. Commun., 4, 483 (2002).
[36]Y. Wu, C. Jiang, C. Wan and R. Holze, J. Power Sources, 111, 329 (2002).
[37]Y.P. Wu, C. Jiang, C. Wan and R. Holze, J. Appl. Electrochem., 32, 1011 (2002).
[38]T. Nakajima, M. Koh, R.N. Singh and M. Shimada, Electrochim. Acta, 44, 2879 (1999).
[39]V. Gupta, T. Nakajima, Y. Ohzawa and H. Iwata, J. Fluorine Chem., 112, 233 (2001).
[40]T. Nakajima, V. Gupta, Y. Ohzawa, H. Iwata, A. Tressaud and E. Durand, J. Fluorine

Chem., 114, 209 (2002).
[41]T. Nakajima, V. Gupta, Y. Ohzawa, M. Koh, R.N. Singh, A. Tressaud and E. Durand, J. Power Sources, 104, 108 (2002).
[42]H. Groult, T. Nakajima, L. Perrigaud, Y. Ohzawa, H. Yashiro, S. Komaba and N. Kumagai, J. Fluorine Chem., 126, 1111 (2006).
[43]T. Nakajima, J. Li, K. Naga, K. Yoneshima, T. Nakai and Y. Ohzawa, J. Power Sources, 133, 243 (2004).
[44]J. Li, K. Naga, Y. Ohzawa, T. Nakajima, A.P. Shames and A.I. Panich, J. Fluorine Chem., 126, 265 (2005).
[45]J. Li, Y. Ohzawa, T. Nakajima and H. Iwata, J. Fluorine Chem., 126, 1028 (2005).
[46]K. Naga, T. Nakajima, Y. Ohzawa, B. Žemva, Z. Mazej and H. Groult, J. Electrochem. Soc., 154, A347 (2007).
[47]K. Naga, T. Nakajima, S. Aimura, Y. Ohzawa, B. Žemva, Z. Mazej, H. Groult and A. Yoshida, J. Power Sources, 167, 192 (2007).
[48]T. Nakajima, S. Shibata, K. Naga, Y. Ohzawa, A. Tressaud, E. Durand, H. Groult and F. Warmont, J. Power Sources, 168, 265 (2007).
[49]K. Matsumoto, J. Li, Y. Ohzawa, T. Nakajima, Z. Mazej and B. Žemva, J. Fluorine Chem., 127, 1383 (2006).
[50]T. Achiha, T. Nakajima and Y. Ohzawa, J. Electrochem. Soc., 154, A827 (2007).
[51]T. Achiha, S. Shibata, T. Nakajima, Y. Ohzawa, A Tressaud and E. Durand, J. Power Sources, 171, 932 (2007).
[52]S. Rozen and C. Gal, Tetrahedron Lett., 25, 449 (1984).
[53]S. Rozen and C. Gal, J. Fluorine Chem., 27, 143 (1985).
[54]M. Koh, H. Yumoto, H. Higashi and T. Nakajima, J. Fluorine Chem., 97, 239 (1999).
[55]O. Ruff and H. Krug, Z. Anorg. Allg. Chem., 190, 270 (1930).
[56]J. W. Grisard, H. A. Bernhard and G. D. Oliver, J. Am. Chem. Soc., 73, 5725 (1951).
[57]J. W. Mellor (Ed.), A Comprehensive Treatise on Inorganic and Theoretical Chemistry, Supplement II. Part I, Longman, Green and Co. (1956) p.147.
[58]F. Tuinstra and J. L. Koenig, J. Chem. Phys., 53, 1126 (1970).
[59]D. S. Knight and W. B. White, J. Mater. Res., 4, 385 (1989).

Chapter 4

Electrochemical behavior of plasma-fluorinated natural graphite in propylene carbonate-containing solvents

4-1 Introduction

Graphitic materials such as natural and synthetic graphites with high crystallinity are mainly used as anodes of lithium-ion batteries in combination with ethylene carbonate (EC)-based solvents. Graphite has several advantages of low electrode potential, small irreversible capacity (high first coulombic efficiency), good cycleability and constant capacity. Natural graphite shows high reversible capacity (~360 $mAhg^{-1}$) close to the theoretical discharge capacity (372 $mAhg^{-1}$) while synthetic graphite often gives slightly lower capacity than natural graphite because of its lower crystallinity. It is well known that EC-based solvents should be employed for graphite anode with high crystallinity for the quick formation of protective surface film (Solid Electrolyte Interface: SEI) with decomposition of a small amount of EC [1]. EC has, however, a high melting point of 36 °C. Therefore the use of propylene carbonate (PC) with a low melting point of -55 °C is desirable for graphite anode. It is unfortunately difficult to use PC-based solvents for graphite since electrochemical reduction of PC vigorously occurs on graphite. It is also known that PC can be used for low crystalline carbons having higher surface disorder than graphite. It suggests that high crystalline graphite may be used in PC-based solvents if surface disordering is attained by surface modification. Surface modification is one of the effective methods for improving electrode characteristics of carbonaceous anodes. Recently various methods of surface modification were reported [2-4]. They include carbon coating [5-17], metal or metal oxide coating [18-24], surface oxidation [25-31], surface fluorination [32-44] and polymer or Si coating [45-51]. These methods improved such electrode characteristics of carbonaceous anodes as reversible capacities, first coulombic efficiencies (irreversible capacities), cycleability and so on. Among them, surface fluorination is effective for improving the electrochemical behavior of graphitic materials. When low crystalline carbons are fluorinated by fluorinating gases, carbon-carbon bond rupture leading to the formation of gaseous fluorocarbons such as CF_4 easily occurs. However, surface-fluorinated layers with covalent C-F bond are formed when natural or synthetic graphite is fluorinated. Fluorination mechanisms of carbon materials are different depending on fluorinating agents or fluorination techniques. Fluorination of graphite by F_2 is an electrophilic reaction in which $F^{\delta+}$

preferentially attacks carbon atom with higher electron density ($C^{\delta-}$) and $F^{\delta-}$ reacts with $C^{\delta+}$, yielding fluorinated layers with C-F covalent bond [52-54]. Surface fluorination of natural graphites and graphitized petroleum cokes by F_2 gave fluorinated layers with high disorder [32-34, 36-39, 41, 44]. On the other hand, the reactions of ClF_3 and NF_3 with carbon materials are radical reactions by chemically active species such as F, Cl, ClF_2 and NF_2 generated by thermal decomposition of ClF_3 and NF_3 [40, 41, 43]. Plasma-fluorination using CF_4 gas is also a radical reaction by radical species such as CF_3 produced under plasma [34, 35, 42]. Radical reactions have surface etching effect easily producing fluorocarbon gases. In fact, no surface fluorine was detected and no increase in surface disorder was observed when graphitized petroleum cokes were fluorinated by ClF_3 and NF_3 at 200-500 °C [40, 41]. However, fluorinated layers with high disorder were formed in the surface region of high crystalline natural graphite even when fluorinated by ClF_3 at 200-300 °C because natural graphite has a strong carbon skeleton [43]. Plasma-fluorination also gave fluorinated layers with high disorder for both natural graphite and graphitized petroleum cokes probably because the sample temperature was low, i.e. 90 °C [34, 35, 42]. Surface disorder of graphitized petroleum cokes was enhanced by the surface fluorination with F_2 [37-39], and plasma-fluorination using CF_4 [42]. The increase in surface disorder of graphitized petroleum cokes led to decrease in their irreversible capacities, i.e. increase in first coulombic efficiencies in EC-based solvent [37-39]. In the case of high purity natural graphite samples with large surface areas, surface disorder was increased by the fluorination not only with F_2 [44] but also with ClF_3 [43]. Electrochemical reduction of PC was highly reduced on the surface-fluorinated samples, which led to large increase in first coulombic efficiencies in PC-containing solvent [43, 44]. In the present study, natural graphite samples with large surface areas were fluorinated by plasma-treatment using CF_4, and effect of surface fluorination on the charge/discharge behavior was investigated in PC-containing solvent.

4-2 Experimental

4-2-1 Plasma-fluorination and characterization of natural graphite samples

Raw materials were natural graphite powder samples with average particle sizes of 5 μm, 10 μm and 15 μm (abbreviated to NG5 μm, NG10 μm and NG15 μm; d_{002} = 0.3355, 0.3354 and 0.3355 nm; purity: >99.95 %) supplied by SEC Carbon Co. Ltd. Their X-ray diffraction patterns are shown in Fig. 1. Natural graphite sample was placed in the center of the chamber on the electrode connected to rf. Plasma-fluorination was made using CF_4 gas under the following conditions: CF_4 flow rate: 8 cm^3/min., total gas pressure: 5.0 Pa, power: 80 W, plasma frequency: 13.56 MHz, sample temperature: 90 °C and plasma-treatment time: 60 min. Surface-fluorinated natural graphite samples were characterized by elemental analysis of C and F, X-ray diffractometry, X-ray photoelectron spectroscopy (XPS), surface area and

meso-pore size distribution measurements using nitrogen gas, and Raman spectroscopy.

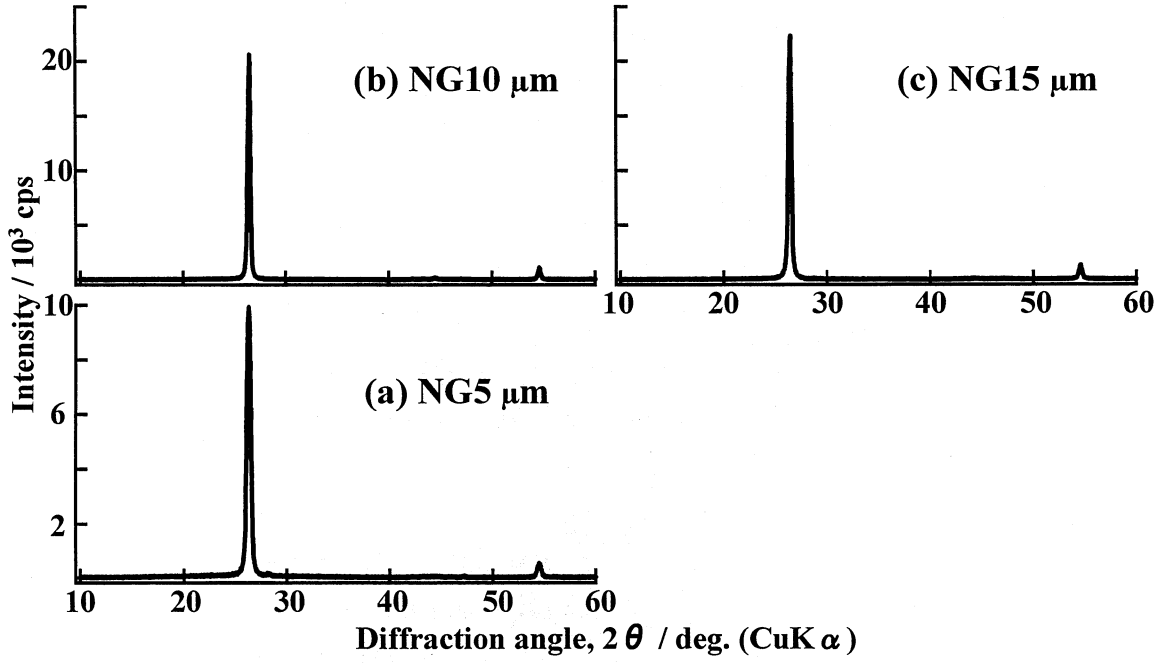

Figure 1. X-ray diffraction patterns of (a) NG5 μm, (b) NG10 μm and (c) NG15 μm.

4-2-2 Electrochemical measurement of plasma-fluorinated natural graphite samples

Three electrode-cell with natural graphite sample as a working electrode and metallic lithium as counter and reference electrodes was used for galvanostatic charge/discharge measurements. Electrolyte solution was 1.0 mol/dm^3 $LiClO_4$ - EC/DEC/PC (1:1:1 vol.). Natural graphite electrode was prepared in the following manner. Natural graphite sample was dispersed in N-methyl-2-pyrrolidone (NMP) containing 12 wt.% poly vinylidene fluoride (PVdF) and slurry was pasted on a copper plate. The electrode was dried at 120 °C under vacuum overnight. After drying, the electrode contained 80 wt.% natural graphite sample and 20 wt.% PVdF. Charge/discharge experiments were performed at a current density of 150 mA/g between 0 and 3.0 V relative to Li/Li^+ in a glove box filled with Ar at 25 °C.

4-3 Results and Discussion

4-3-1 Surface composition and structure of plasma-fluorinated natural graphite samples

X-ray diffraction pattern of natural graphite samples was not changed by plasma-fluorination. The change in *d* values of (002) diffraction lines was negligible. Table I gives composition of plasma-fluorinated samples, obtained by elemental analysis. Fluorine content was very small, i.e. in the range of 0.3-0.6 at.% less than 1.0 at.%. Surface fluorine

concentration obtained by XPS was in the range of 14.8-17.3 at.%. There is no large difference in these data among three natural graphite samples. Surface fluorine concentrations were similar to those obtained when the same natural graphite samples were fluorinated by F_2 ($3x10^4$ Pa) (11.1-15.3 at.% at 200 °C and 17.7-20.5 at.% at 300 °C) [44]. When they were fluorinated by ClF_3 under the same conditions, the lower fluorine concentrations were obtained (0-6.6 at.% at 200 °C and 0.9-12.7 at.% at 300 °C) [43]. In addition, surface fluorine concentration increased with decreasing surface area, i.e. from NG5 μm to NG15 μm. Fluorocarbon gases such as CF_4 is mainly produced in the case of NG5 μm having a large surface area since high temperature fluorination of a carbon material by ClF_3 is a radical reaction with surface etching effect [40, 41, 43]. Plasma-fluorination with CF_4 is also a radical reaction [34, 35, 42]. However, the formation reaction of fluorocarbon gases is probably slow in plasma-fluorination because the sample temperature was low, 90 °C. This may be the reason that the surface fluorine concentrations obtained in the present study are similar to those obtained when the same natural graphite samples were fluorinated by F_2. Surface oxygen was slightly reduced by plasma-fluorination in all samples.

Table I. Composition of plasma-fluorinated natural graphite samples, obtained by elemental analysis.

	Plasma-fluorinated		
Sample	**C (at.%)**	**O (at.%)**	**F (at.%)**
NG5 μm	**99.3**	**0.1**	**0.6**
NG10 μm	**99.5**	**0.1**	**0.4**
NG15 μm	**99.7**	**0.0**	**0.3**

Table II. Surface composition of plasma-fluorinated natural graphite samples, obtained by XPS.

	Original		Plasma-fluorinated		
Sample	**C (at.%)**	**O (at.%)**	**C (at.%)**	**O (at.%)**	**F (at.%)**
NG5 μm	**91.2**	**8.8**	**75.1**	**17.3**	**7.6**
NG10 μm	**91.6**	**8.4**	**78.5**	**14.8**	**6.7**
NG15 μm	**90.5**	**9.5**	**77.6**	**15.1**	**7.3**

Raman spectra of original and plasma-fluorinated natural graphite samples are shown in Fig. 2. High crystalline natural graphite powder usually shows a similar Raman spectrum. G-bands at 1580 cm^{-1} indicating graphitic structure are strong while D-bands at 1360 cm^{-1} indicating disordered structure are weak. G-bands were slightly broadened by plasma-fluorination. Table III gives *R* values calculated as peak intensity ratios of D-band to G-band. *R* values of surface-fluorinated samples were larger than those of non-fluorinated ones, increasing with increasing particle size of natural graphite, i.e. from NG5 μm to NG15

μm. The increase in *R* value of NG5 μm by plasma-fluorination was the same as that of NG5 μm fluorinated by F_2 at 300 °C [44]. In the case of NG10 μm and NG15 μm, the increase in *R* values by plasma-fluorination were also the same as those obtained for the samples fluorinated by F_2 at 200 °C, but smaller than those obtained by the fluorination with F_2 at 300 °C [44].

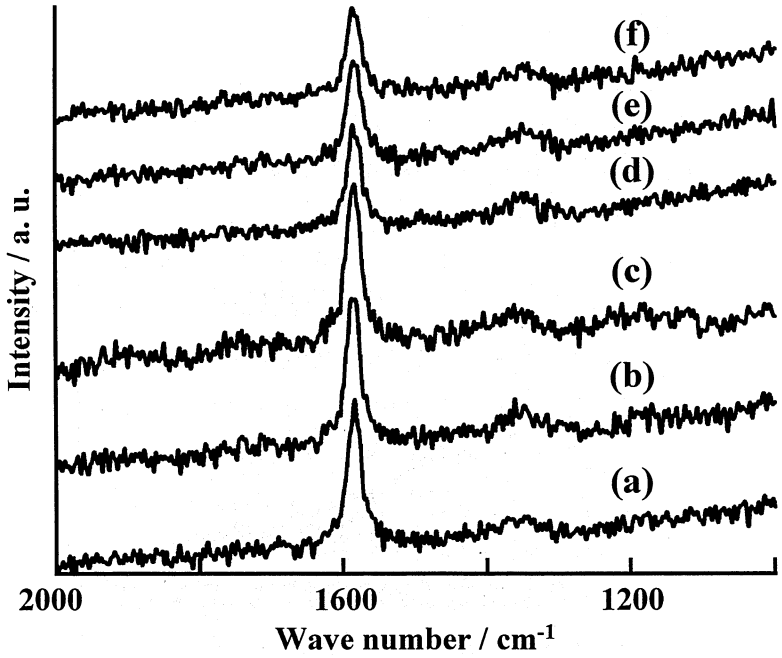

Figure 2. Raman spectra of original and plasma-fluorinated natural graphite samples.
(a) NG5 μm, (b) NG10 μm, (c) NG15 μm, (d) plasma-fluorinated NG5 μm,
(e) plasma-fluorinated NG10 μm, (f) plasma-fluorinated NG15 μm.

Table III. *R* values ($=I_D/I_G$) calculated from peak intensity ratios of Raman spectra.

Sample	Original	Plasma-fluorinated
NG5 μm	0.24	0.27
NG10 μm	0.25	0.33
NG15 μm	0.26	0.39

Table IV gives surface areas of original and plasma-fluorinated samples. In all samples, surface areas were reduced by plasma-fluorination because plasma-fluorination is a radical reaction having surface etching effect. Fig. 3 shows meso-pore size distribution of original and plasma-fluorinated samples. Meso-pores were totally reduced by surface etching effect of plasma-fluorination, however, those with diameters of 1.5-2.0 nm were increased by breaking of carbon-carbon bonds.

Table IV. BET surface areas of plasma-fluorinated natural graphite samples.

Sample	Original (m^2g^{-1})	Plasma-fluorinated (m^2g^{-1})
NG5 μm	13.6	12.3
NG10 μm	9.0	7.2
NG15 μm	7.0	5.9

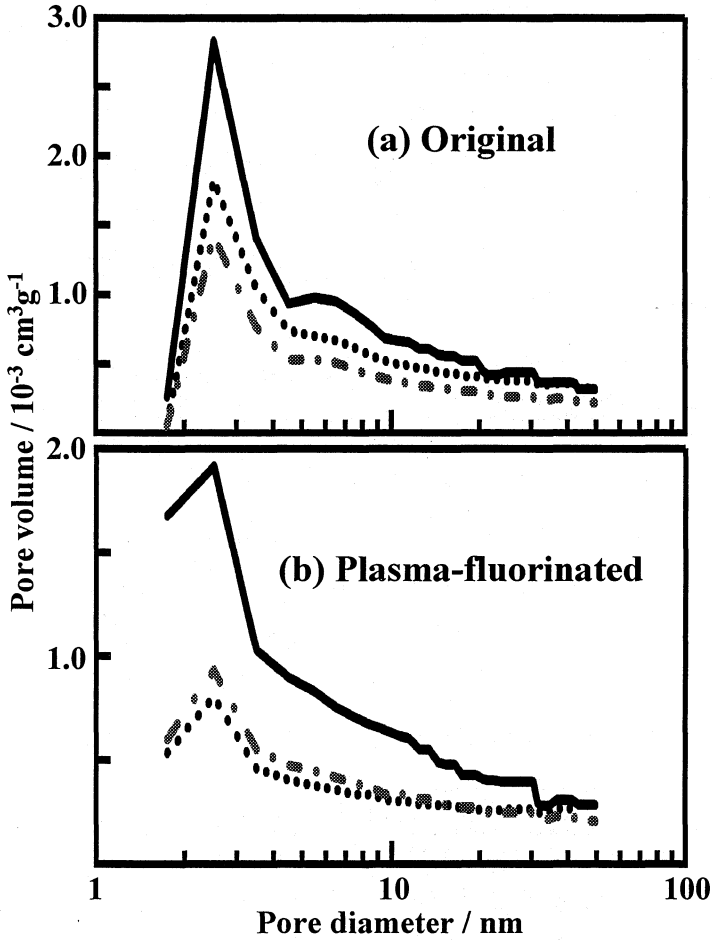

Figure 3. Meso-pore size distribution of original and surface-fluorinated natural graphite samples. (a) Original , (b) Plasma-fluorinated,
———: NG5 μm, ·····: NG10 μm, — · — · —: NG15 μm.

4-3-2 Charge/discharge characteristics of plasma-fluorinated natural graphite samples in 1.0 mol/dm^3 $LiClO_4$ - EC/DEC/PC (1:1:1 vol.)

Degree of surface disorder, i.e. crystallinity of surface region of natural graphite samples would be an important structural factor influencing SEI formation. X-ray diffraction patterns shown in Fig. 1 and d_{002} values of natural graphite samples indicate that crystallinity of these three samples are similar to each other. *R* values obtained from Raman spectra are also nearly the same for all natural graphite samples, which means that surface disorder is almost the same for three natural graphite samples. This result suggests that there is no large difference in the rates of SEI formation by the decomposition of PC per unit surface area of three natural graphite samples if an actual current density is the same. Therefore difference in the surface areas should be taken into account for the electrochemical decomposition of PC. Fig. 4 shows first charge/discharge potential curves, and charge capacities and coulombic efficiencies as a function of cycle number for original and plasma-fluorinated natural graphite samples, obtained at 150 mA/g. In case of non-fluorinated samples, the longer potential plateaus at ca. 0.8 V vs. Li/Li^+ indicating the reduction of PC were observed with increasing particle size, i.e. with decreasing surface area from NG5 μm to NG15 μm. First charge capacity decreased with decreasing surface area of natural graphite while first discharge capacity increased as given in Table V. Therefore first coulombic efficiency of non-fluorinated sample highly diminished with decreasing surface area. As reported in a previous paper [44], the same samples gave high first coulombic efficiencies in EC-based solvent at 60 mA/g (NG5 μm: 81.4 %, NG10 μm: 82.2 %, NG15 μm: 85.4 %). The results show that decomposition of EC is reduced with decreasing surface area in EC-based solvent, indicating that SEI is quickly formed by decomposition of a small amount of EC. However, the decomposition of PC increased with decreasing surface area as shown in Fig. 4 and Table V. The area of edge plane, where desolvation of PC and reduction of PC and Li^+ ion, followed by Li insertion may mainly occur, decreases with decreasing total surface area, i.e. from NG5 μm to NG15 μm. In addition, the ratio of edge plane to total surface area is high in fine graphite powder such as NG5 μm (≈ 50 %), but decreases with decreasing total surface area. Actual current density therefore increases with decreasing area of edge plane, that is, from NG5 μm to NG15 μm. Since SEI formation on high crystalline graphite is more difficult in PC-based solvent than in EC-based one, decomposition of PC would be accelerated with decrease in the area of edge plane, that is, with increase in actual current density. First coulombic efficiencies for NG5 μm were high in both EC- and PC-containing solvents because NG5 μm has the largest area of edge plane among three natural graphite samples, which may promote the smooth formation of SEI on NG5 μm even in PC-containing solvent.

Effect of plasma-fluorination varied depending on the average particle size of natural graphite. NG5 μm with the largest surface area showed almost the same charge/discharge behavior before and after fluorination as shown in Figs. 4(a) and 4(b) and Table V probably

because the increase in *R* value i.e. surface disorder and decrease in surface area by surface fluorination were very small as given in Tables III and IV. Effect of plasma-fluorination was found in NG10 μm and NG15 μm with relatively smaller surface areas. Large potential plateaus at ca. 0.8 V vs. Li/Li^+ indicating decomposition of PC were highly reduced on plasma-fluorinated NG10 μm and NG15 μm as shown in Figs. 4(c) and 4(e). First discharge capacities for NG10 μm and NG15 μm decreased to 455 and 450 $mAhg^{-1}$ similar to that of NG5 μm, 440 $mAhg^{-1}$ by plasma-fluorination (Table V). As a consequence, first coulombic efficiencies for NG10 μm and NG15 μm increased from 58.7 and 43.7 % to 68.5 and 63.0 %, i.e. the increments of first coulombic efficiencies were 9.7 and 19.3 %, respectively, as given in Table V. When the same natural graphite samples were fluorinated by F_2 at 200 °C and 300 °C, first coulombic efficiencies were 70.3 and 71.9 % for NG10 μm and 66.0 and 64.0 % for NG15 μm at 150 mA/g [44]. The increments of first coulombic efficiencies were 11.6-13.2 % and 20.3-22.3 % for NG10 μm and NG15 μm, which are only slightly larger than 9.7 and 19.3 % obtained in the present study. This may be due to the difference in *R* values between plasma-fluorination using CF_4 and fluorination with F_2. *R* values of plasma-fluorinated NG10 μm and NG15 μm were similar to those obtained for the same graphites fluorinated by F_2 at 200 °C, but smaller than those obtained for the samples fluorinated at 300 °C [44]. Plasma-fluorination reduced surface areas as given in Table IV while fluorination of the same natural graphites by F_2 increased surface areas [44]. Decrease in the surface areas may increase actual current density leading to increase in electrochemical decomposition of PC. However, first discharge capacities for plasma-fluorinated samples given in Table V were nearly the same as those obtained for the same graphites fluorinated by F_2 [44]. This suggests that increase in small meso-pores with diameter of 1.5-2.0 nm by plasma-fluorination brought about the increase in actual area of edge plane, i.e. electrode area, leading to reduction of electrochemical decomposition of PC. Coulombic efficiencies soon approached 100 % after 1st cycle for all samples and cycleability was good except plasma-fluorinated NG15 μm. Decrease in charge capacity of plasma-fluorinated NG15 μm with cycling may arise from slight reduction of electrical contact with copper current collector due to expansion and shrinking of graphite by intercalation and deintercalation of Li^+ ions.

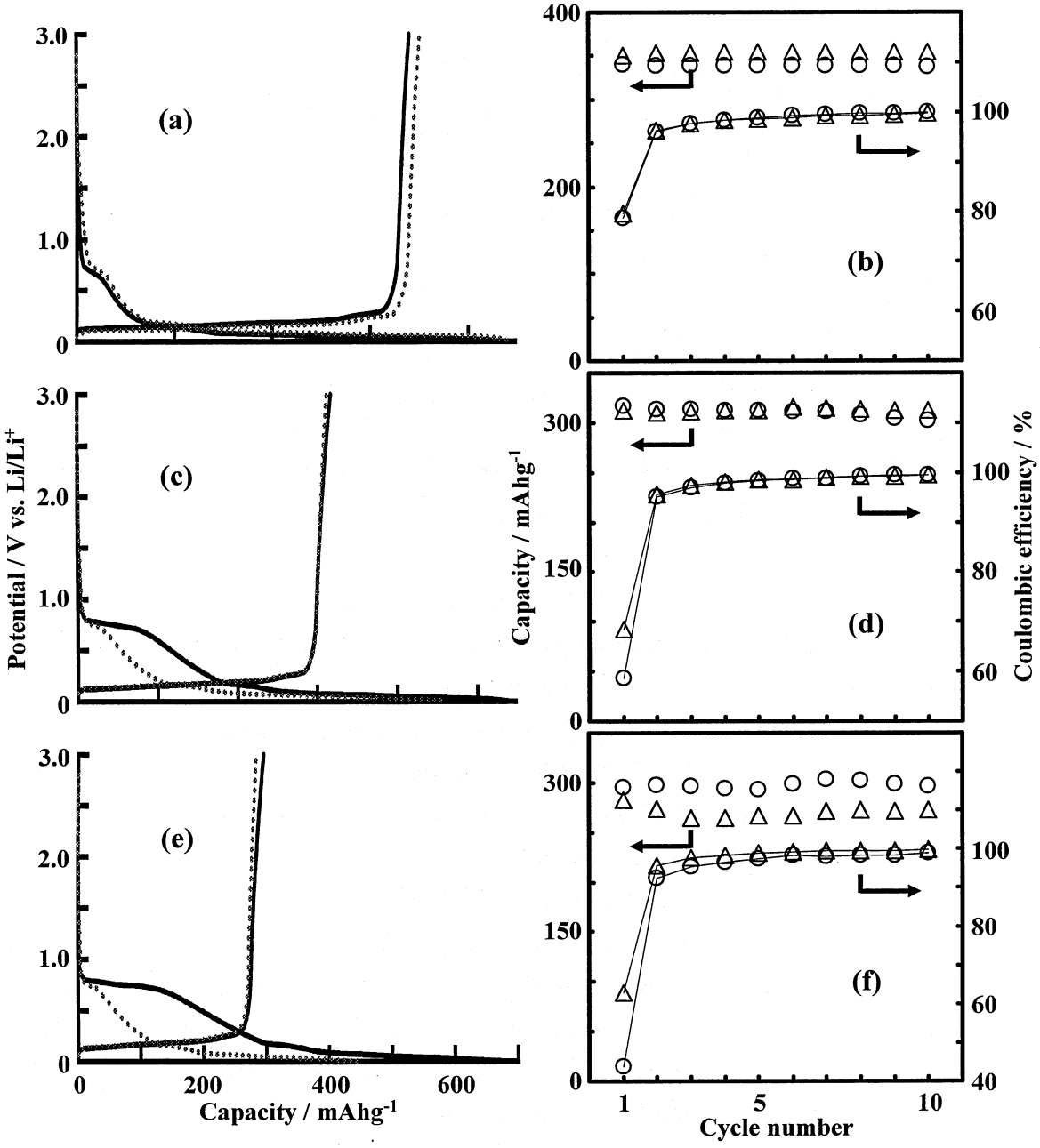

Figure 4. First charge/discharge curves, charge capacities and coulombic efficiencies for original and surface-fluorinated natural graphite samples,
obtained at 150 mA/g in 1.0 mol/dm^3 $LiClO_4$ - EC/DEC/PC (1:1:1 vol.).
(a), (b) NG5 μm; (c), (d) NG10 μm; (e), (f) NG15 μm.
———: original, ·····: plasma-fluorinated natural graphite.
○: original, △: plasma-fluorinated natural graphite.

Table V. First charge/discharge capacities and first coulombic efficiencies for original and plasma-fluorinated natural graphite samples at 150 mA/g.

Sample	First discharge capacity / $mAhg^{-1}$	First charge capacity / $mAhg^{-1}$	First coulombic efficiency / %
Original			
NG5 μm	**432**	**340**	**78.7**
NG10 μm	**540**	**317**	**58.7**
NG15 μm	**675**	**295**	**43.7**
Fluorinated			
NG5 μm	**440**	**351**	**79.6**
NG10 μm	**455**	**312**	**68.5**
NG15 μm	**450**	**283**	**63.0**

4-4 Conclusions

Plasma-fluorination of natural graphite powder samples with average particle sizes of 5, 10 and 15 μm (NG5 μm, NG10 μm and NG15 μm) was performed to prepare natural graphites with high surface disorder, and charge/discharge properties of plasma-fluorinated samples were investigated in 1.0 mol/dm^3 $LiClO_4$ - EC/DEC/PC (1:1:1 vol.). Electrochemical decomposition of PC increased with increasing particle size, i.e. with decreasing surface area of edge plane of non-fluorinated sample probably due to increase in actual current density. Plasma-fluorination increased surface disorder of three natural graphite samples though surface areas were reduced by radical reaction having surface etching effect. Fluorine contents in fluorinated graphite samples were small, 0.3-0.6 at.%, and surface fluorine concentrations were in the range of 14.8-17.3 at.%. Plasma-fluorination highly reduced the electrochemical decomposition of PC on NG10 μm and NG15 μm. As a consequence, first coulombic efficiencies for plasma-fluorinated NG10 μm and NG15 μm increased by 9.7 and 19.3 % at 150 mA/g, respectively.

References

[1] R. Fong, U. von Sacken, and J.R. Dahn, J. Electrochem. Soc. 137, 2009 (1990).

[2] T. Nakajima, and H. Groult (eds.), "Fluorinated Materials for Energy Conversion", Elsevier, Oxford, 2005.

[3] T. Takamura, Bul. Chem. Soc. Jpn. 75, 21 (2002).

[4] L.J. Ning, Y.P. Wu, S.B. Fang, E. Rahm, and R. Holze, J. Power Sources 133, 229 (2004).

[5] H. Wang, and M. Yoshio, J. Power Sources 93, 123 (2001).
[6] S. Soon, H. Kim, and S.M. Oh, J. Power Sources 94, 68 (2001).
[7] M. Yoshio, H. Wang, K. Fukuda, Y. Hara, and Y. Adachi, J. Electrochem. Soc. 147, 1245 (2000).
[8] H. Wang, M. Yoshio, T. Abe, and Z. Ogumi, J. Electrochem. Soc. 149, A499 (2002).
[9] M. Yoshio, H. Wang, K. Fukuda, T. Umeno, N. Dimov, and Z. Ogumi, J. Electrochem. Soc. 149, A1598 (2002).
[10] Y.-S. Han, and J.-Y. Lee, Electrochim. Acta 48, 1073 (2003).
[11] Y. Ohzawa, M. Mitani, T. Suzuki, V. Gupta, and T. Nakajima, J. Power Sources 122, 153 (2003).
[12] Y. Ohzawa, M. Mitani, J. Li, and T. Nakajima, Mater. Sci. & Eng. B, 113, 91 (2004).
[13] Y. Ohzawa, Y. Yamanaka, K. Naga, and T. Nakajima, J. Power Sources 146, 125 (2005).
[14] J.-H. Lee, H.-Y Lee, S.-M. Oh, S.-J. Lee, K.-Y. Lee, and S.-M. Lee, J. Power Sources, 166 (2007).
[15] Y. Ohzawa, K. Mizuno, and T. Nakajima, Carbon, 46, 562 (2008).
[16] Y. Ohzawa, and T. Nakajima, Carbon, 46, 565 (2008).
[17] Y. Ohzawa, R, Minamikawa, T. Okada, and T. Nakajima, Carbon, 46, 1628 (2008).
[18] R. Takagi, T. Okubo, K. Sekine, and T. Takamura, Electrochemistry 65, 333 (1997).
[19] T. Takamura, K. Sumiya, J. Suzuki, C. Yamada, and K. Sekine, J. Power Sources 81/82, 368 (1999).
[20] Y. Wu, C. Jiang, C. Wan, and E. Tsuchida, Electrochem. Commun. 2, 626 (2000).
[21] S.-S. Kim, Y. Kadoma, H. Ikuta, Y. Uchimoto, and M. Wakihara, Electrochem. Solid-State Lett. 4, A109 (2001).
[22] J.K. Lee, D.H. Ryu, J.B. Ju, Y.G. Shul, B.W. Cho, and D. Park, J. Power Sources 107, 90 (2002).
[23] I.R.M. Kottegoda, Y. Kadoma, H. Ikuta, Y. Uchimoto, and M. Wakihara, Electrochem. Solid-State Lett. 5, A275 (2002).
[24] I.R.M. Kottegoda, Y. Kadoma, H. Ikuta, Y. Uchimoto, and M. Wakihara, J. Electrochem. Soc. 152, A1595 (2005).
[25] E. Peled, C. Menachem, D. Bar-Tow, and A. Melman, J. Electrochem. Soc. 143, L4 (1996)
[26] J. S. Xue, and J. R. Dahn, J. Electrochem. Soc. 142, 3668 (1995).
[27] Y. Ein-Eli, and V.R. Koch, J. Electrochem. Soc. 144, 2968 (1997).
[28] Y. Wu, C. Jiang, C. Wan, and E. Tsuchida, J. Mater. Chem. 11, 1233 (2001).
[29] Y.P. Wu, C. Jiang, C. Wan, and R. Holze, Electrochem. Commun. 4, 483 (2002).
[30] Y. Wu, C. Jiang, C. Wan, and R. Holze, J. Power Sources 111, 329 (2002).
[31] Y.P. Wu, C. Jiang, C. Wan, and R. Holze, J. Appl. Electrochem. 32, 1011 (2002).
[32] T. Nakajima, M. Koh, R.N. Singh, and M. Shimada, Electrochim. Acta 44, 2879 (1999).
[33] V. Gupta, T. Nakajima, Y. Ohzawa, and H. Iwata, J. Fluorine Chem. 112, 233 (2001).

[34]T. Nakajima, V. Gupta, Y. Ohzawa, H. Iwata, A. Tressaud, and E. Durand, J. Fluorine Chem. 114, 209 (2002).

[35]T. Nakajima, V. Gupta, Y. Ohzawa, M. Koh, R.N. Singh, A. Tressaud, and E. Durand, J. Power Sources 104, 108 (2002).

[36]H. Groult, T. Nakajima, L. Perrigaud, Y. Ohzawa, H. Yashiro, S. Komaba, and N. Kumagai, J. Fluorine Chem. 126, 1111 (2006).

[37]T. Nakajima, J. Li, K. Naga, K. Yoneshima, T. Nakai, and Y. Ohzawa, J. Power Sources 133, 243 (2004).

[38]J. Li, K. Naga, Y. Ohzawa, T. Nakajima, A.P. Shames, and A.I. Panich, J. Fluorine Chem. 126, 265 (2005).

[39]J. Li, Y. Ohzawa, T. Nakajima, and H. Iwata, J. Fluorine Chem. 126, 1028 (2005).

[40]K. Naga, T. Nakajima, Y. Ohzawa, B. Žemva, Z. Mazej, and H. Groult, J. Electrochem. Soc., 154, A347 (2007).

[41]K. Naga, T. Nakajima, S. Aimura, Y. Ohzawa, B. Žemva, Z. Mazej, H. Groult, and A. Yoshida, J. Power Sources 167, 192 (2007).

[42]T. Nakajima, S. Shibata, K. Naga, Y. Ohzawa, A. Tressaud, E. Durand, H. Groult, and F. Warmont, J. Power Sources 168, 265 (2007).

[43]K. Matsumoto, J. Li, Y. Ohzawa, T. Nakajima, Z. Mazej, and B. Žemva, J. Fluorine Chem. 127, 1383 (2006).

[44]T. Achiha, T. Nakajima, and Y. Ohzawa, J. Electrochem. Soc., 154, A827 (2007).

[45]S. Kuwabata, N. Tsumura, S. Goda, C.R. Martin, and H. Yoneyama, J. Electrochem. Soc. 145, 1415 (1998).

[46]M. Gaberscek, M. Bele, J. Drofenik, R. Dominko, and S. Pejovnik, Electrochem. Solid State Lett. 3, 171 (2000).

[47]J. Drofenik, M. Gaberscek, R. Dominko, M. Bele, and S. Pejovnik, J. Power Sources 94, 97 (2001).

[48]M. Bele, M. Gaberscek, R. Dominko, J. Drofenik, K. Zupan, P. Komac, K. Kocevar, I. Musevic, and S. Pejovnik, Carbon 40, 1117 (2002).

[49]M. Gaberscek, M. Bele, J. Drofenik, R. Dominko, and S. Pejovnik, J. Power Sources 97/98, 67 (2001).

[50]B. Veeraraghavan, J. Paul, B. Haran, and B. Popov, J. Power Sources 109, 377 (2002).

[51]M. Holzapfel, H. Buqa, F. Krumeich, P. Novak, F.M. Petrat, and C. Veit, Electrochem. Solid-State Lett. 8, A516 (2005).

[52]S. Rozen, and C. Gal, Tetrahedron Lett., 25, 449 (1984).

[53]S. Rozen, and C. Gal, J. Fluorine Chem., 27, 143 (1985).

[54]M. Koh, H. Yumoto, H. Higashi, and T. Nakajima, J. Fluorine Chem., 97, 239 (1999).

Chapter 5

Thermal stability and electrochemical properties of nonflammable fluoro-carbonates for lithium-ion battery

5-1 Introduction

Lithium-ion batteries are currently used as important electric sources for many electronic instruments such as computers, mobile phones, watches and so on. Recently the demand as electric sources for electric vehicles is rapidly increasing. Lithium-ion batteries with high power densities are especially requested for this purpose. However, lithium-ion batteries have a possibility of firing and/or explosion at high temperatures, by short circuit, by overcharging and so on since they use flammable organic solvents differently from other secondary batteries with aqueous electrolyte solutions. The safety problem is one of the most important issues for the practical use of lithium-ion batteries. To increase the thermal and oxidation stability of lithium-ion batteries, new additives or solvents have been investigated [1-26]. Most of them are phosphorus compounds (phosphates) having flame retardant properties. Thermal stability and electrochemical properties of trimethyl phosphate (TMP) were investigated in various solvent mixtures [1-5]. TMP was mixed by 20-30 % as one of the component of solvent mixtures. Phosphates with phenyl groups such as triphenyl phosphate (TPP), tributyl phosphate (TBP) and cresyl diphenyl phosphate (CDP) were added to solvents by 3-5 wt.% as additives, which improved thermal stability of the batteries [6-9]. K. Xu et al. examined fluorine-containing phosphorus compounds: tris-(2,2,2-trifluoroethyl) phosphate (TFP), bis-(2,2,2-trifluoroethyl) methyl phosphate (BMP) and (2,2,2-trifluoroethyl) diethyl phosphate (TDP) [10-13]. They were mixed with solvents by 20-40 % to investigate thermal stability and electrochemical behavior. Among three phosphates examined, it was shown that TFP was the best candidate. Thermal stability of TFP, TPP and vinyl ethylene carbonate (VEC) was also investigated [14]. Other phosphorus compounds examined as flame retardant solvents or additives are 4-isopropyl phenyl diphenyl phosphate (IPPP) [15, 16], diphenyloctyl phosphate (DPOF) [17, 18], hexamethyl phosphoramide (HMPA) [19], dimethyl methyl phosphonate (DMMP) [20], dimethyl (2-methoxyethoxy) methyl phosphonate (DMMEMP) [21], tri-(β-chloromethyl) phosphate (TCEP) [22], and aromatic phosphorus-containing esters [23]. Cyclohexyl benzene [21], hexamethoxycyclotriphosphazene [24], lithium difluoro (oxalato) borate [25] and allyl tris (2,2,2-trifluoroethyl) carbonate [26] were also studied. It was shown that these phosphorus

compounds improved thermal stability of lithium-ion batteries. In addition to phosphorus compounds mentioned above, organo-fluorine compounds have high stability against oxidation because introduction of fluorine atoms into organic compounds reduces HOMO/LUMO energies. Decrease in HOMO energies gives high anti-oxidation ability to organo-fluorine compounds. Therefore organo-fluorine compounds are different type candidates as flame retardant solvents for lithium-ion batteries. However, the decrease in LUMO energies due to introduction of fluorine atoms into organic compounds simultaneously elevates reduction potentials of organic compounds [27], which facilitate electrochemical decomposition of fluorine compounds. If electrochemical reduction of fluorine compounds continues for a long time without forming protective surface film (Solid Electrolyte Interface: SEI) on carbonaceous anode, irreversible capacity unfortunately increases. However, if decomposed products quickly forms SEI, such fluorine compounds can be used as solvents. Another important problem is miscibility of fluorine compounds with polar solvents for lithium-ion batteries such as EC (ethylene carbonate), PC (propylene carbonate), DEC (diethyl carbonate) and so on. In the present study, electrochemical redox reactions of fluorine compounds were investigated and charge/discharge characteristics of natural graphite electrodes were evaluated in fluorine compound-containing solvents for the application of organo-fluorine compounds to flame retardant solvents for lithium-ion batteries.

5-2 Experimental

5-2-1 Natural graphite samples

Natural graphite powder samples (purity: >99.95 %) with average particle sizes of 5, 10, 15, 25 and 40 μm (abbreviated to NG5 μm, NG10 μm, NG15 μm, NG25 μm and NG40 μm) were used for cyclic voltammetry and charge/discharge cycling. The d_{002} values obtained by X-ray diffractometry (XRD-6100, Shimadzu) were 0.3355, 0.3354, 0.3355, 0.3358 and 0.3358 nm for NG5 μm, NG10 μm, NG15 μm, NG25 μm and NG40 μm, respectively. Surface structure of natural graphite samples were investigated by BET surface area measurement (Tristar 3000, Shimadzu) and Raman spectroscopy (NRS-1000, Jasco) with Nd:YVO_4 laser (532 nm).

5-2-2 Fluorine compounds

The following fluorine compounds with carbonate structures (purity: 99.9 %, H_2O <10 ppm), synthesized in Daikin Industries, Ltd., were used in the present study.

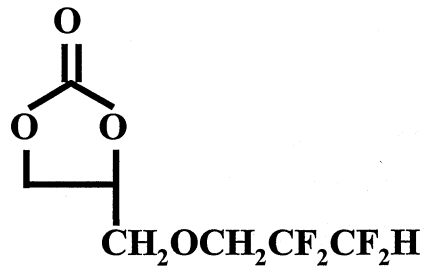

A: 4-(2,2,3,3-tetrafluoropropoxymethyl)-[1,3]-dioxolan-2-one

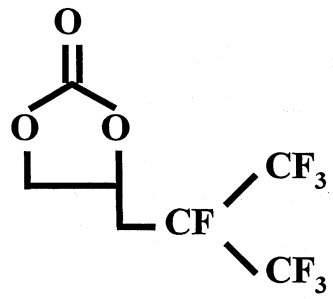

B: 4-(2,3,3,3-tetrafluoro-2-trifluoromethyl-propyl)-[1,3]-dioxolan-2-one

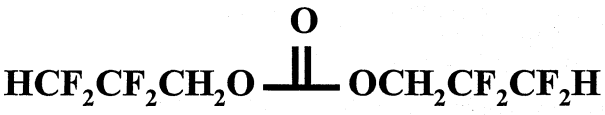

C: bis-(2,2,3,3-tetrafluoro-propyl) carbonate

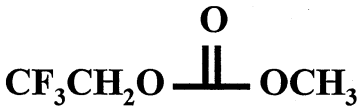

D: 2,2,2-trifluoroethyl methyl carbonate

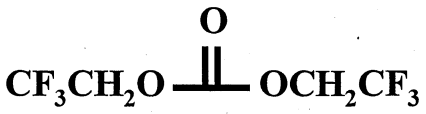

E: bis-(2,2,2-trifluoroethyl) carbonate

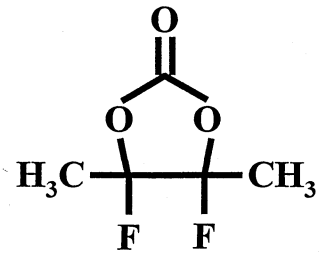

F: 4,5-difluoro-4,5-dimethyl-[1,3]-dioxolan-2-one

HOMO and LUMO energies of fluorine compounds **A**, **B**, **C**, **D**, **E** and **F** were calculated by Spartan'06 semi-empirical method using AM1, being compared with those for the same type compounds consisting of C, H and O: 4-propoxymethyl-[1,3]-dioxolan-2-one (**A**-H), 4-(2-methyl-propyl)-[1,3]-dioxolan-2-one (**B**-H), bis-propyl carbonate (**C**-H), methylethyl carbonate (**D**-H), diethyl carbonate (**E**-H) and 4,5-H-4,5-dimethyl-[1,3]-dioxolan-2-one (**F**-H), in which fluorine atoms are replaced by hydrogen.

Thermal stability of 0.67 mol/dm^3 $LiClO_4$ - EC/DEC/PC (1:1:1 vol.) and EC/DEC/PC/(**A**, **B**, **C**, **D**, **E** or **F**) (1:1:1 vol.) were examined by differential scanning calorimetry (DSC) at 5 °C/min between room temperature and 300 °C (Shimadzu, DSC-60). For DSC measurement, Al airtight cell containing a mixture of the electrolyte solution (3 μℓ) and NG15 μm (0.8 mg)

5-2-3 Electrochemical measurements

Oxidation currents for 0.67 mol/dm^3 $LiClO_4$ - EC/DEC (1:1 vol.), EC/DEC/PC (1:1:1 vol.) and EC/DEC/(**A**, **B**, **C**, **D**, **E** or **F**) (1:1:1 vol.) (Kishida Chemicals, Co. Ltd., H_2O: 2-5 ppm for EC/DEC and PC) were measured by linear sweep of potential at 0.1 mV/s using Pt wire electrode (Hokuto Denko, HZ-5000). Counter and reference electrodes were copper plate and lithium foil, respectively.

Three-electrode cell with natural graphite as a working electrode and lithium foil as counter and reference electrodes were used for cyclic voltammetry study and galvanostatic charge/discharge experiments. Natural graphite electrode was prepared as follows. Natural graphite powder was dispersed in N-methyl-2-pyrrolidone (NMP) containing 12 wt.% poly vinylidene fluoride (PVdF) and the slurry was pasted on a copper current collector. The electrode was dried at 120 °C under vacuum for half a day. After drying, the electrode contained 80 wt.% graphite and 20 wt.% PVdF. Electrolyte solutions were prepared by mixing the fluorine compound **A**, **B**, **C**, **D**, **E** or **F** with 1.0 mol/dm^3 $LiClO_4$ - EC/DEC (1:1 vol.) and/or 1.0 mol/dm^3 $LiClO_4$ - EC/DEC/PC (1:1:1 vol.) (Kishida Chemicals, Co. Ltd., H_2O: 2-5 ppm). Fluorine compounds **A**, **B**, **C**, **D**, **E** and **F** are mixed with EC/DEC and EC/DEC/PC in whole range of composition at room temperature. For cyclic voltammetry study, 0.5 mol/dm^3 $LiClO_4$ - EC/DEC/(**A**, **B** or **C**) (1:1:2 vol.) and 0.5 mol/dm^3 $LiClO_4$ - EC/DEC/PC/(**D**, **E** or **F**) (1:1:1:3 vol.) were used. Cyclic voltammograms were obtained using NG5 μm at a scan rate of 0.1 mV/s for **A**, **B** or **C**-mixed electrolyte solution and using NG15 μm at a scan rate of 0.1 mV/s for **D**, **E** or **F**-mixed one (Hokuto Denko, HZ-5000). For galvanostatic charge/discharge experiments, the mixing ratios of solvents were 1:1:1 vol. in 0.67 mol/dm^3 $LiClO_4$ - EC/DEC/(**A**, **B** or **C**) and 1:1:1:1.5 vol. in 0.67 mol/dm^3 $LiClO_4$ - EC/DEC/PC/(**A**, **B**, **C**, **D**, **E** or **F**). Preparation of 1.0 mol/dm^3 $LiClO_4$ - EC/DEC/(**A**, **B**, **C**, **D**, **E** or **F**) (1:1:1 vol.) can be made at room temperature by dissolving $LiClO_4$ in 0.67 mol/dm^3 $LiClO_4$ - EC/DEC. However, the 0.67 mol/dm^3 $LiClO_4$ - EC/DEC and EC/DEC/PC solutions were used in the present study to simplify the experiments. Galvanostatic charge/discharge

cyclings were performed at a current density of 60 mA/g between 0 and 3.0 V vs. Li/Li^+ reference electrode in a glove box filled with Ar at 25 °C (Hokuto Denko, HJ1001 SM8A).

5-3 Results and Discussion

5-3-1 Surface structure of natural graphite samples

Table I shows BET surface areas and total pore volumes and *R* values of natural graphite samples used in this study. Surface area decreased with increasing particle size of natural graphite powder. In particular NG5 μm and NG10 μm have large surface areas. Change in the pore volume has the same trend. In mesopore size distributions, NG5 μm, NG10 μm and NG15 μm have the larger peaks at a diameter of 2.3 nm in mesopore distributions while NG25 μm and NG40 μm show the smaller peaks at a diameter of 2.0 nm. The peak height decreased with increasing average particle size of natural graphite powder. The Raman spectra of five natural graphite samples had strong G-bands (1580 cm^{-1}) and very week D-bands (1360 cm^{-1}) as shown Fig.1. The peak intensity ration of D-band to G-band is defined as the *R* value (= I_D/I_G) indicating the degree of surface disorder of carbon materials. *R* values of five natural graphite samples were in range of 0.23-0.27, which shows that the surface disorders of five samples are similar to each other.

Table I. Surface structure of natural graphite samples.

Natural graphite	Surface area (m^2g^{-1})	Pore volume (cm^3g^{-1})	*R* value ($=I_D/I_G$)
NG5 μm	**13.9**	**0.047**	**0.23**
NG10 μm	**9.2**	**0.035**	**0.23**
NG15 μm	**6.9**	**0.026**	**0.25**
NG25 μm	**3.7**	**0.009**	**0.26**
NG40 μm	**3.2**	**0.010**	**0.27**

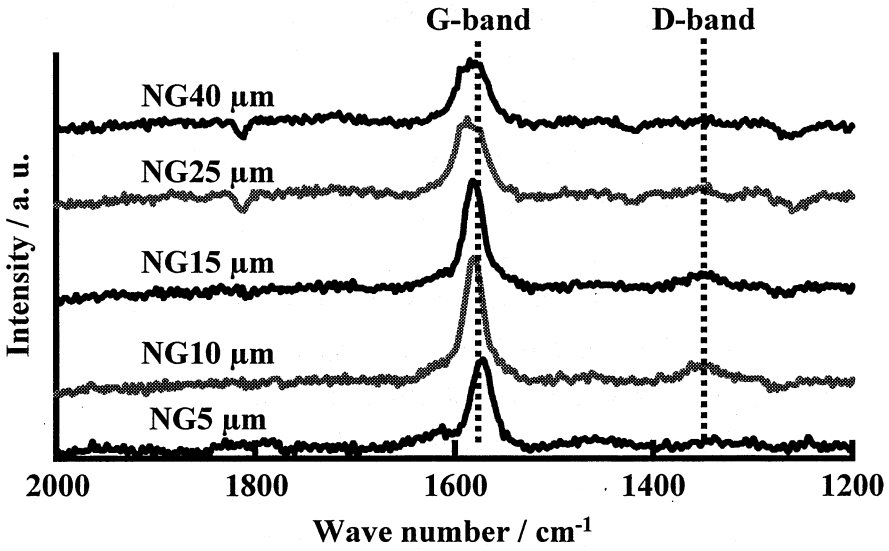

Figure 1. Raman spectra of natural graphite samples.

5-3-2 HOMO and LUMO energies of fluorine compounds

Substitution of fluorine for hydrogen increases anti-oxidation ability of organic compounds. Table II shows HOMO and LUMO energies of fluorine compounds **A**, **B**, **C**, **D**, **E** and **F** used in the present study in comparison with those for **A**-H, **B**-H, **C**-H, **D**-H, **E**-H and **F**-H consisting of only C, H and O. HOMO energies are the lower in fluorine compounds **A**, **B**, **C**, **D**, **E** and **F** than **A**-H, **B**-H, **C**-H, **D**-H, **E**-H and **F**-H, respectively. It suggests that fluorine compounds **A**, **B**, **C**, **D**, **E** and **F** are stronger against electrochemical oxidation than **A**-H, **B**-H, **C**-H, **D**-H, **E**-H and **F**-H, respectively. However, LUMO energies are simultaneously decreased by fluorine introduction into organic compounds. It also suggests that the compounds **A**, **B**, **C**, **D**, **E** and **F** are electrochemically reduced at higher potentials than **A**-H, **B**-H, **C**-H, **D**-H, **E**-H and **F**-H, respectively.

Table II. HOMO and LUMO energies of fluorine compounds and the same type carbonates consisting of C, H and O, calculated by Spatan'06 semi-empirical method using AM1.

Compound	A-H	A	B-H	B
HOMO energy (kJ/mol)	-1068.5	-1146.0	-1122.1	-1183.6
LUMO energy (kJ/mol)	100.4	64.2	111.3	-1.3

Compound	C-H	C	D-H	D
HOMO energy (kJ/mol)	-1100.2	-1151.1	-1105.0	-1165.0
LUMO energy (kJ/mol)	100.6	15.5	133.5	60.2

Compound	E-H	E	F-H	F
HOMO energy (kJ/mol)	-1099.4	-1207.0	-1150.4	-1191.2
LUMO energy (kJ/mol)	132.4	2.0	133.6	86.9

5-3-3 Thermal stability of fluorine compounds

Figure 2 shows DSC profiles for the mixtures of 0.67 mol/dm^3 $LiClO_4$ - EC/DEC/PC/(**A**, **B**, **C**, **D**, **E** or **F**) and NG15 μm. Exothermic reactions of EC/DEC/PC/(**A**, **B**, **C**, **D**, **E** or **F**) started at 290, 289, 296, 290, 289 and 249 °C, respectively. The starting temperatures were higher in EC/DEC/PC/(**A**, **B**, **C**, **D** or **E**) than in EC/DEC/PC (271 °C). In addition, exothermic peaks of EC/DEC/PC/(**A**, **B**, **C**, **D** or **E**) were observed at 301, 300<, 300, 300< and 296 °C, respectively, which were also higher than that for EC/DEC/PC (281 °C). The thermal stability of **F** is slightly lower than that for EC/DEC/PC. Thus the mixing of organo-fluorine compounds (**A**, **B**, **C**, **D** or **E**) with EC/DEC/PC highly increases thermal stability of electrolyte solutions.

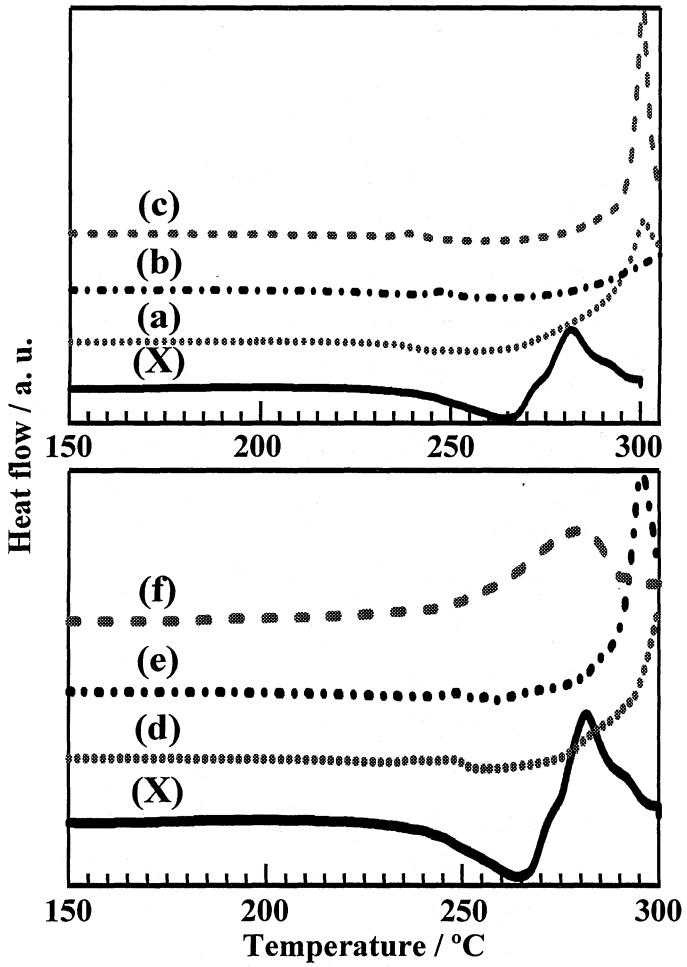

Figure 2. DSC profiles for mixtures of 0.67 mol/dm^3 $LiClO_4$
- EC/DEC/PC/(**A**, **B**, **C**, **D**, **E** or **F**) (1:1:1:1.5 vol.) and NG15 μm.
(X) EC/DEC/PC, (a) EC/DEC/PC/**A**, (b) EC/DEC/PC/**B**, (c) EC/DEC/PC/**C**
(d) EC/DEC/PC/**D**, (e) EC/DEC/PC/**E**, (f) EC/DEC/PC/**F**

5-3-3 Electrochemical oxidation of fluorine compounds

Figure 3 shows oxidation currents in EC/DEC, EC/DEC/PC and fluorine compound-containing EC/DEC and EC/DEC/PC solutions. Oxidative decomposition started at ca. 6.0 V vs. Li/Li^+ for all solutions. Gas evolution was also observed above 6.0 V vs. Li/Li^+. However, oxidation currents were much smaller in EC/DEC/(**A**, **B** or **C**) and EC/DEC/(**D**, **E** or **F**) than in both EC/DEC and EC/DEC/PC at the higher potentials than 6.0 V vs. Li/Li^+, being largely diminished by the mixing of fluorine compound by 33.3 vol. Large reduction of oxidation currents would have been caused by the decrease in electrode area due to adsorption of stable fluorine compounds on a Pt electrode surface. Thus the mixing of organo-fluorine compounds with EC/DEC and EC/DEC/PC highly increases anti-oxidation ability of electrolyte solutions.

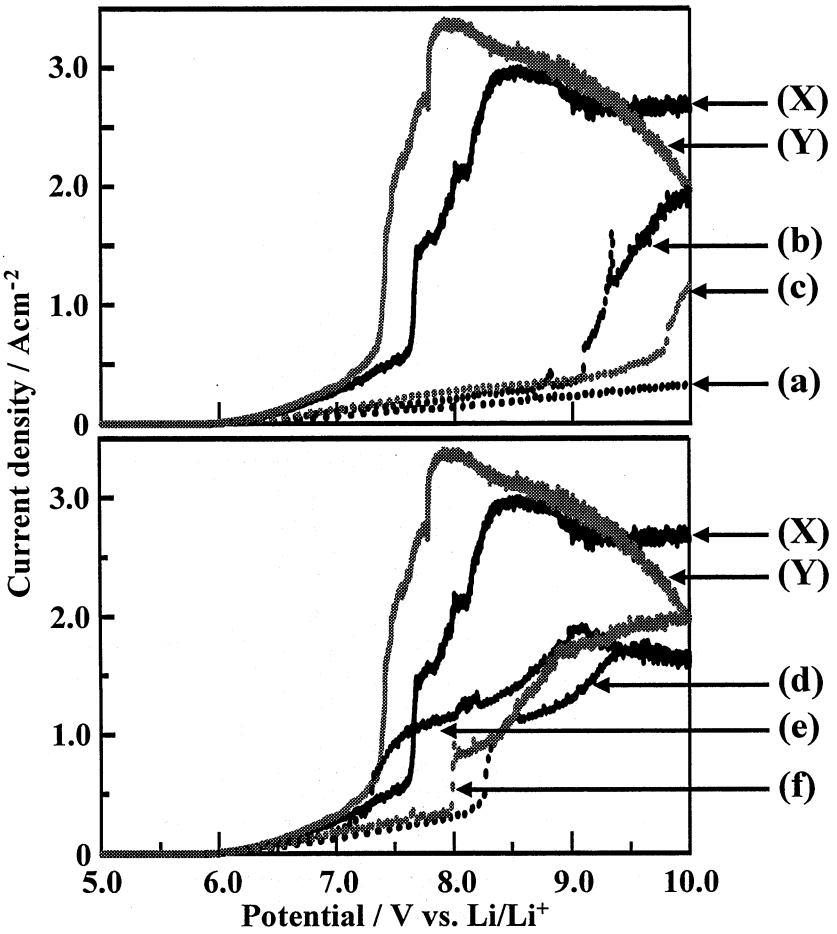

Figure 3. Linear sweep voltammograms for Pt wire electrode
in 0.67 mol/dm^3 $LiClO_4$ - EC/DEC (1:1 vol.), EC/DEC/PC (1:1:1 vol.),
EC/DEC/(**A**, **B**, **C**, **D**, **E** or **F**) (1:1:1 vol.).
(X) EC/DEC, (Y) EC/DEC/PC, (a) EC/DEC/**A**,(b) EC/DEC/**B**
(c) EC/DEC/**C**, (d) EC/DEC/PC/**D**, (e) EC/DEC/PC/**E**, (f) EC/DEC/PC/**F**.

5-3-4 Electrochemical reduction of fluorine compounds

Cyclic voltammograms obtained in fluorine compound-containing solvents were shown in Fig. 4, in which the large reduction currents indicating the decomposition of fluorine compounds **A**, **B**, **C**, **D**, **E** and **F** were observed. The electrochemical reduction of **A**, **B**, **C**, **D**, **E** and **F** started at 2.0, 2.2, 1.9, 2.3, 2.7 and 2.4 V vs. Li/Li$^+$, respectively. Since the reduction of EC, DEC and PC starts at 1.4, 1.3 and 1.0-1.6 V vs. Li/Li$^+$ [28, 29], respectively, Fig. 4 shows that all fluorine compounds used in the present study are reduced at the higher potentials than EC, DEC and PC as suggested by the result of molecular orbital calculation in Table II.

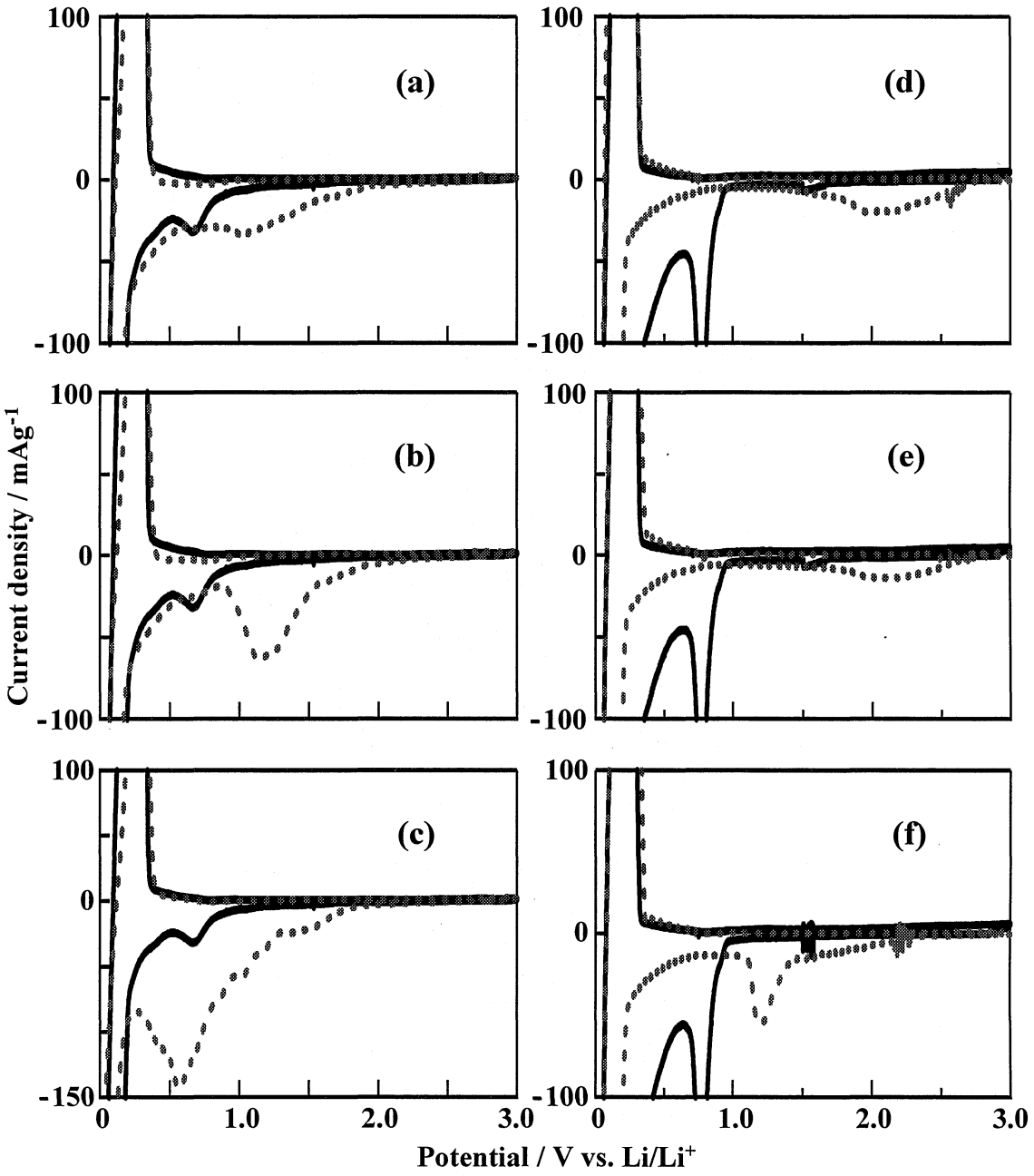

Figure 4. Cyclic voltammograms for natural graphite (NG5 μm or NG15μm)
in 0.5 mol/dm^3 $LiClO_4$ - EC/DEC/(**A**, **B** or **C**) (1:1:2 vol.) and
EC/DEC/PC/(**D**, **E** or **F**) (1:1:1:1.5 vol.). (a) EC/DEC/**A**, (b) EC/DEC/**B**, (c) EC/DEC/**C**,
——— : EC/DEC, ····· : EC/DEC/(**A**, **B** or **C**).
(d) EC/DEC/PC/**D**, (e) EC/DEC/PC/**E**, (f) EC/DEC/PC/**F**
——— : EC/DEC/PC, ····· : EC/DEC/PC/(**D**, **E** or **F**).
Scan speed: 0.1 mV/s, NG sample: NG5 μm for (a), (b) and (c), NG15 μm for (d), (e) and (f).

5-3-5 Charge/discharge behavior of natural graphite samples in fluorine compound -containing solvents

In 0.67 mol/dm^3 $LiClO_4$ - EC/DEC and EC/DEC/(**A**, **B** or **C**) solutions, charge/discharge capacities and coulombic efficiencies at the first cycle were similar to each other (Table III. (a), Table IV. (a) and Table V. (a)). Charge capacities at the first cycle were in the range of 358-329 mAhg^{-1} in both EC/DEC and EC/DEC/(**A**, **B** or **C**), slightly decreasing from NG5 to NG40 μm, i.e., with increasing average particle size. The first coulombic efficiency increased from 75.1 % (NG5 μm) to 85.7 % (NG40 μm) with decreasing surface area of natural graphite though the actual current density increases with decreasing surface area. It means that SEI is quickly formed on natural graphite powder by the decomposition of EC and fluorine compound **A**, **B** or **C**. In EC/DEC/(**A**, **B** or **C**), the first coulombic efficiencies were in the range of 76.3-87.1, 74.4-88.4, and 72.3-87.5 %, respectively, also increasing from NG5 to NG40 μm. In the case of NG15 μm, the first coulombic efficiencies slightly increased by the addition of **B** and **C** to EC/DEC. The results show that fluorine compounds **A**, **B** and **C** contribute well to the SEI formation without increasing the irreversible capacity. First charge capacities somewhat decreased with increasing average particle size of natural graphite probably due to the slow Li diffusion in graphene layers.

Table III. First charge/discharge capacities and first coulombic efficiencies for natural graphite samples in 0.67 mol/dm^3 $LiClO_4$ - (a) EC/DEC/**A** (1:1:1 vol.) and (b) EC/DEC/PC/**A** (1:1:1:1.5 vol.).

(a) 0.67 mol/dm^3 $LiClO_4$ - EC/DEC/A (1:1:1 vol.)

Natural Graphite	First discharge capacity / mAhg^{-1}		First charge capacity / mAhg^{-1}		First coulombic efficiency / %	
	EC/DEC	EC/DEC/A	EC/DEC	EC/DEC/A	EC/DEC	EC/DEC/A
NG5 μm	476	467	358	357	75.1	76.3
NG10 μm	446	427	348	333	78.0	77.9
NG15 μm	439	434	341	329	77.7	75.9
NG25 μm	407	413	348	342	85.6	82.7
NG40 μm	387	378	332	329	85.7	87.1

(b) 0.67 mol/dm^3 $LiClO_4$ - EC/DEC/PC/A (1:1:1:1.5 vol.)

Natural Graphite	First discharge capacity / mAhg^{-1}		First charge capacity / mAhg^{-1}		First coulombic efficiency / %	
	EC/DEC /PC	EC/DEC /PC/A	EC/DEC /PC	EC/DEC /PC/A	EC/DEC /PC	EC/DEC /PC/A
NG5 μm	485	489	349	350	72.1	71.7
NG10 μm	551	475	341	332	61.9	69.8
NG15 μm	608	481	352	334	58.0	69.4
NG25 μm	622	447	337	342	54.1	75.7
NG40 μm	579	452	314	314	54.3	69.6

Table IV. First charge/discharge capacities and first coulombic efficiencies for natural graphite samples in 0.67 mol/dm^3 $LiClO_4$ - (a) EC/DEC/**B** (1:1:1 vol.) and (b) EC/DEC/PC/**B** (1:1:1:1.5 vol.).

(a) 0.67 mol/dm^3 $LiClO_4$ - EC/DEC/B (1:1:1 vol.)

Natural Graphite	First discharge capacity / mAhg^{-1}		First charge capacity / mAhg^{-1}		First coulombic efficiency / %	
	EC/DEC	EC/DEC/B	EC/DEC	EC/DEC/B	EC/DEC	EC/DEC/B
NG5 μm	476	476	358	354	75.1	74.4
NG10 μm	446	430	348	345	78.0	80.3
NG15 μm	439	413	341	349	77.7	84.4
NG25 μm	407	402	348	329	85.6	82.0
NG40 μm	387	379	332	335	85.7	88.4

(b) 0.67 mol/dm^3 $LiClO_4$ - EC/DEC/PC/B (1:1:1:1.5 vol.)

Natural Graphite	First discharge capacity / mAhg^{-1}		First charge capacity / mAhg^{-1}		First coulombic efficiency / %	
	EC/DEC /PC	EC/DEC /PC/B	EC/DEC /PC	EC/DEC /PC/B	EC/DEC /PC	EC/DEC /PC/B
NG5 μm	485	479	349	347	72.1	72.4
NG10 μm	551	458	341	356	61.9	77.8
NG15 μm	608	403	352	329	58.0	81.6
NG25 μm	622	402	337	329	54.1	82.0
NG40 μm	579	361	314	317	54.3	87.7

Table V. First charge/discharge capacities and first coulombic efficiencies for natural graphite samples in 0.67 mol/dm^3 $LiClO_4$ - (a) EC/DEC/**C** (1:1:1 vol.) and (b) EC/DEC/PC/**C** (1:1:1:1.5 vol.).

(a) 0.67 mol/dm^3 $LiClO_4$ - EC/DEC/C (1:1:1 vol.)

Natural Graphite	First discharge capacity / mAhg^{-1}		First charge capacity / mAhg^{-1}		First coulombic efficiency / %	
	EC/DEC	EC/DEC/C	EC/DEC	EC/DEC/C	EC/DEC	EC/DEC/C
NG5 μm	476	494	358	357	75.1	72.3
NG10 μm	446	434	348	349	78.0	80.3
NG15 μm	439	422	341	354	77.7	84.0
NG25 μm	407	406	348	350	85.6	86.2
NG40 μm	387	390	332	341	85.7	87.5

(b) 0.67 mol/dm^3 $LiClO_4$ - EC/DEC/PC/C (1:1:1:1.5 vol.)

Natural Graphite	First discharge capacity / mAhg^{-1}		First charge capacity / mAhg^{-1}		First coulombic efficiency / %	
	EC/DEC /PC	EC/DEC /PC/C	EC/DEC /PC	EC/DEC /PC/C	EC/DEC /PC	EC/DEC /PC/C
NG5 μm	485	485	349	354	72.1	73.0
NG10 μm	551	509	341	331	61.9	65.1
NG15 μm	608	556	352	350	58.0	63.0
NG25 μm	622	434	337	349	54.1	80.3
NG40 μm	579	423	314	331	54.3	78.3

Table VI. First charge/discharge capacities and first coulombic efficiencies for natural graphite samples in 0.67 mol/dm^3 $LiClO_4$ - (a) EC/DEC/PC/**D**, (b) EC/DEC/PC/**E** and (c) EC/DEC/PC/**F** (1:1:1:1.5 vol.).

(a) 0.67 mol/dm^3 $LiClO_4$ - EC/DEC/PC/D (1:1:1:1.5 vol.)

	First discharge capacity / mAhg^{-1}		First charge capacity / mAhg^{-1}		First coulombic efficiency / %	
Natural Graphite	EC/DEC /PC	EC/DEC /PC/D	EC/DEC /PC	EC/DEC /PC/D	EC/DEC /PC	EC/DEC /PC/D
NG15 μm	608	529	352	341	58.0	64.4
NG25 μm	622	517	337	354	54.1	68.4

(b) 0.67 mol/dm^3 $LiClO_4$ - EC/DEC/PC/E (1:1:1:1.5 vol.)

	First discharge capacity / mAhg^{-1}		First charge capacity / mAhg^{-1}		First coulombic efficiency / %	
Natural Graphite	EC/DEC /PC	EC/DEC /PC/E	EC/DEC /PC	EC/DEC /PC/E	EC/DEC /PC	EC/DEC /PC/E
NG15 μm	608	464	352	356	58.0	76.7
NG25 μm	622	431	337	348	54.1	80.8

(c) 0.67 mol/dm^3 $LiClO_4$ - EC/DEC/PC/F (1:1:1:1.5 vol.)

	First discharge *capacity / mAhg^{-1}*		First charge *capacity / mAhg^{-1}*		First coulombic *efficiency / %*	
Natural Graphite	EC/DEC /PC	EC/DEC /PC/F	EC/DEC /PC	EC/DEC /PC/F	EC/DEC /PC	EC/DEC /PC/F
NG15 μm	608	482	352	362	58.0	75.1
NG25 μm	622	448	337	352	54.1	78.7

SEI formation on high crystalline natural graphite is slow in PC-containing solvents, which normally causes large increase in irreversible capacity. In fact, first coulombic efficiency decreased from 72.1 % (NG5 μm) to 54.3 % (NG40 μm) with decreasing surface area, i.e. with increasing actual current density in 0.67 mol/dm^3 $LiClO_4$ - EC/DEC/PC as shown Table III, IV, V and VI. However, discharge capacities at first cycle were decreased by addition of the fluorine compounds to EC/DEC/PC except NG5 μm. The decrease in the first discharge capacities for natural graphite samples were in the range of 76-127, 93-220, 42-188, 79-105, 144-191 and 126-174 mAhg^{-1} in EC/DEC/PC/(**A**, **B**, **C**, **D**, **E** or **F**), respectively, increasing from NG10 to NG40 μm. Charge capacities were similar to each other in both EC/DEC/PC and EC/DEC/PC/(**A**, **B**, **C**, **D**, **E** or **F**) in most of the cases (charge capacities: 352-314 mAhg^{-1} in EC/DEC/PC, 350-314 mAhg^{-1} in EC/DEC/PC/**A**, 356-317 mAhg^{-1} in EC/DEC/PC/**B**, 354-331 mAhg^{-1} in EC/DEC/**C**, 341-354 mAhg^{-1} in EC/DEC/PC/**D**, 348-356 mAhg^{-1} in EC/DEC/PC/**E** and 352-362 mAhg^{-1} in EC/DEC/PC/**F**). Consequently the first coulombic efficiencies were increased by the mixing of the fluorine compounds with

EC/DEC/PC as shown in Tables III-VI except NG5 μm. The addition of fluorine compounds was not effective for increasing the first coulombic efficiencies of NG5 μm probably because of its large surface area, where actual current density was relatively small. Nevertheless the results clearly show that the fluorine compounds **A**, **B**, **C**, **D**, **E** and **F** can be used as solvents for all natural graphite samples including NG5 μm because no increase in irreversible capacity was observed. The increase in the first coulombic efficiency by the addition of a fluorine compound was larger as the surface area of natural graphite decreased, i.e., from NG10 to NG40 μm, which suggests that high values of the first coulombic efficiencies can also be obtained at high current densities. These results mean that the addition of **A**, **B**, **C**, **D**, **E** and **F** to the EC/DEC/PC mixture highly facilitates SEI formation on natural graphite electrodes of NG10-NG40 μm. Among the three fluorine compounds examined, **B** was the best in increasing the first coulombic efficiencies of natural graphite electrodes. The same phenomena were also seen in the first charge/discharge potential curves obtained in 0.67 mol/dm^3 $LiClO_4$ - EC/DEC/PC and EC/DEC/PC/(**A**, **B**, **C**, **D**, **E** or **F**) solutions (Figs. 5-8). In 0.67 mol/dm^3 $LiClO_4$ - EC/DEC/PC, potential plateaus indicating the electrochemical reduction of PC are observed at 0.8 V vs. Li/Li^+. The potential plateau becomes longer with decreasing surface area from NG5 to NG40 μm, consistent with the decrease in the first coulombic efficiency. The potential plateaus showing the reduction of PC almost disappeared by mixing fluorine compounds **A**, **B**, **C**, **D**, **E** or **F** with EC/DEC/PC as shown in Figs. 5-8 except NG5 μm. In the case of NG5 μm, no change in the potential curves was observed by the addition of fluorine compounds. Figures 9-12 show charge capacities and coulombic efficiencies as a function of cycle number, obtained in 0.67 mol/dm^3 $LiClO_4$ - EC/DEC/PC/(**A**, **B**, **C**, **D**, **E** or **F**). Cycleability was good in all cases, and coulombic efficiencies approached 100 % after several cycles. The first coulombic efficiencies were increased by the addition of fluorine compounds **A**, **B**, **C**, **D**, **E** and **F** to EC/DEC/PC except for NG5 μm. This trend was more evident with increasing average particle size of natural graphite. Even after the first cycle, coulombic efficiencies were higher in EC/DEC/PC/(**A**, **B**, **C**, **D**, **E** or **F**) solutions than in EC/DEC/PC itself in many cases. In the case of NG10 and NG15 μm, the charge capacities were slightly lower in EC/DEC/PC/(**A**, **B**, **C** or **D**) solutions than in EC/DEC/PC in most of the cases, which could be due to the increase in the resistances of SEI films containing fluorine groups because SEI resistance was increased by the introduction of fluorine groups into SEI, while charge transfer resistance was reduced [30]. The results obtained show that the mixing of the fluorine compounds **A**, **B**, **C**, **D**, **E** and **F** with EC/DEC/PC not only improves the antioxidation ability of electrolyte solutions but also increases the first coulombic efficiencies, i.e., reduces irreversible capacities.

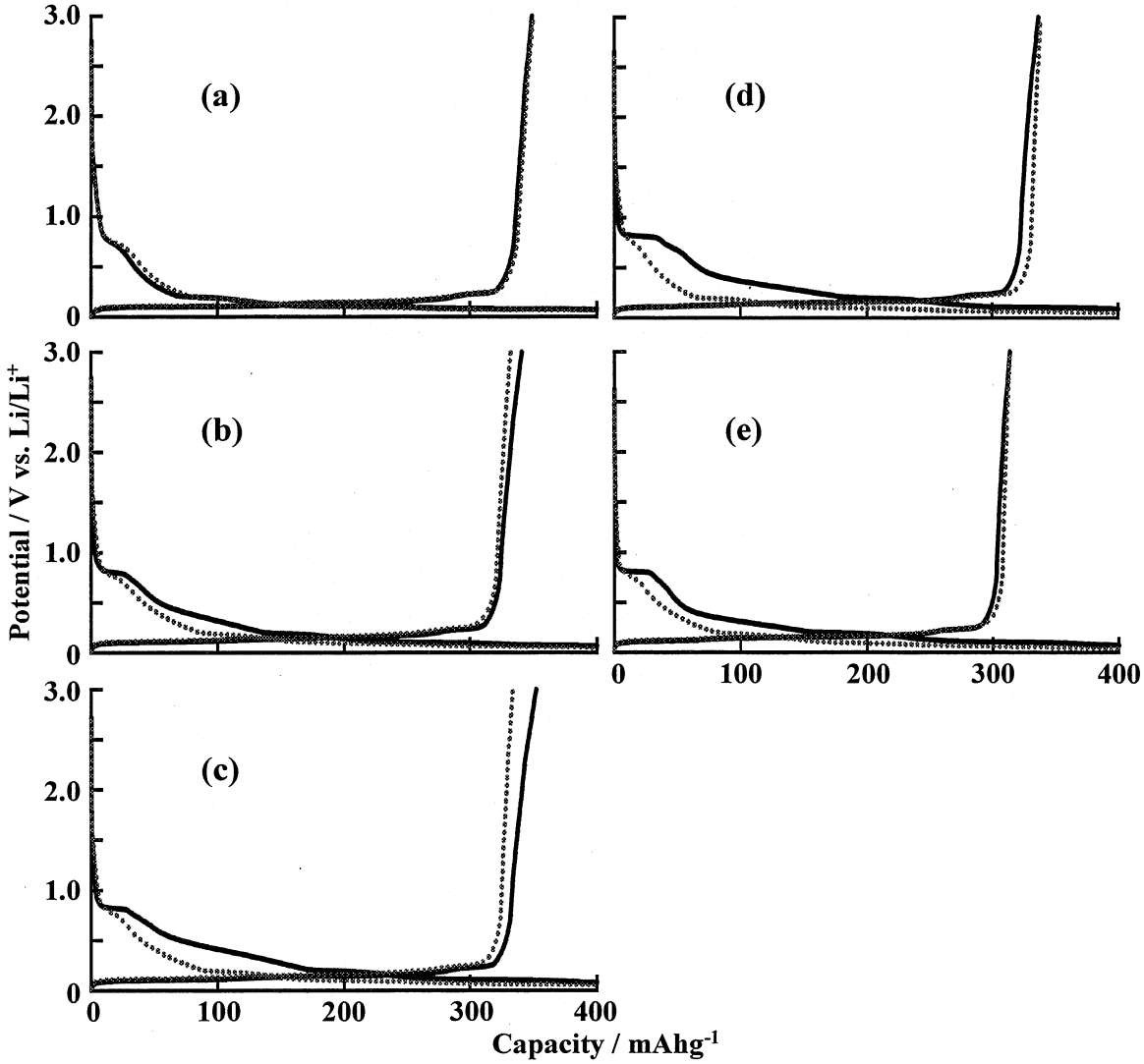

Figure 5. First charge/discharge potential curves for natural graphite samples in 0.67 mol/dm^3 $LiClO_4$ - EC/DEC/PC (1:1:1 vol.) and EC/DEC/PC/**A** (1:1:1:1.5 vol.). (a) NG5 μm, (b) NG10 μm, (c) NG15 μm, (d) NG25 μm, (e) NG40 μm. ———: EC/DEC/PC, ·····: EC/DEC/PC/**A**.

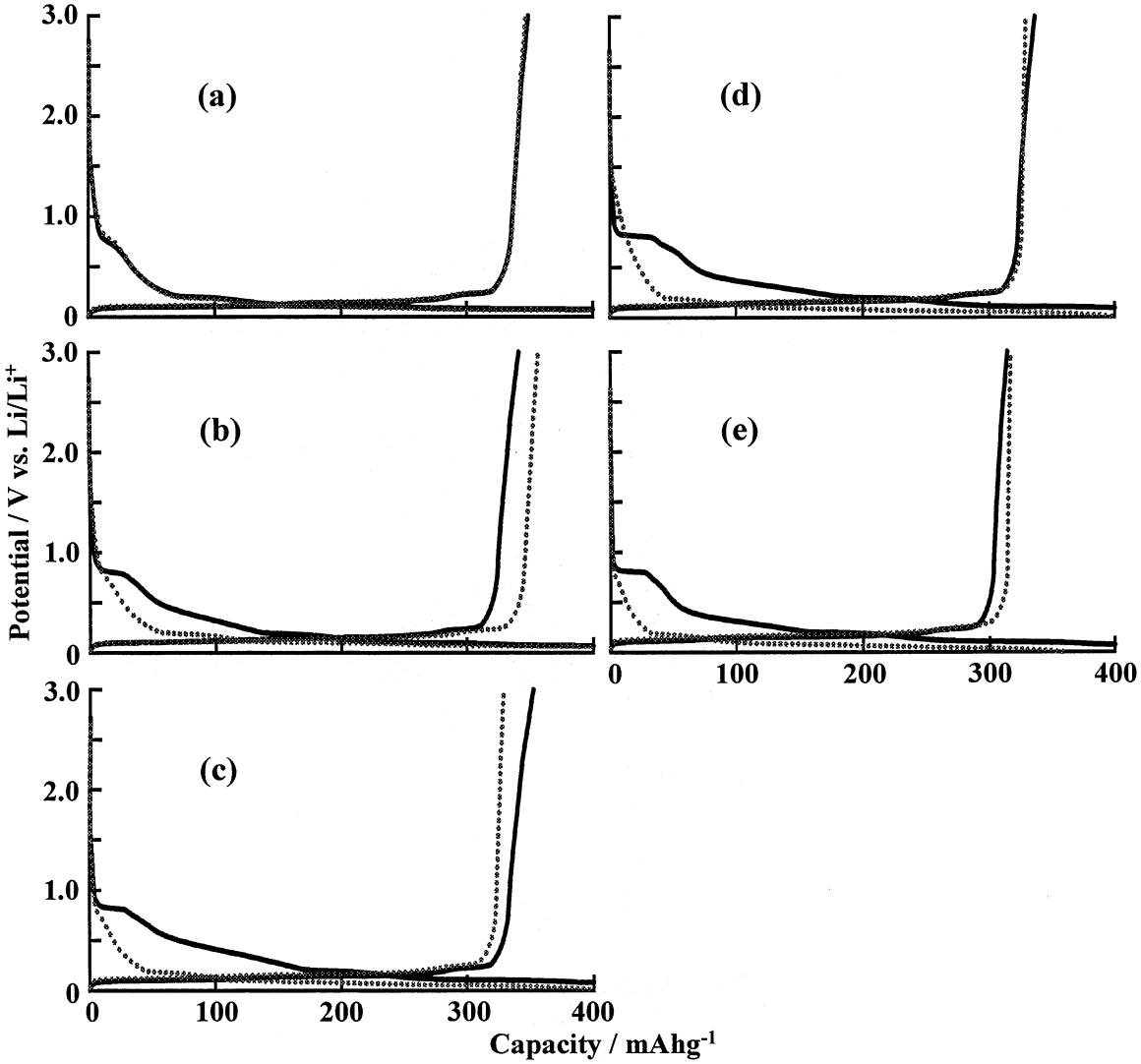

Figure 6. First charge/discharge potential curves for natural graphite samples in 0.67 mol/dm^3 $LiClO_4$ - EC/DEC/PC (1:1:1 vol.) and EC/DEC/PC/**B** (1:1:1:1.5 vol.). (a) NG5 μm, (b) NG10 μm, (c) NG15 μm, (d) NG25 μm, (e) NG40 μm. ———: EC/DEC/PC, ·····: EC/DEC/PC/**B**.

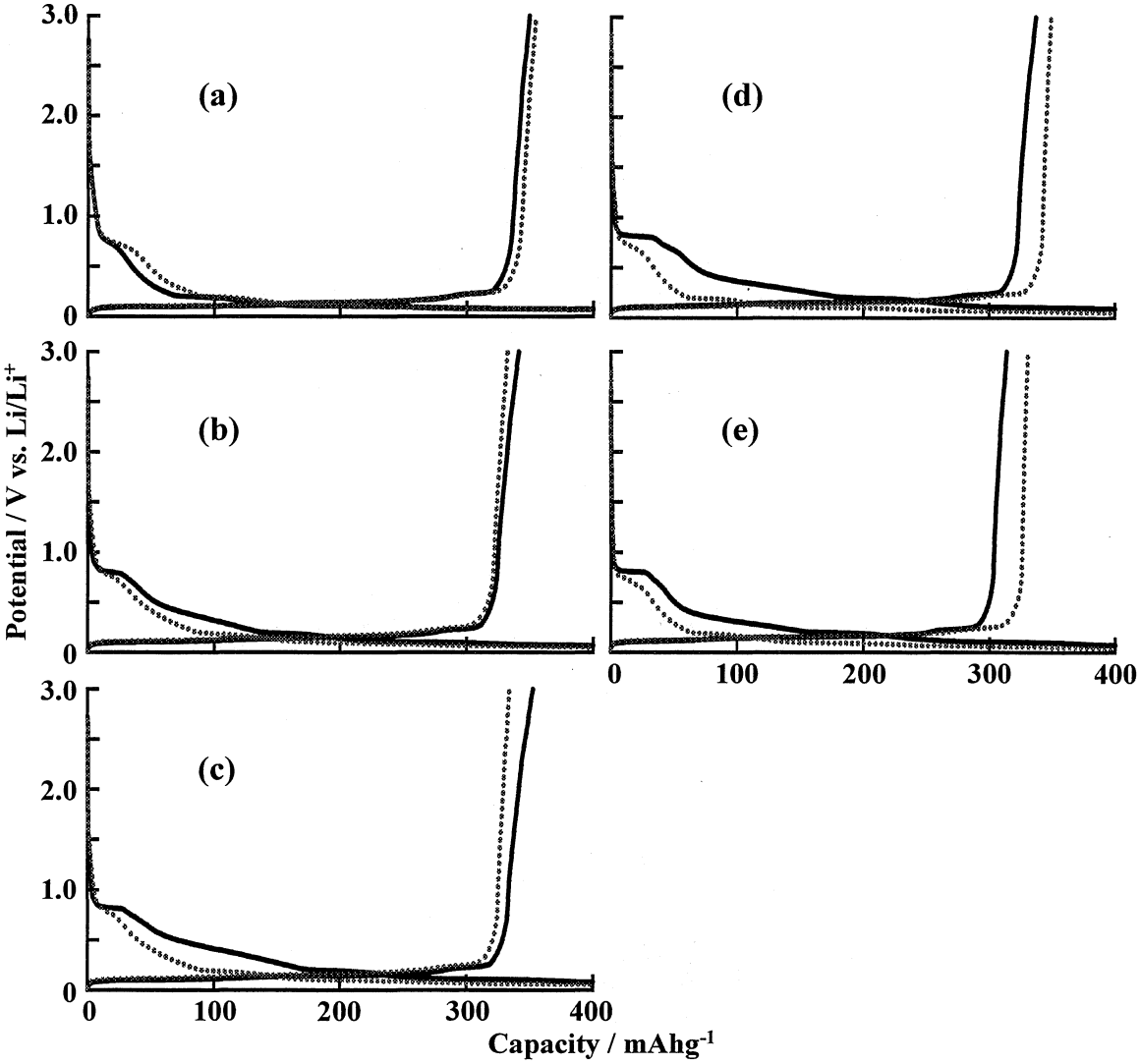

Figure 7. First charge/discharge potential curves for natural graphite samples in 0.67 mol/dm^3 $LiClO_4$ - EC/DEC/PC (1:1:1 vol.) and EC/DEC/PC/**C** (1:1:1:1.5 vol.). (a) NG5 μm, (b) NG10 μm, (c) NG15 μm, (d) NG25 μm, (e) NG40 μm. ———: EC/DEC/PC, ·····: EC/DEC/PC/**C**.

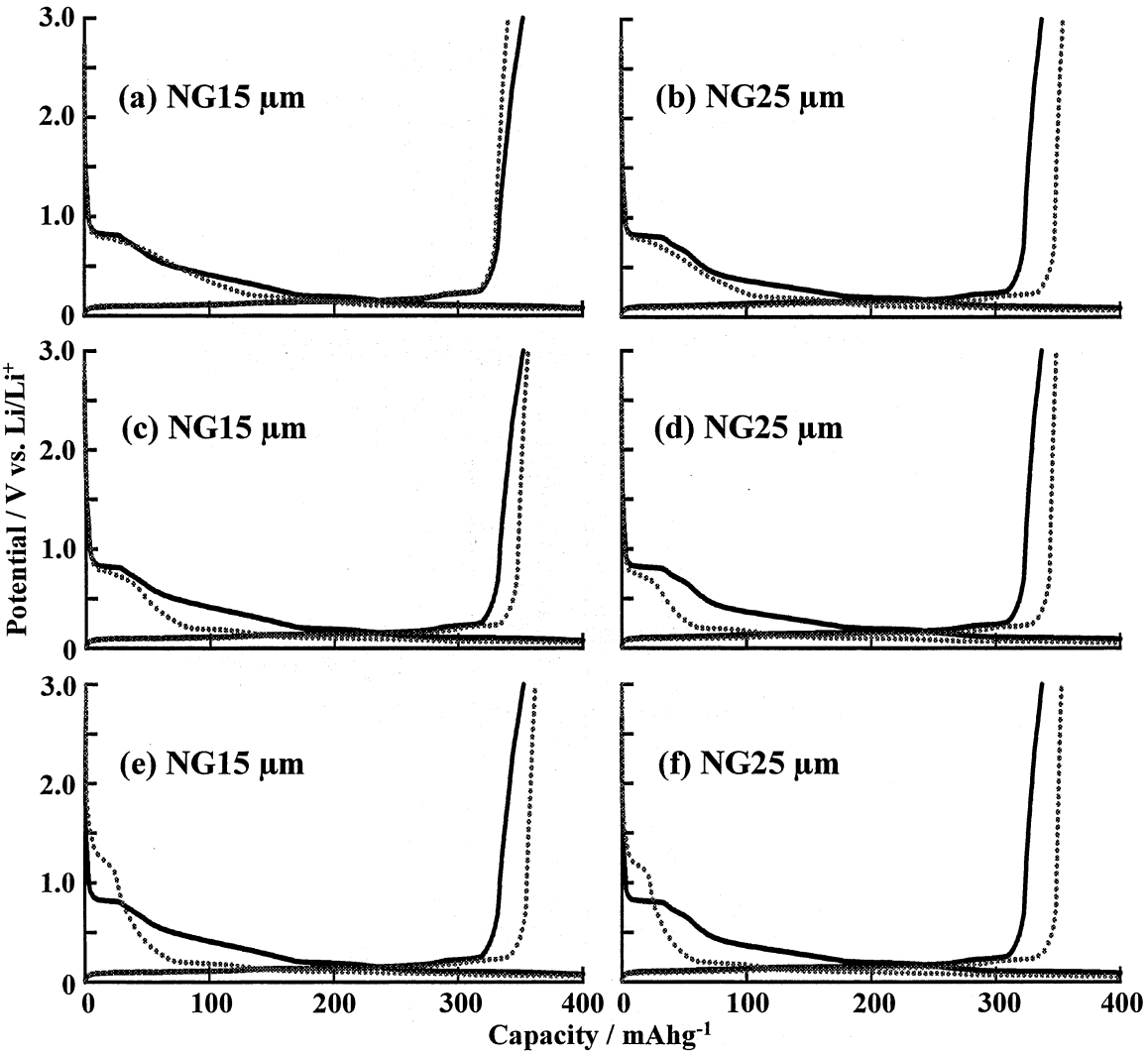

Figure 8. First charge/discharge potential curves for natural graphite samples in 0.67 mol/dm^3 $LiClO_4$ - EC/DEC/PC (1:1:1 vol.) and EC/DEC/PC/(**D**, **E** or **F**) (1:1:1:1.5 vol.).
(a), (b): EC/DEC/PC/**D**, (c), (d): EC/DEC/PC/**E**, (e), (f): EC/DEC/PC/**F**.
———: EC/DEC/PC, ·····: EC/DEC/PC/(**D**, **E** or **F**).

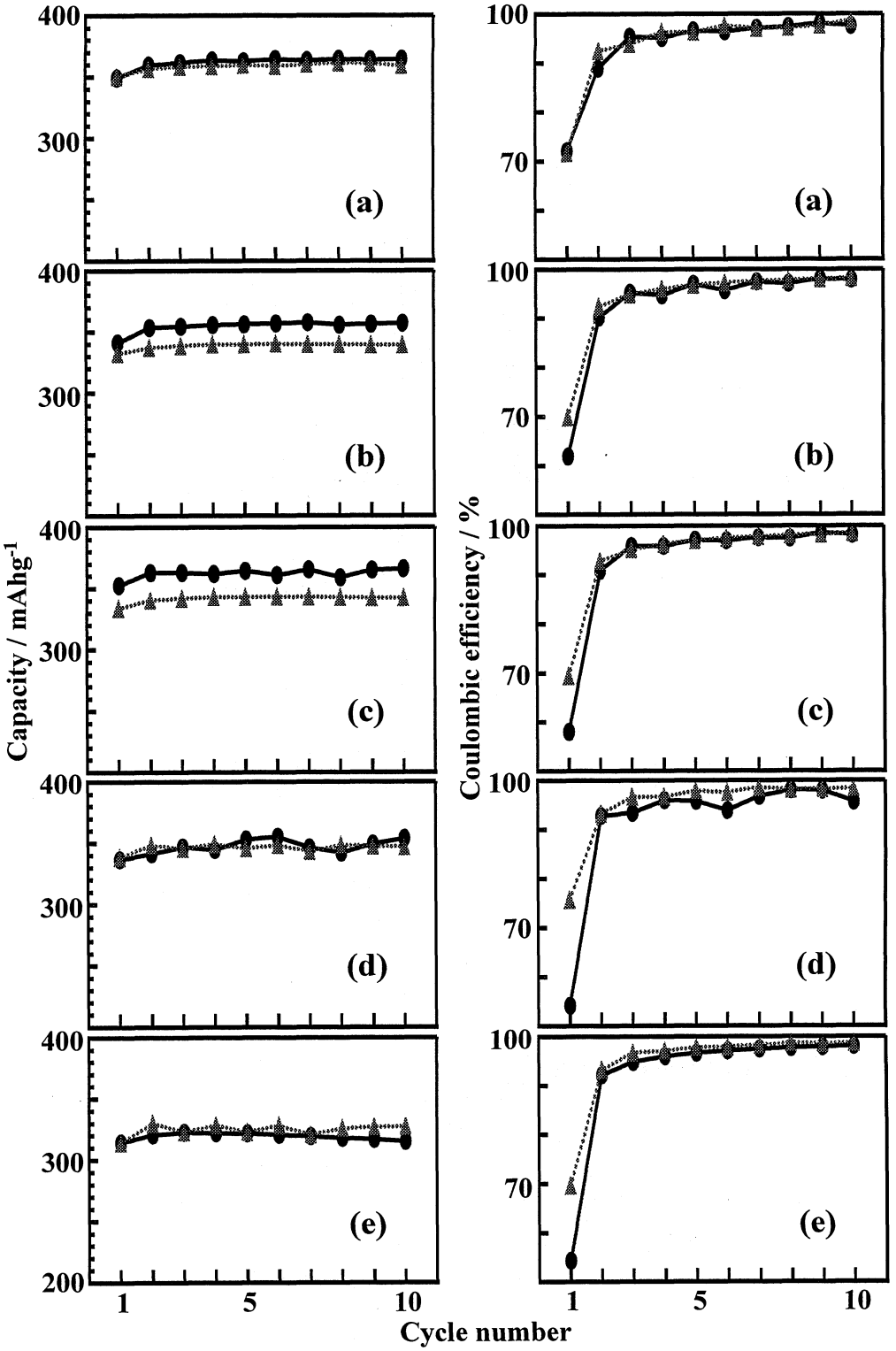

Figure 9. Charge capacities and coulombic efficiencies for natural graphite samples in 0.67 mol/dm^3 $LiClO_4$ - EC/DEC/PC (1:1:1 vol.) and EC/DEC/PC/A (1:1:1:1.5 vol.). (a) NG5 μm, (b) NG10 μm, (c) NG15 μm, (d) NG25 μm, (e) NG40 μm.
—●—: EC/DEC/PC, ·····▲·····: EC/DEC/PC/A.

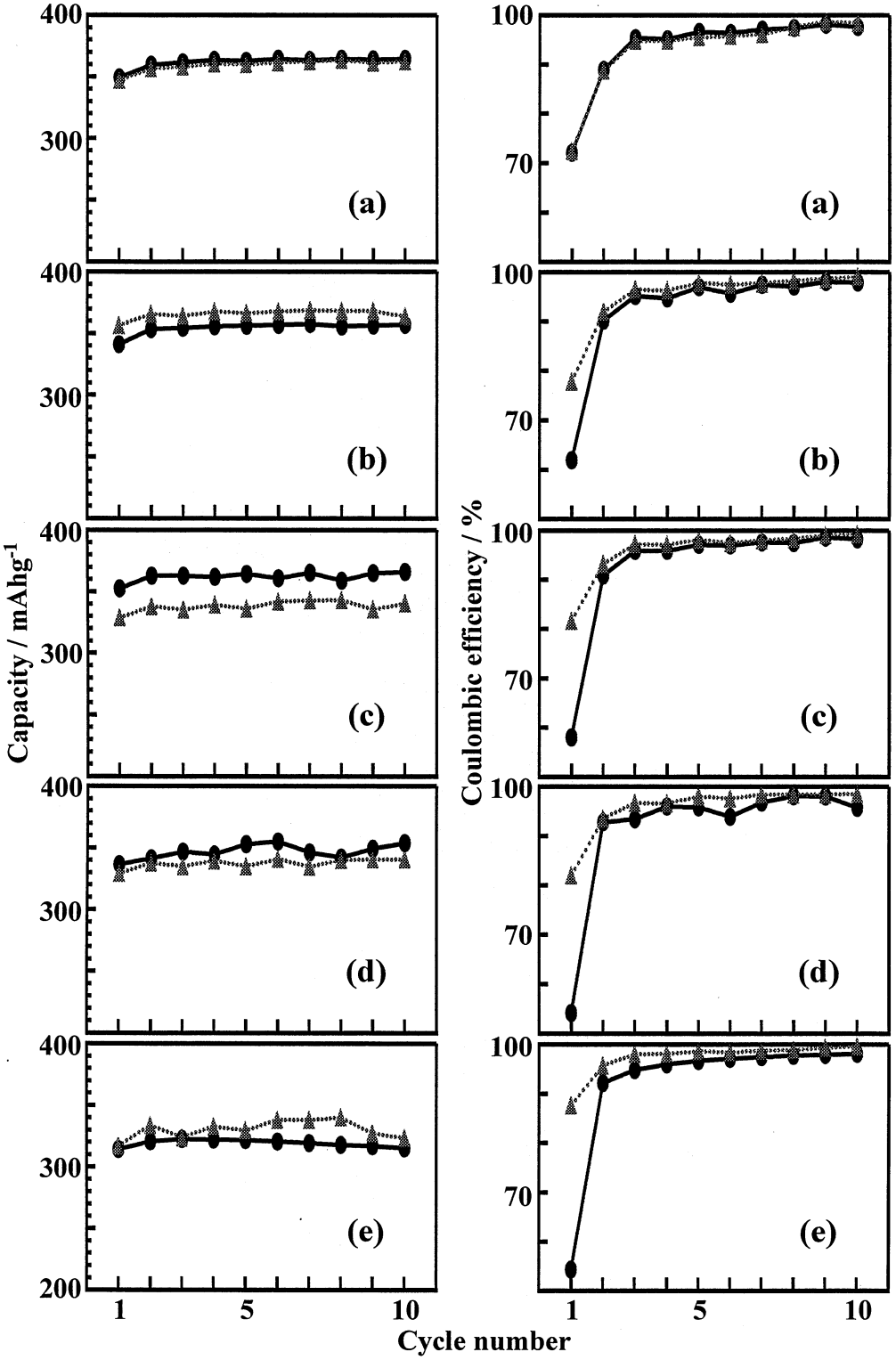

Figure 10. Charge capacities and coulombic efficiencies for natural graphite samples in 0.67 mol/dm^3 $LiClO_4$ - EC/DEC/PC (1:1:1 vol.) and EC/DEC/PC/**B** (1:1:1:1.5 vol.). (a) NG5 μm, (b) NG10 μm, (c) NG15 μm, (d) NG25 μm, (e) NG40 μm.
—●—: EC/DEC/PC, ·····▲·····: EC/DEC/PC/**B**.

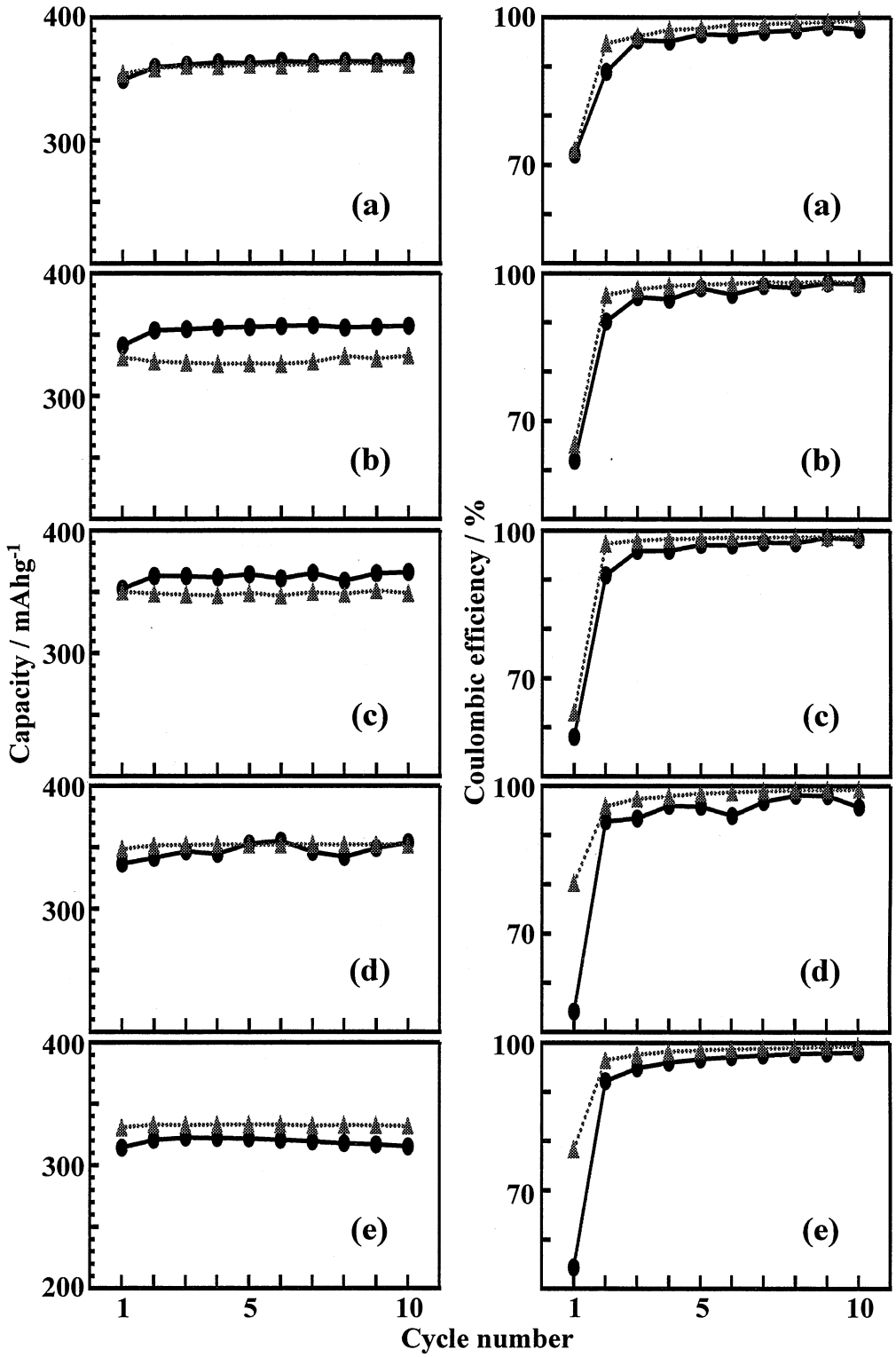

Figure 11. Charge capacities and coulombic efficiencies for natural graphite samples in 0.67 mol/dm^3 $LiClO_4$ - EC/DEC/PC (1:1:1 vol.) and EC/DEC/PC/**C** (1:1:1:1.5 vol.). (a) NG5 μm, (b) NG10 μm, (c) NG15 μm, (d) NG25 μm, (e) NG40 μm.
—●—: EC/DEC/PC, ·····▲·····: EC/DEC/PC/**C**.

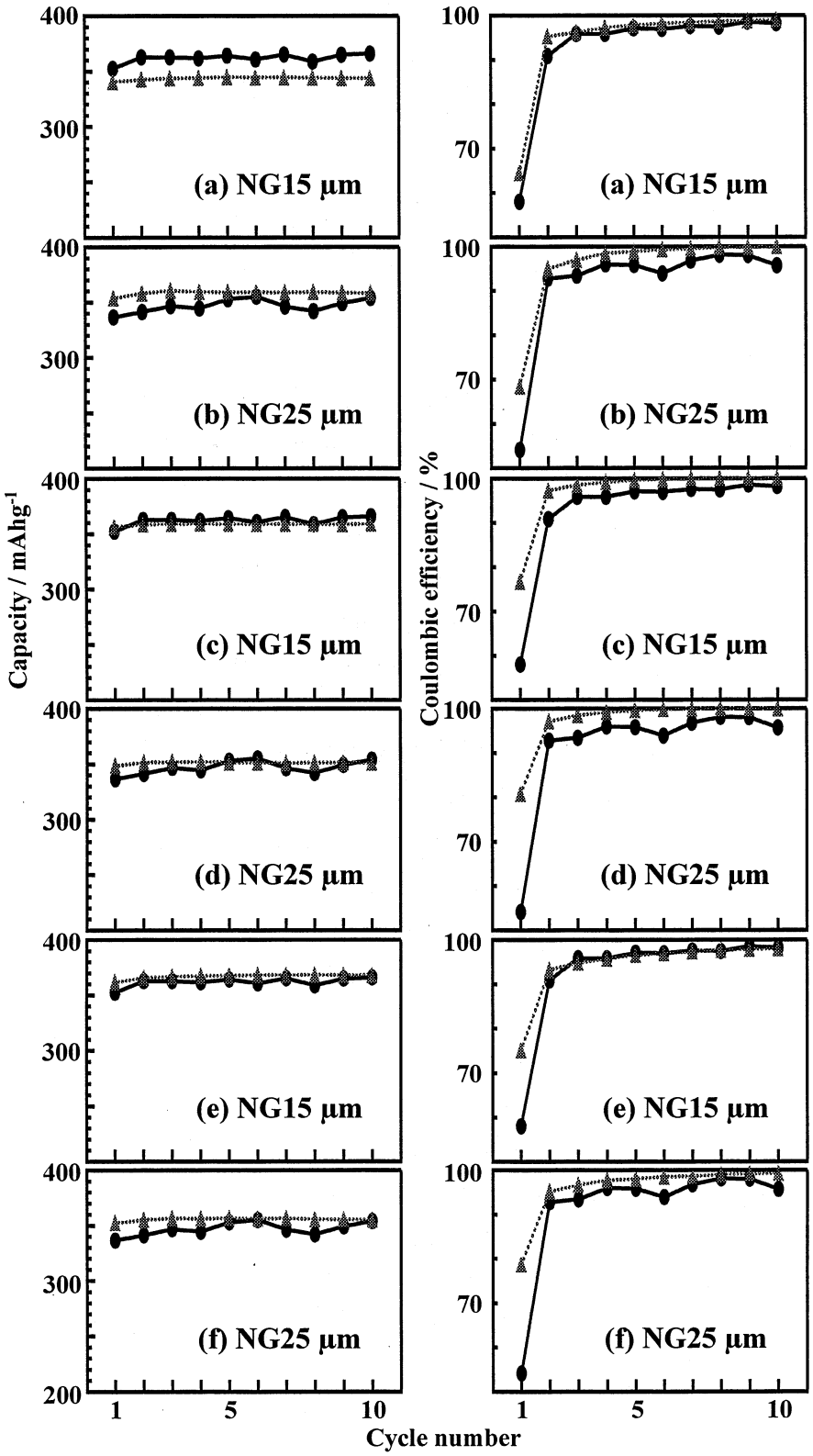

Figure 12. Charge capacities and coulombic efficiencies for natural graphite samples in 0.67 mol/dm^3 $LiClO_4$ - EC/DEC/PC (1:1:1 vol.)

and EC/DEC/PC/(**D**, **E** or **F**) (1:1:1:1.5 vol.).

(a) (b) EC/DEC/PC/**D**, (c) (d) EC/DEC/PC/**E**, (e) (f) EC/DEC/PC/**F**.

—●—: EC/DEC/PC, ·····▲·····: EC/DEC/PC/(**D**, **E** or **F**).

5-4 Conclusions

The electrochemical behavior of organo-fluorine compounds has been studied in EC/DEC and EC/DEC/PC mixtures using natural graphite electrodes. Electrochemical oxidation using a Pt wire electrode was largely suppressed by the mixing of fluorine compounds **A**, **B**, **C**, **D**, **E** and **F** with EC/DEC and EC/DEC/PC. The oxidation current was much smaller in 0.67 mol/dm^3 $LiClO_4$ - EC/DEC/(**A**, **B** or **C**) and EC/DEC/PC/(**D**, **E** or **F**) than in 0.67 mol/dm^3 $LiClO_4$ - EC/DEC and EC/DEC/PC at potentials higher than 6.0 V vs. Li/Li$^+$. A cyclic voltammetry study showed that the electrochemical reduction of fluorine compounds **A**, **B**, **C**, **D**, **E** and **F** started at ca. 1.9-2.7 V vs. Li/Li$^+$, which is a higher potential than those of EC, DEC, and PC. However charge/discharge capacities and first coulombic efficiencies were nearly the same in 0.67 mol/dm^3 $LiClO_4$ - EC/DEC and EC/DEC/(**A**, **B** or **C**). Furthermore the mixing of fluorine compound **A**, **B**, **C**, **D**, **E** or **F** with EC/DEC/PC diminished the electrochemical reduction of PC at the first cycle, highly increasing the first coulombic efficiencies for natural graphite electrodes in 0.67 mol/dm^3 $LiClO_4$ - EC/DEC/PC/(**A**, **B**, **C**, **D**, **E** or **F**) except NG5 μm in 0.67 mol/dm^3 $LiClO_4$ - EC/DEC/PC/(**A**, **B** or **C**). The increment in the first coulombic efficiency by the mixing of the fluorine compound with EC/DEC/PC increased with decreasing surface area of natural graphite from NG10 to NG40 μm. These results show that fluorine compounds **A**, **B**, **C**, **D**, **E** and **F** not only give antioxidation ability to electrolyte solutions but also contribute to the SEI formation on natural electrodes. From the viewpoint of thermal and electrochemical oxidation stability, fluoro-carbonates, **A**, **B**, **C**, **D** and **E** are good candidates as nonflammable solvents for lithium-ion batteries.

References

[1] X. Wang, E. Yasukawa, and S. Kasuya, J. Electrochem. Soc., 148, A1058 (2001).

[2] X. Wang, E. Yasukawa, and S. Kasuya, J. Electrochem. Soc., 148, A1066 (2001).

[3] K. Xu, M. S. Ding, S. Zhang, J. L. Allen, and T. R. Jow, J. Electrochem. Soc., 149, A622 (2002).

[4] X. L. Yao, S. Xie, C. H. Chn, Q. S. Wang, J. H. Sun, Y. L. Li, and S. X. Lu, J. Power Sources, 144, 170 (2005).

[5] X. Wang, C. Yamada, H. Naito, G. Segami, and K. Kibe, J. Electrochem. Soc., 153, A135 (2006).

[6] Y. E. Hyung, D. R. Vissers, and K. Amine, J. Power Sources, 119-121, 383 (2003).

[7] E.-G. Shim, T.-H. Nam, J.-G. Kim, H.-S. Kim, and S.-I Moon, J. Power Sources, 172, 919 (2007).

[8] T.-H. Nam, E-G. Shim, J-G. Kim, H.-S. Kim, and S.-I Moon, J. Electrochem. Soc., 154, A957 (2007).

[9] D. Zhou, W. Li, C. Tan, X. Zuo, and Y. Huang, J. Power Sources, 184, 589 (2008).
[10] K. Xu, S. Zhang, J. L. Allen, and T. R. Jow, J. Electrochem. Soc., 149, A1079 (2002).
[11] K. Xu, M. S. Ding, S. Zhang, J. L. Allen, and T. R. Jow, J. Electrochem. Soc., 150, A161 (2003).
[12] K. Xu, S. Zhang, J. L. Allen, and T. R. Jow, J. Electrochem. Soc., 150, A170 (2003).
[13] S. S. Zhang, K. Xu, and T. R. Jow, J. Power Sources, 113, 166 (2003).
[14] D. H. Doughty, E. P. Roth, C. C. Crafts, G. Nagasubramanian, G. Henriksen, and K. Amine, J. Power Sources, 146, 116 (2005).
[15] Q. Wang, J. Sun, X. Yao, and C. Chen, Electrochem. Solid-State Lett., 8, A467 (2005).
[16] Q. Wang, J. Sun, and C. Chen, J. Power Sources, 162, 1363 (2006).
[17] E.-G. Shim, T.-H. Nam, J.-G. Kim, H.-S. Kim, and S.-I. Moon, J. Power Sources, 175, 533 (2008).
[18] T.-H. Nam, E.-G. Shim, J.-G. Kim, H.-S. Kim, and S.-I. Moon, J. Power Sources, 180, 561 (2008)
[19] S. Izquierdo-Gonzales, W. Li, and B. L. Lucht, J. Power Sources, 135, 291 (2004).
[20] H. F. Xiang, Q. Y. Jin, C. H. Chen, X. W. Ge, S. Guo, and J. H. Sun, J. Power Sources, 174, 335 (2007).
[21] L. Wu, Z. Song, L. Liu, X Guo, L. Kong, H. Zhan, Y. Zhou, and Z. Li, J. Power Sources, 188, 570 (2009).
[22] Y.-B. He, Q. Liu, Z.-Y. Tang, Y.-H. Chen, and Q.-S. Song, Electrochim. Acta, 52, 3534 (2007).
[23] B. K. Mandal, A. K. Padhi, Z. Shi, S. Chakraborty, and R. Filler, J. Power Sources, 161, 1341 (2006).
[24] C. W. Lee, R. Venkatachalapathy, and J. Prakash, Electrochem. Solid-State Lett., 3, 63 (2000).
[25] A, Chen, Y. Qin, J. Liu, and K. Amine, Electrochem. Solid-State Lett., 12, A69 (2009).
[26] S. Chen, Z. Wang, H. Zhao, H. Qiao, H. Luan, and L. Chen, J. Power Sources, 187, 229 (2009).
[27] T. Nakajima, K. Dan, M. Koh, T. Ino, and T. Shimizu, J. Fluorine Chem., 111, 167 (2001).
[28] X. Zhang, R. Kostecki, T. . Richardson, J. K. Pugh, and P. N. Ross, Jr., J. Electrochem. Soc., 148, A1341 (2001).
[29] J. M. Vollmer, L. A. Curtiss, D. R. Vissers, and K. Amine, J. Electrochem. Soc., 151, A178 (2004).
[30] J. Li, K. Naga, Y. Ohzawa, T. Nakajima, and H. Iwata, J. Fluorine Chem., 126, 1028 (2005).

Chapter 6

Thermal stability and electrochemical properties of fluorine-containing ethers and ester as nonflammable solvents for lithium-ion batteries

6-1 Introduction

Lithium-ion batteries with high rate charge and discharge are urgently requested for their application to hybrid cars and electric vehicles. However, lithium-ion batteries have a possibility of firing and/or explosion at high temperatures, by short circuit, by overcharging and so on since they use flammable organic solvents. The high safety is one of the most important issues for the practical use of lithium-ion batteries, especially for the application to hybrid cars and electric vehicles. In order to improve the thermal and oxidation stability of lithium-ion batteries, new additives or solvents for electrolyte solutions have been investigated [1-35]. Most of them are phosphorus compounds (phosphates) having flame retardant properties. Thermal stability and electrochemical properties of trimethyl phosphate (TMP) were investigated in various solvents [1-5], with which TMP was mixed by 20-30%. Phosphates with phenyl groups such as triphenyl phosphate (TPP), tributyl phosphate (TBP) and cresyl diphenyl phosphate (CDP) were added to solvents by 3-5 wt% as additives, which improved thermal stability of lithium-ion batteries [6-9]. Fluorine-containing phosphorus compounds such as tris-(2,2,2-trifluoroethyl) phosphate (TFP), bis-(2,2,2-trifluoroethyl) methyl phosphate (BMP) and (2,2,2-trifluoroethyl) diethyl phosphate (TDP) [10-13] were mixed with solvents by 20-40% to investigate thermal stability and electrochemical properties. Among these phosphates, it was shown that TFP was the best compound. Thermal stability of TFP, TPP and vinyl ethylene carbonate (VEC) was also studied [14]. Other phosphorus compounds examined as flame retardant solvents or additives are 4-isopropyl phenyl diphenyl phosphate (IPPP) [15, 16], diphenyloctyl phosphate (DPOF) [17, 18], hexamethyl phosphoramide (HMPA) [19], dimethyl methyl phosphonate (DMMP) [20], tri-(β-chloromethyl) phosphate (TCEP) [21], and aromatic phosphorus-containing esters [22], dimethyl methyl phosphate (DMMP) [23], trimethyl phosphate (TEP) [24], dimethyl (2-methoxyethoxy) methyl phosphate (DMMEMP) [25] and diphenyloctyl phosphate (DPOF) [26]. It was shown that these phosphorus compounds improved thermal stability of lithium-ion batteries. In addition, cyclohexyl benzene [21], hexamethoxycyclotriphosphazene [27], fluorinated phophazenes [28], lithium difluoro (oxalate) borate (LiDFOB) [29], and vinyl-tris-(methoxydiethoxy) silane (VTMS) [30] were also investigated. Several papers were

quite recently published for the effect of organo-fluorine compounds on the electrochemical oxidation stability and charge/discharge behavior [31-34]. It was reported in these papers that fluoro-esters [31], allyl tris-(2,2,2-trifluoroethyl) carbonate (ATFEC) [32], 2-trifluoromethyl-3-methoxy perfluoropentane (TMMP) [33], and fluoro-carbonates [34] gave the positive effects to oxidation stability of electrolyte solutions and battery performance. In our previous paper [34], mixing of cyclic or linear fluoro-carbonate with 1.0 mol/dm^3 $LiClO_4$ - EC (ethylene carbonate)/DEC (diethyl carbonate)/PC(propylene carbonate) highly increased not only oxidation stability of electrolyte solutions but also first coulombic efficiencies for natural graphite electrode [34]. Fluoro-carbonates used are very stable against electrochemical oxidation at high potentials. They are electrochemically reduced at the higher potentials than EC, DEC and PC, easily forming protective surface film (Solid Electrolyte Interface: SEI) on graphite electrode. Mixing of the fluoro-carbonates therefore enables the use of PC-containing solvents for graphite electrode. It was also found that these fluoro-carbonates can be used for 1.0 mol/dm^3 $LiClO_4$ - EC/DEC without decreasing first coulombic efficiency [34]. Fluorine substitution of organic compounds reduces HOMO/LUMO levels [34, 35]. Organo-fluorine compounds are new type candidates as nonflammable solvents for lithium-ion batteries because the decrease in HOMO levels gives high oxidation stability to fluorine compounds. However, the decrease in LUMO levels due to fluorine substitution simultaneously increases reduction potentials of organic compounds, which causes electrochemical decomposition of fluorine compounds. If electrochemical reduction of fluorine compounds continues without forming SEI on carbon anode, irreversible capacity largely increases. However, if decomposed products quickly form SEI, such fluorine compounds can be used as nonflammable solvents. Other important problems are miscibility of fluorine compounds with polar solvents for lithium-ion batteries such as EC, PC, DEC and solubilities of inorganic electrolytes. The fluoro-carbonates examined in a previous paper [34] solved these problems, meeting the request as nonflammable solvents for lithium-ion batteries. In the present study, thermal stability and electrochemical reactions of fluoro-ethers, fluoro-ester and fluoro-carbonates were investigated and charge/discharge characteristics of natural graphite electrodes were studied in the fluorine compound-mixed electrolyte solutions to develop new nonflammable solvents for lithium-ion batteries.

6-2 Experimental

6-2-1 Natural graphite samples

Natural graphite samples (purity: >99.95 %) with average particle sizes of 15 and 25 μm (abbreviated to NG15 μm and NG25 μm) were used for cyclic voltammetry and charge/discharge cycling. The d_{002} values obtained by X-ray diffractometry (XRD-6100, Shimadzu) were 0.3355 and 0.3358 nm for NG15 μm and NG25 μm, respectively. Surface

areas and meso-pore volumes obtained by BET surface area measurement (Tristar 3000, Shimadzu) were 6.9 and 3.7 m^2/g, and 0.026 and 0.009 cm^3/g for NG15 μm and NG25 μm, respectively. Peak intensity ratios of D-band to G-band ($R=I_D/I_G$) obtained by Raman spectroscopy (NRS-1000, Jasco) with Nd:YVO_4 laser (532 nm) were nearly the same as each other (0.25 and 0.26. for NG15 μm and NG25 μm, respectively).

6-2-2 Organo-fluorine compounds

The following ether, ester and carbonate type organo-fluorine compounds (purity: 99.9 %, H_2O: <10 ppm), synthesized in Daikin Industries, Ltd., were examined in the present study. Among them, the compounds, I-III were used only for differential scanning calorimetry (DSC) measurement because their electrochemical properties were already reported in a previous paper [34].

$HCF_2CF_2CH_2OCF_2CF_2H$

A: 3-(1,1,2,2-tetrafluoroethoxy)-1,1,2,2-tetrafluoropropane

$HCF_2CF_2CH_2OCF_2CFClH$

B: 3-(2-chloro-1,1,2-trifluoroethoxy)-1,1,2,2-tetrafluoropropane

$HCF_2COOC_2H_5$

C: ethyl 2,2-difluoroacetate

HOMO and LUMO energies of organo-fluorine compounds **A**, **B** and **C** were calculated by Spartan'06 semi-empirical method using AM1, being compared with those for the same type compounds without F: ethoxy propane (**A**-H), 2-chloroethoxy propane (**B**-H) and ethyl acetate (**C**-H), in which H is substituted for F.

6-2-3 Thermal stability of organo-fluorine compound-mixed electrolyte solutions

Thermal stability of organo-fluorine compound-mixed electrolyte solutions was examined by differential scanning calorimetry (DSC-60, Shimadzu). DSC measurement was carried out using an airtight Al cell containing a mixture of 0.67 mol/dm^3 $LiClO_4$ - EC/DEC/PC (1:1:1 vol., 3 μℓ) (Kishida Chemicals, Co. Ltd., H_2O: <10 ppm for 1.0 mol/dm^3 - EC/DEC and PC) or EC/DEC/PC(**A**, **B** and **C**) (1:1:1:1.5 vol., 3μℓ) and NG15 μm (0.8 mg) between room temperature and 300 °C at a temperature scan speed of 5 °C/min.

6-2-4 Electrochemical measurements

Oxidation currents for 0.67 mol/dm^3 $LiClO_4$ - EC/DEC/PC (1:1:1 vol.) and EC/DEC/PC/(**A**, **B** and **C**) (1:1:1:1.5 vol.) were measured by linear sweep of potential at 0.1 mV/s using Pt wire electrode (Hokuto Denko, HZ-5000). Counter and reference electrodes were lithium foil. Three-electrode cell with natural graphite as a working electrode and lithium foil as counter and reference electrodes was used for cyclic voltammetry study and galvanostatic charge/discharge experiments. Natural graphite electrode was prepared as follows. Natural graphite powder was dispersed in N-methyl-2-pyrrolidone (NMP) containing 12 wt.% poly vinylidene fluoride (PVdF) and the slurry was pasted on a copper current collector. The electrode was dried at 120°C under vacuum for half a day. After drying, the electrode contained 80 wt.% graphite and 20 wt.% PVdF. Electrolyte solutions were prepared by mixing the fluorine compound **A**, **B** and **C** with 1.0 mol/dm^3 $LiClO_4$ - EC/DEC/PC (1:1:1 vol.). Organo-fluorine compounds **A**, **B** and **C** are mixed with 1.0 mol/dm^3 $LiClO_4$ - EC/DEC and EC/DEC/PC in whole range of composition at room temperature. For cyclic voltammetry study, 0.5 mol/dm^3 $LiClO_4$ - EC/DEC/PC/(**A**, **B** and **C**) (1:1:1:1.5 vol.) was used. Cyclic voltammograms were obtained using NG15 μm at a scan rate of 0.1 mV/s (Hokuto Denko, HZ-5000). The 0.67 mol/dm^3 $LiClO_4$ - EC/DEC/PC/(**A**, **B** and **C**) (1:1:1:1.5 vol.) was used for galvanostatic charge/discharge experiments. Preparation of 1.0 mol/dm^3 $LiClO_4$ - EC/DEC/(**A**, **B** and **C**) (1:1:1 vol.) and EC/DEC/PC/(**A**, **B** and **C**) (1:1:1:1.5 vol.) can be made at room temperature by dissolving $LiClO_4$ in 0.67 mol/dm^3 $LiClO_4$ - EC/DEC/(**A**, **B** and **C**) and EC/DEC/PC/(**A**, **B** and **C**) (1:1:1:1.5 vol.), respectively. However, the 0.67 mol/dm^3 $LiClO_4$ - EC/DEC/PC/(**A**, **B** and **C**) (1:1:1:1.5 vol.) was used for charge/discharge cyclings to simplify the experiments. Galvanostatic charge/discharge cyclings were performed using NG15 μm and NG25 μm at a current density of 60 mA/g between 0 and 3.0 V vs. Li/Li^+ reference electrode in a glove box filled with Ar at 25 °C (Hokuto Denko, HJ1001 SM8A).

6-3 Results and Discussion

6-3-1 HOMO and LUMO energies of organo-fluorine compounds

Table I shows HOMO and LUMO energies of organo-fluorine compounds used in the present study and the same type compounds in which fluorine atoms are replaced by hydrogen. Both HOMO and LUMO levels are decreased by fluorine substitution. The decrements in the HOMO and LUMO energies are qualitatively proportional to the numbers of substituted fluorine atoms. The result suggests that oxidation stability of organic compounds is improved by fluorine substitution, however, their reduction simultaneously becomes easy, i.e. their reduction potentials are elevated.

Table I. HOMO and LUMO energies of fluorine-containing ethers and ester and the same type compounds without F, calculated by Spartan'06 semiempirical method using AM1.

Compound	A-H	A	B-H	B	C-H	C
HOMO energy (kJ/mol)	-1002.5	-1154.4	-1031.7	-1143.2	-1069.9	-1100.8
LUMO energy (kJ/mol)	285.2	23.0	122.9	-12.4	109.1	40.9

6-3-2 Thermal stability of fluorine compound-mixed electrolyte solutions

Thermal stability of fluorine compound-mixed electrolyte solutions mixed with NG15 μm was evaluated by DSC measurement. DSC curves obtained are shown in Fig. 1. The 0.67 mol/dm^3 $LiClO_4$ - EC/DEC/PC had an exothermic peak at 281 °C (Fig. 1(a)). Exothermic peaks for fluoro-ethers, **A** and **B**-mixed solutions were observed both at a slightly higher temperature of 286 °C (Fig. 1(b) and (c)). Fluoro-ester, **C**-mixed solution gave an exothermic peak at a similar temperature of 284 °C (Fig. 1(d)). The DSC measurement showed that fluoro-ethers, **A** and **B** improve the thermal stability of lithium-ion batteries.

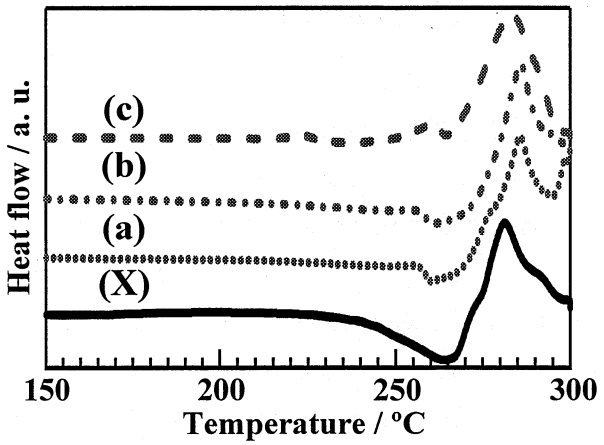

Figure 1. DSC profiles for 0.67 mol/dm^3 $LiClO_4$ - EC/DEC/PC/(**A**, **B** or **C**) (1:1:1:1.5 vol.) (X) EC/DEC/PC, (a) EC/DEC/PC/**A**, (b) EC/DEC/PC/**B**, (c) EC/DEC/PC/**C**

6-3-3 Electrochemical oxidation of fluorine compound-mixed electrolyte solutions

Figure 2 shows oxidation currents for 0.67 mol/dm^3 $LiClO_4$ - EC/DEC/PC and EC/DEC/PC/(**A**, **B** and **C**). No oxidation current was observed until 6.0 V vs. Li/Li$^+$. After 6.0 V vs. Li/Li$^+$, the larger oxidation currents flowed in 0.67 mol/dm^3 $LiClO_4$ - EC/DEC/PC than in fluorine compound-mixed solutions. In particular, oxidation current abruptly increased at 7.3 V vs. Li/Li$^+$ in 0.67 mol/dm^3 $LiClO_4$ - EC/DEC/PC (Fig. 2(X)). Much smaller oxidation currents were observed in fluoro-ethers, **A** and **B**-mixed solutions (Fig. 2(a) and (b)), which

shows that fluoro-ethers, **A** and **B** have high stability against electrochemical oxidation. The oxidation current observed in fluoro-ester, **C**-mixed solution was relatively larger than in other fluorine compound-mixed ones (Fig. 2(c)). However, even in these cases, the oxidation currents were smaller than that in 0.67 mol/dm^3 $LiClO_4$ - EC/DEC/PC without fluorine compound before and after 7.3 V vs. Li/Li$^+$.

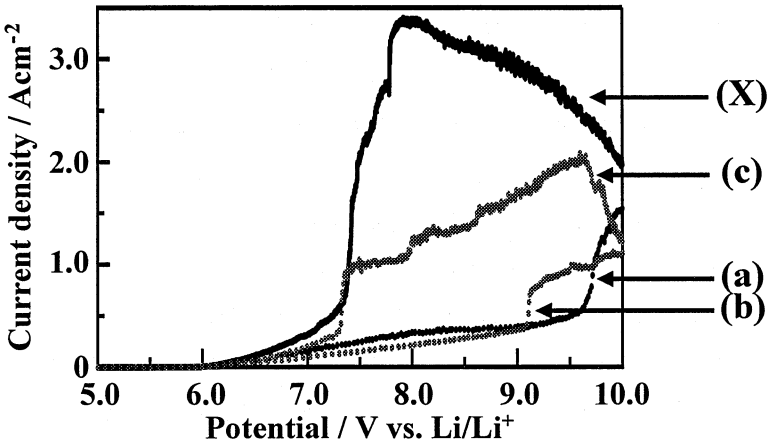

Figure 2. Linear sweep voltammograms for Pt wire electrode in 0.67 mol/dm^3 $LiClO_4$ - EC/DEC/PC (1:1:1 vol.) and EC/DEC/PC/(**A**, **B** or **C**) (1:1:1:1.5 vol.).
(X) EC/DEC/PC, (a) EC/DEC/PC/**A**, (b) EC/DEC/PC/**B**, (c) EC/DEC/PC/**C**.

6-3-4 Electrochemical reduction of fluorine compound-mixed electrolyte solutions

Fluorine substitution of organic compounds reduces LUMO levels, i.e. elevates their reduction potentials. Figure 3 shows cyclic voltammograms obtained for 0.67 mol/dm^3 $LiClO_4$ - EC/DEC/PC and EC/DEC/PC/(**A**, **B** and **C**). Reduction currents started to flow at 2.1, 2.3 and 2.6 V vs. Li/Li$^+$ for 0.67 mol/dm^3 $LiClO_4$ - EC/DEC/PC/(**A**, **B** and **C**), respectively. Since electrochemical reduction of EC, DEC, and PC starts at 1.4, 1.3 and 1.0-1.6 V vs. Li/Li$^+$, respectively [36, 37], organo-fluorine compounds, **A-C** electrochemically decompose at the higher potentials than those for EC, DEC and PC. Fluoro-ether, **A** is electrochemically stable and **B** is also stable at a higher potential than 1.0 V vs. Li/Li$^+$, where only small reduction currents similar to that in 0.67 mol/dm^3 $LiClO_4$ - EC/DEC/PC were observed. Fluoro-ester, **C** easily decomposed between 1.0 and 2.6 V vs. Li/Li$^+$, where the larger current flowed than in Fig. 3(a) and (b).

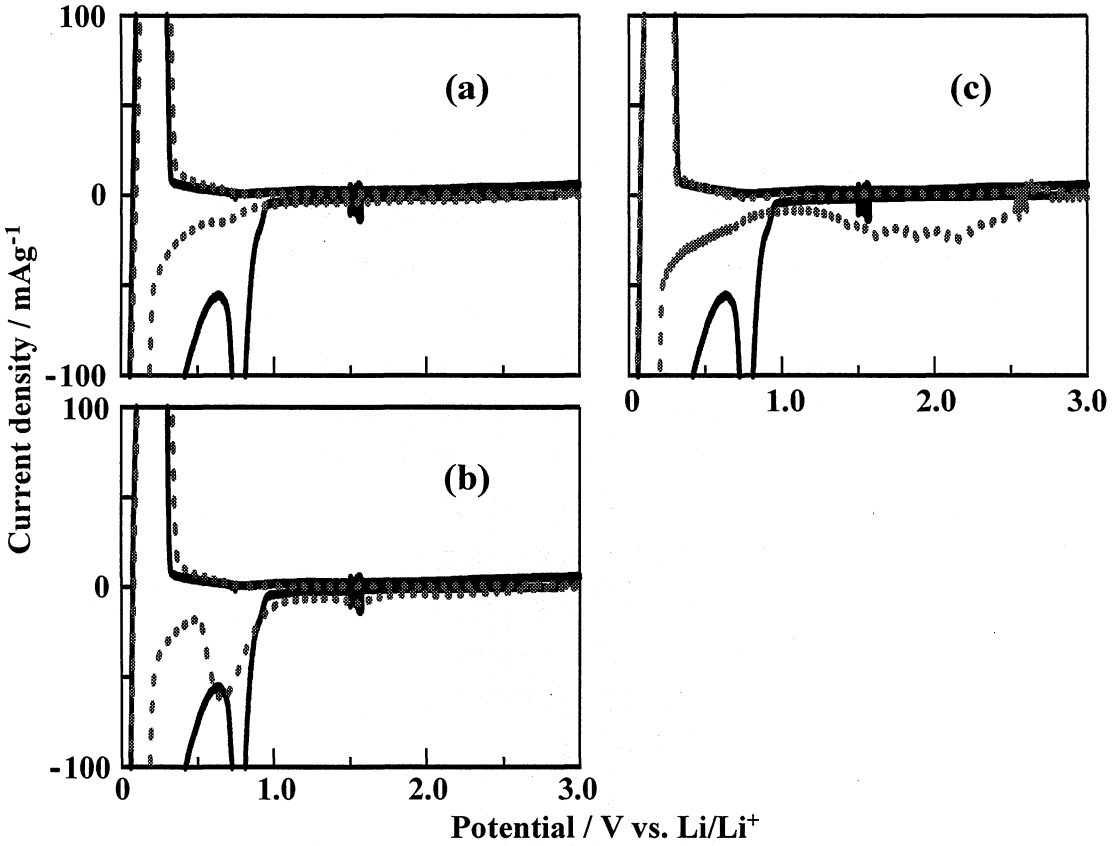

Figure 3. Cyclic voltammograms for natural graphite
in 0.5 mol/dm^3 $LiClO_4$ - EC/DEC/PC/(**A**, **B** or **C**) (1:1:1:1.5 vol.).
(a) EC/DEC/PC/**A**, (b) EC/DEC/PC/**B**, (c) EC/DEC/PC/**C**.
——— : EC/DEC/PC, ····· : EC/DEC/PC/(**A**, **B** or **C**).

6-3-5 Charge/discharge characteristics of natural graphite samples in fluorine compound-mixed electrolyte solutions

First charge/discharge curves shown in Fig. 4 clearly indicate that potential plateaus at 0.8 V vs. Li/Li$^+$ due to the electrochemical reduction of PC were reduced and the electrode potentials were quickly lowered, approaching that of lithium-intercalated graphite by mixing of organo-fluorine compounds with 0.67 mol/dm^3 $LiClO_4$ - EC/DEC/PC, which suggests that the fluorine compounds electrochemically decompose prior to the decomposition of PC and facilitate the SEI formation. Fluoro-ethers, **A** and **B** were quite effective for the quick formation of SEI on graphite electrodes. In the electrolyte solutions containing the organo-fluorine compounds, **A** and **B** first coulombic efficiencies increased by 20-31 % as summarized in Table II. Even in the solution with fluorine compound **C**, first coulombic efficiency increased by about 15 %. Table II indicates that first discharge capacities were largely reduced by mixing of organo-fluorine compounds. The decrements of first discharge capacities were 144-180 and 122-215 mAhg^{-1} for NG15 μm and NG25 μm, respectively,

which is the main reason for the increase in first coulombic efficiencies. Thus organo-fluorine compounds decompose at the higher potentials than PC, EC and DEC, contributing to the formation of SEI on graphite. The charge capacities for NG15 μm were similar to each other in the solutions with and without organo-fluorine compounds. Those for NG25 μm were slightly increased by mixing of organo-fluorine compounds as shown in Fig. 4 and Table II. Fluorine-containing chemical species would be incorporated in SEI. Diffusion of Li^+ ion may be easier in the SEI containing fluorine species because surface free energies of organo-fluorine compounds are low. Since surface area of NG25 μm is smaller than that of NG15 μm, actual current density would be larger for NG25 μm than NG15 μm. The higher kinetics for NG25 μm may have increased the first charge capacities. Charge capacities and coulombic efficiencies for NG15 μm and NG25 μm are shown in Figs. 5 and 6, respectively as a function of cycle number. Cycleability for natural graphite samples was good and coulombic efficiencies quickly approached 100% after first cycle. The results revealed that the organo-fluorine compounds examined in the study contributed to quick formation of SEI on natural graphite electrodes, increasing first coulombic efficiencies. From the viewpoint of thermal and electrochemical oxidation stability, fluoro-ethers **A** and **B** are good candidates as nonflammable solutions for lithium-ion batteries.

Table II. First charge/discharge capacities and coulombic efficiencies for natural graphite electrode in 0.67 mol/dm^3 $LiClO_4$ - EC/DEC/PC (1:1:1 vol.) and EC/DEC/PC/(**A**, **B** or **C**) (1:1:1:1.5 vol.).

Electrolyte	Discharge capacity / mAhg^{-1}		Charge capacity / mAhg^{-1}		Coulombic efficiency / %	
	NG15μm	NG25μm	NG15μm	NG25μm	NG15μm	NG25μm
EC/DEC/PC	608	622	352	337	58.0	54.1
EC/DEC/PC/A	438	407	345	348	78.8	85.4
EC/DEC/PC/B	428	432	336	343	78.5	79.3
EC/DEC/PC/C	464	500	345	348	74.4	69.7

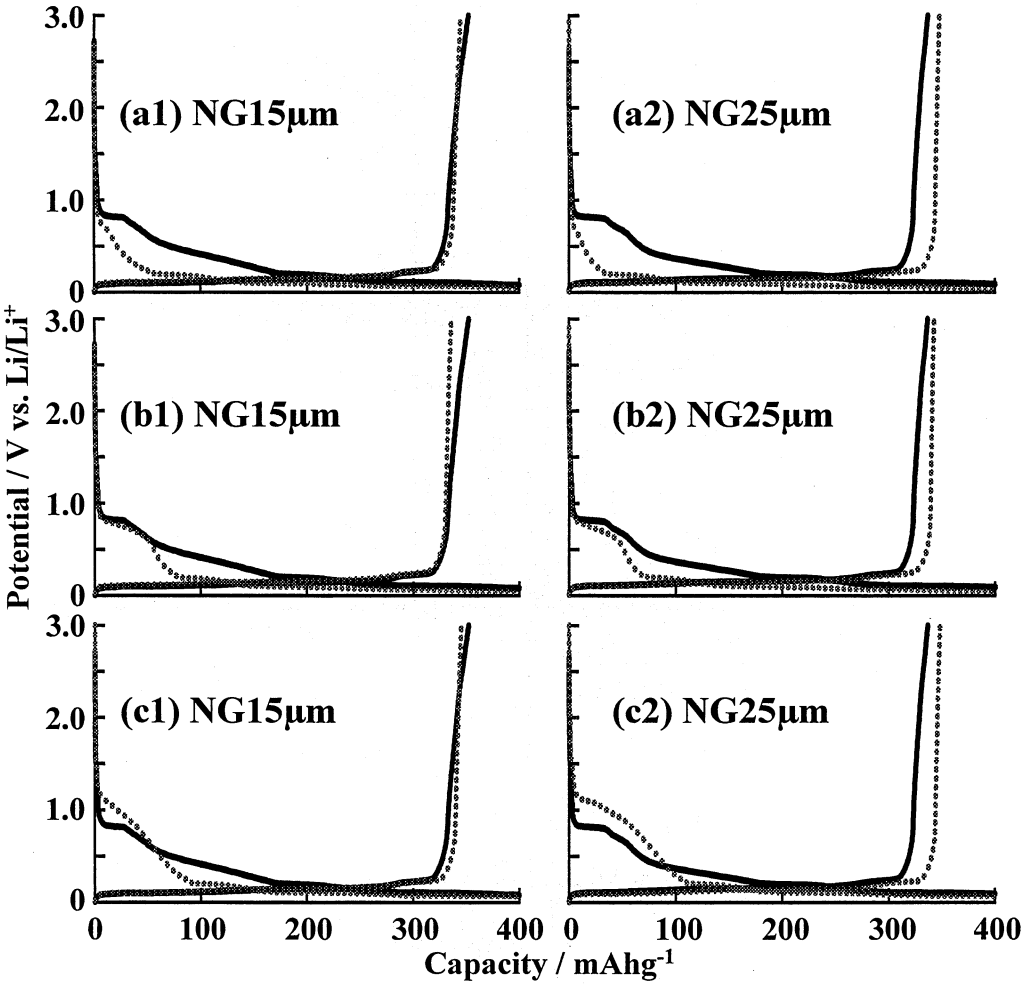

Figure 4. First charge/discharge potential curves for natural graphite samples in 0.67 mol/dm^3 $LiClO_4$ - EC/DEC/PC (1:1:1 vol.) and EC/DEC/PC/(**A**, **B** or **C**) (1:1:1:1.5 vol.). (a1), (a2) EC/DEC/PC/**A**, (b1), (b2) EC/DEC/PC/**B**, (c1), (c2) EC/DEC/PC/**C**.
———: EC/DEC/PC, ·····: EC/DEC/PC/(**A**, **B** or **C**).

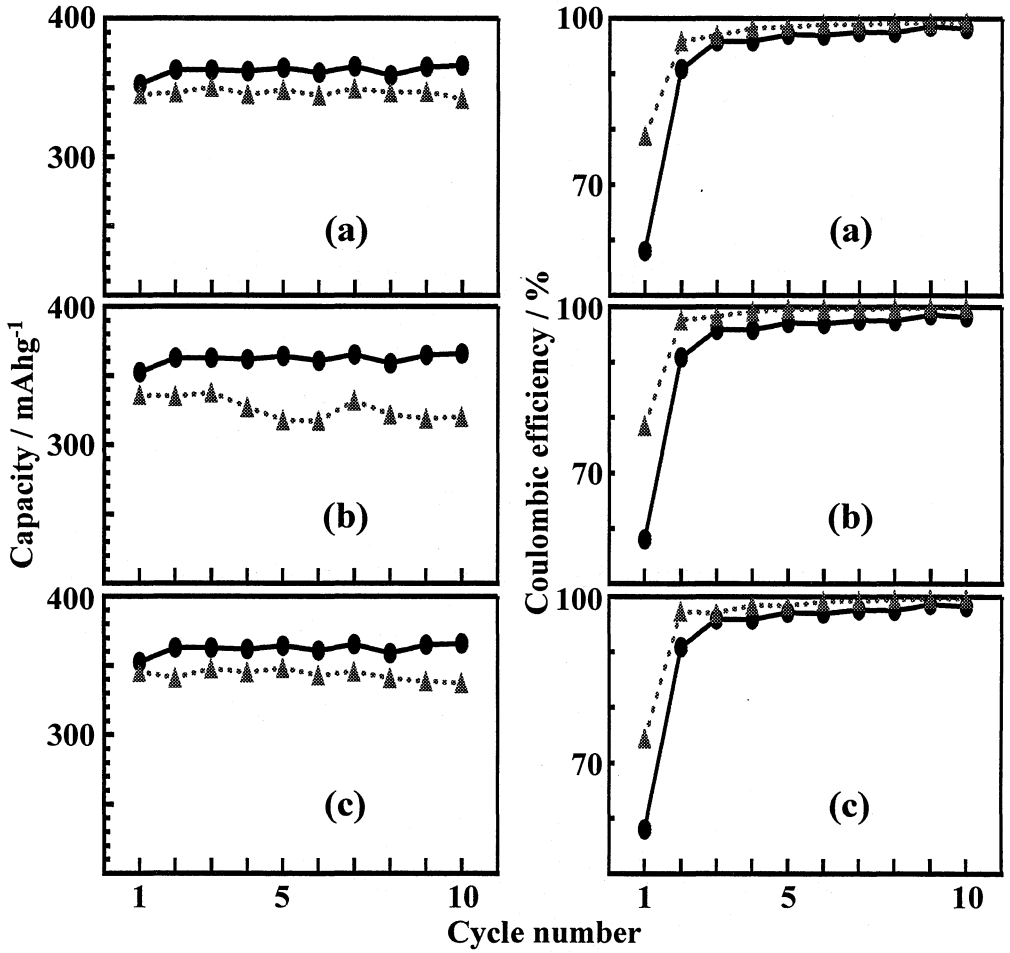

Figure 5. Charge capacities and coulombic efficiencies for NG15μm in 0.67 mol/dm^3 $LiClO_4$ - EC/DEC/PC (1:1:1 vol.) and EC/DEC/PC/(**A**, **B** or **C**) (1:1:1:1.5 vol.).
(a) EC/DEC/PC/**A**, (b) EC/DEC/PC/**B**, (c) EC/DEC/PC/**C**.
—•—: EC/DEC/PC, ·····▲·····: EC/DEC/PC /(**A**, **B** or **C**).

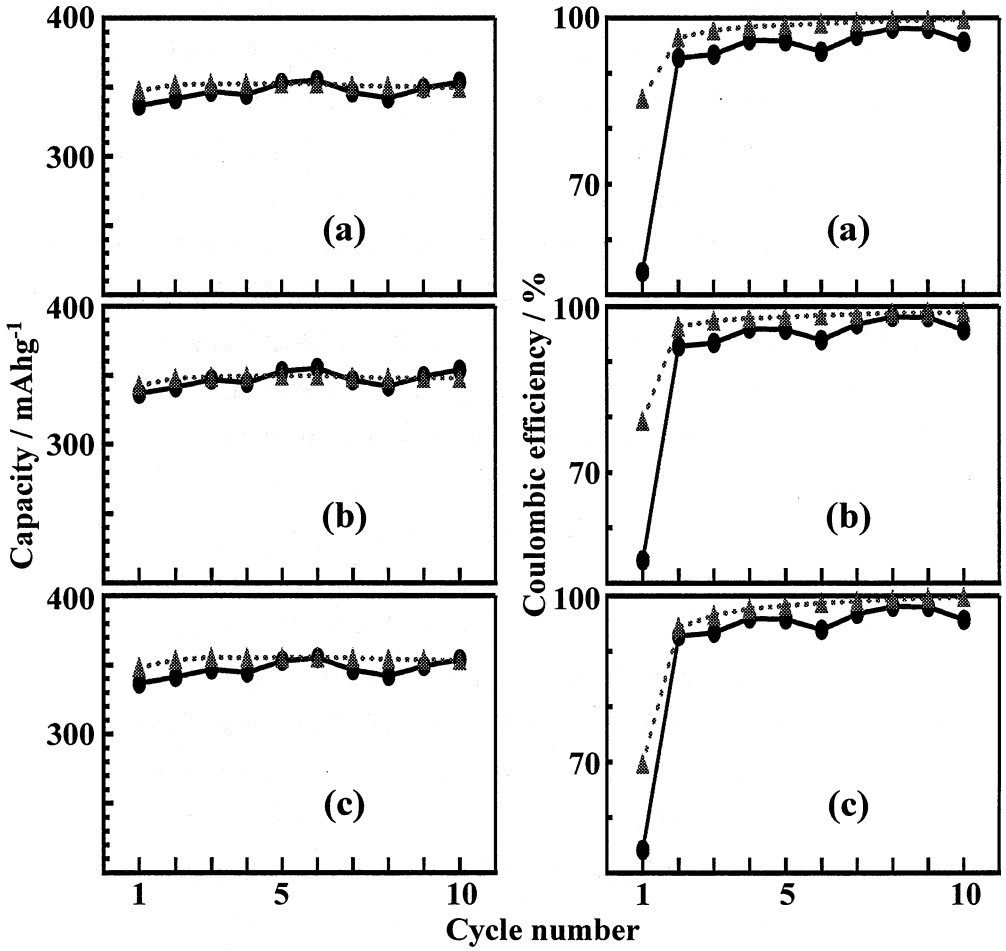

Figure 6. Charge capacities and coulombic efficiencies for NG25μmin 0.67 mol/dm^3 $LiClO_4$ - EC/DEC/PC (1:1:1 vol.) and EC/DEC/PC/(**A**, **B** or **C**) (1:1:1:1.5 vol.).
(a) EC/DEC/PC/**A**, (b) EC/DEC/PC/**B**, (c) EC/DEC/PC/**C**.
—•—: EC/DEC/PC, ·····▲·····: EC/DEC/PC /(**A**, **B** or **C**).

6-4 Conclusions

Thermal stability were evaluated by DSC for 0.67 mol/dm^3 $LiClO_4$ - EC/DEC/PC (1:1:1 vol.) and EC/DEC/PC/(**A**, **B** and **C**) (1:1:1:1.5 vol.). Exothermic peaks for fluorine compound-mixed electrolyte solutions were observed at higher temperatures than that for 0.67 mol/dm^3 $LiClO_4$ - EC/DEC/PC, which shows the higher thermal stability of fluorine compound-mixed solutions. Electrochemical oxidation currents measured using Pt wire electrode were much smaller in 0.67 mol/dm^3 $LiClO_4$ - EC/DEC/PC/(**A** and **B**) than in 0.67 mol/dm^3 $LiClO_4$ - EC/DEC/PC, which shows also high stability of fluorine compound-mixed electrolyte solutions against electrochemical oxidation. The **C**-mixed solution also gave the smaller oxidation current before and after 7.3 V vs. Li/Li$^+$. Electrochemical reduction of organo-fluorine compounds occurred at the higher potentials than those for EC, DEC and PC. However, charge/discharge experiments indicated that fluorine compound-mixed electrolyte solutions highly increased first coulombic efficiencies for both NG15 μm and NG25 μm. The results revealed that fluoro-ethers, **A** and **B** are good candidates as nonflammable solvents because they not only improved thermal and electrochemical oxidation stability of electrolyte solutions but also highly increased first coulombic efficiencies due to quick formation of SEI on graphite in PC-containing solvents.

References

[1] X. Wang, E. Yasukawa, and S. Kasuya, J. Electrochem. Soc., 148, A1058 (2001).

[2] X. Wang, E. Yasukawa, and S. Kasuya, J. Electrochem. Soc., 148, A1066 (2001).

[3] K. Xu, M. S. Ding, S. Zhang, J. L. Allen, and T. R. Jow, J. Electrochem. Soc., 149, A622 (2002).

[4] X. L. Yao, S. Xie, C. H. Chn, Q. S. Wang, J. H. Sun, Y. L. Li, and S. X. Lu, J. Power Sources, 144, 170 (2005).

[5] X. Wang, C. Yamada, H. Naito, G. Segami, and K. Kibe, J. Electrochem. Soc., 153, A135 (2006).

[6] Y. E. Hyung, D. R. Vissers, and K. Amine, J. Power Sources, 119-121, 383 (2003).

[7] E.-G. Shim, T.-H. Nam, J.-G. Kim, H.-S. Kim, and S.-I Moon, J. Power Sources, 172, 919 (2007).

[8] T.-H. Nam, E-G. Shim, J-G. Kim, H.-S. Kim, and S.-I Moon, J. Electrochem. Soc., 154, A957 (2007).

[9] D. Zhou, W. Li, C. Tan, X. Zuo, and Y. Huang, J. Power Sources, 184, 589 (2008).

[10] K. Xu, S. Zhang, J. L. Allen, and T. R. Jow, J. Electrochem. Soc., 149, A1079 (2002).

[11] K. Xu, M. S. Ding, S. Zhang, J. L. Allen, and T. R. Jow, J. Electrochem. Soc., 150, A161 (2003).

[12] K. Xu, S. Zhang, J. L. Allen, and T. R. Jow, J. Electrochem. Soc., 150, A170 (2003).

[13] S. S. Zhang, K. Xu, and T. R. Jow, J. Power Sources, 113, 166 (2003).
[14] D. H. Doughty, E. P. Roth, C. C. Crafts, G. Nagasubramanian, G. Henriksen, and K. Amine, J. Power Sources, 146, 116 (2005).
[15] Q. Wang, J. Sun, X. Yao, and C. Chen, Electrochem. Solid-State Lett., 8, A467 (2005).
[16] Q. Wang, J. Sun, and C. Chen, J. Power Sources, 162, 1363 (2006).
[17] E.-G. Shim, T.-H. Nam, J.-G. Kim, H.-S. Kim, and S.-I. Moon, J. Power Sources, 175, 533 (2008).
[18] T.-H. Nam, E.-G. Shim, J.-G. Kim, H.-S. Kim, and S.-I. Moon, J. Power Sources, 180, 561 (2008).
[19] S. Izquierdo-Gonzales, W. Li, and B. L. Lucht, J. Power Sources, 135, 291 (2004).
[20] H. F. Xiang, Q. Y. Jin, C. H. Chen, X. W. Ge, S. Guo, and J. H. Sun, J. Power Sources, 174, 335 (2007).
[21] Y.-B. He, Q. Liu, Z.-Y. Tang, Y.-H. Chen, and Q.-S. Song, Electrochim. Acta, 52, 3534 (2007).
[22] B. K. Mandal, A. K. Padhi, Z. Shi, S. Chakraborty, and R. Filler, J. Power Sources, 161, 1341 (2006).
[23] H. F. Xiang, Q. Y. Jin, R. Wang, C. H. Chen, and X. W. Ge, J. Power Sources, 179, 351 (2008).
[24] B. S. Lalia, T. Fujita, N. Yoshimoto, M. Egashira, and M. Morita, J. Power Sources, 186, 211 (2009).
[25] L. Wu, Z. Song, L. Liu, X. Guo, L. Kong, H. Zhan, Y. Zhou, and Z. Li, J. Power Sources, 188, 570 (2009).
[26] E.-G. Shim, T.-H. Nam, J.-G. Kim, H.-S. Kim, and S.I. Moon, Electrochim. Acta, 54, 2276 (2009).
[27] C. W. Lee, R. Venkatachalapathy, and J. Prakash, Electrochem. Solid-State Lett., 3, 63 (2000).
[28] T. Tsujikawa, K. Yabuta, T. Matsushita, T. Matsushima, K. Hayashi, and M. Arakawa, J. Power Sources, 189, 429 (2009).
[29] Z. Chen, Y. Qin, J. Liu, and K. Amine, Electrochem. Solid-State Lett., 12, A69 (2009).
[30] H. P. Zhang, Q. Xia, B. Wang, L. C. Yang, Y. P. Wu, D. L. Sun, C. L. Gan, H. J. Luo, A. W. Bebeda, and T. V. Ree, Electrochem. Commun., 11, 526 (2009).
[31] K. A. Smith, M. C. Smart, G. K. S. Prakash, and B. V. Ratnakumar, ECS Trans., 11, 91 (2008).
[32] S. Chen, Z. Wang, H. Zhao, H. Qiao, H. Luan, and L. Chen., J. Power Sources, 187, 229 (2009).
[33] K. Naoi, E. Iwama, N. Ogihara, Y. Nakamura, H. Segawa, and Y. Ino, J. Electrochem. Soc., 156, A272 (2009).
[34] T. Achiha, T. Nakajima, Y. Ohzawa, M. Koh, A. Yamauchi, M. Kagawa, and H. Aoyama, J. Electrochem. Soc., 156, A483 (2009).

[35]T. Nakajima, K. Dan, M. Koh, T. Ino, and T. Shimizu, J. Fluorine Chem., 111, 167 (2001).

[36]X. Zhang, R. Kostecki, T. Richardson, J. K. Pugh, and P. N. Ross, Jr., J. Electrochem. Soc., 148, A1341 (2001).

[37]J. M. Vollmer, L. A. Curtiss, D. R. Vissers, and K. Amine, J. Electrochem. Soc., 151, A178 (2004).

Chapter 7

Conclusions

Chapter 1 describes the details of lithium-ion batteries and carbonaceous anodes. Surface modification is one of the effective methods for improving electrode performance. Surface modification methods such as surface fluorination, surface oxidation, metal or metal oxide coating, polymer coating, and so on, were used to improve the electrochemical properties of carbonaceous anodes. Many kinds of composite electrodes were also presented. To increase the thermal and oxidation stability of lithium-ion batteries, nonflammable additives or solvents have been investigated. They include phosphates with methyl, ethyl or phenyl groups, fluorine-containing phosphorus compounds, organo-fluorine compounds and so on. This chapter summarized the results recently obtained on these subjects. In addition, the purpose of the present study and outline of each chapter were described.

Chapters 2-4 present the results on the surface structure changes and charge/discharge behavior of natural graphite (NG5 μm, NG10 μm and NG15 μm) fluorinated by different fluorinating agents samples (F_2 gas, ClF_3 gas, NF_3 gas and plasma-fluorination using CF_4 gas) in propylene carbonate-containing solvents. Natural graphite powder samples (NG5 μm, NG10 μm and NG15 μm) were fluorinated by F_2 gas ($3x10^4$ Pa at 200 °C and 300 °C for 2 min.), ClF_3 and NF_3 gases ($1x10^5$ Pa at 200 °C and 300 °C for 5 min.), and plasma-fluorination using CF_4 gas (CF_4 flow rate: 8 cm^3/min., total gas pressure: 5.0 Pa, power: 80 W, plasma frequency: 13.56 MHz, sample temperature: 90 °C and plasma-treatment time: 60 min.) in order to prepare natural graphite with high surface disorder, and electrochemical behavior of surface-fluorinated samples were examined in 1.0 mol/dm^3 $LiClO_4$ - EC/DEC/PC (1:1:1 vol.).

In the fluorination with F_2 gas, increase in surface areas and total pore volumes by surface fluorination was smaller for NG10 μm and NG15 μm than for NG5 μm. However, surface disorder was highly increased in NG10 μm and NG15 μm, but less in NG5 μm. Cyclic voltammetry study indicated that decomposition of PC on original graphite samples increased with increasing particle size of natural graphite, i.e. with decreasing the area of edge plane. Surface fluorination highly reduced the electrochemical decomposition of PC on NG10 μm and NG15 μm. Due to decrease in the decomposition of PC, first coulombic efficiencies for NG10 μm and NG15 μm increased by 9.9-13.2 % and 20.3-23.3 %, respectively. The increase in first columbic efficiencies is attributed to the increase in surface disorder providing a large amount of surface defects and probably actual electrode area by surface fluorination. Surface fluorine would also contribute to SEI formation by giving LiF.

The fluorination with ClF_3 and NF_3 gases increased meso-pores with diameter of 2.0 nm due to surface fluorination while those with diameters of 2.5 and 3.0 nm were reduced. *R* values obtained from Raman spectra increased with increasing fluorination temperature and particle size of natural graphite sample, indicating increase in surface disorder by surface fluorination. These surface structure changes would have reduced the electrochemical decomposition of PC at 1st cycle, i.e. increased first coulombic efficiencies, which was more clearly observed at a high current density of 150 mA/g and mainly for NG10 μm and NG15 μm having the larger particle sizes. The increase in first coulombic efficiencies for NG10 μm and NG15 μm fluorinated by ClF_3 reached ca. 10 and 20 %, respectively.

In the case of plasma-fluorination, fluorination increased surface disorder of three natural graphite samples though surface areas were reduced by radical reaction having surface etching effect. Plasma-fluorination highly reduced the electrochemical decomposition of PC on NG10 μm and NG15 μm. As a consequence, first coulombic efficiencies for plasma-fluorinated NG10 μm and NG15 μm increased by 9.7 and 19.3 % at 150 mA/g, respectively.

Chapters 5-6 deal with thermal stability and electrochemical properties of nonflammable organo-fluorine compounds (fluoro-ethers, fluoro-ester and fluoro-carbonates) for lithium-ion battery. Electrochemical behavior of organo-fluorine compounds has been investigated in EC/DEC and EC/DEC/PC mixtures using natural graphite electrodes.

In chapter 5, electrochemical oxidation using a Pt wire electrode was largely suppressed by the mixing of fluoro-carbonates **A**, **B**, **C**, **D**, **E** and **F** with EC/DEC. The oxidation current was much smaller in 0.67 mol/dm^3 $LiClO_4$ - EC/DEC/(**A**, **B**, **C**, **D**, **E** or **F**) than in 0.67 mol/dm^3 $LiClO_4$ - EC/DEC and EC/DEC/PC at potentials higher than 6.0 V vs. Li/Li^+. Cyclic voltammetry study showed that the electrochemical reduction of fluoro-carbonates **A**, **B**, **C**, **D**, **E** and **F** started at 1.9-2.7 V vs. Li/Li^+, which are higher potentials than those of EC, DEC, and PC. However charge/discharge capacities and first coulombic efficiencies were nearly the same in 0.67 mol/dm^3 $LiClO_4$ - EC/DEC and EC/DEC/(**A**, **B** or **C**). Furthermore the mixing of fluoro-carbonates **A**, **B**, **C**, **D**, **E** or **F** with EC/DEC/PC diminished the electrochemical reduction of PC at the first cycle, highly increasing the first coulombic efficiencies for natural graphite electrodes in 0.67 mol/dm^3 $LiClO_4$ - EC/DEC/PC/(**A**, **B**, **C**, **D**, **E** or **F**) except the data obtained for NG5 μm in 0.67 mol/dm^3 $LiClO_4$ - EC/DEC/PC/(**A**, **B** or **C**). The increment in the first coulombic efficiency by the mixing of the fluoro-carbonates with EC/DEC/PC increased with decreasing surface area of natural graphite from NG10 μm to NG40 μm. These results show that fluorine compounds **A**, **B**, **C**, **D**, **E** and **F** not only give antioxidation ability to electrolyte solutions but also contribute to the SEI formation on natural graphite electrodes. From the viewpoint of thermal and electrochemical oxidation stability, fluoro-carbonates, **A**, **B**, **C**, **D** and **E** are good candidates as nonflammable solvents for lithium-ion batteries.

Chapter 6 describes thermal stability and electrochemical behavior of fluoro-ethers (**A** and

B), fluoro-ester(**C**). Thermal stability was evaluated by DSC for 0.67 mol/dm^3 $LiClO_4$ - EC/DEC/PC (1:1:1 vol.) and EC/DEC/PC/(**A**, **B** or **C**) (1:1:1:1.5 vol.). Exothermic peaks for fluorine compound-mixed electrolyte solutions were observed at higher temperatures than that for 0.67 mol/dm^3 $LiClO_4$ - EC/DEC/PC, which shows the higher thermal stability of fluorine compound-mixed solutions. Electrochemical oxidation currents measured using Pt wire electrode were much smaller in 0.67 mol/dm^3 $LiClO_4$ - EC/DEC/PC/(**A** and **B**) than in 0.67 mol/dm^3 $LiClO_4$ - EC/DEC/PC, which shows also high stability of fluorine compound-mixed electrolyte solutions against electrochemical oxidation. The **C**-mixed solution also gave the smaller oxidation current before and after 7.3 V vs. Li/Li$^+$. Electrochemical reduction of organo-fluorine compounds occurred at the higher potentials than those for EC, DEC and PC. However, charge/discharge experiments indicated that fluorine compound-mixed electrolyte solutions highly increased first coulombic efficiencies for both NG15 μm and NG25 μm. The results revealed that fluoro-ethers, **A** and **B** are good candidates as nonflammable solvents because they not only improved thermal and electrochemical oxidation stability of electrolyte solutions but also highly increased first coulombic efficiencies due to quick formation of SEI on graphite in PC-containing solvents.

List of publications

1. "Electrochemical behavior of surface-fluorinated graphite in propylene carbonate-containing solvent",
   T. Nakajima, **T. Achiha**, Y. Ohzawa, A.M. Panich, and A.I. Shames, *J. Phys. & Chem. of Solids*, 69, 1292-1295 (2007).

2. "Electrochemical behavior of surface-fluorinated natural graphite in propylene carbonate-containing solvent",
   T. Achiha, T. Nakajima, and Y. Ohzawa, *J. Electrochem. Soc.*, 154, A827-A833 (2007).

3. "Charge/discharge behavior of plasma-fluorinated natural graphites in propylene carbonate-containing solvent",
   T. Achiha, S. Shibata, T. Nakajima, Y. Ohzawa, A. Tressaud, and E. Durand, *J. Power Sources*, 171, 932-937 (2007).

4. "Electrochemical Properties of Natural Graphite Fluorinated by ClF_3 and NF_3 in Propylene Carbonate-Containing Solvent",
   X. Cheng, J. Li, **T. Achiha**, T. Nakajima, Y. Ohzawa, Z. Mazej, and B. Žemva, *J. Electrochem. Soc.*, 155, A405-A413 (2008).

5. "Electrochemical Behavior of Nonflammable Organo-Fluorine Compounds for Lithium Ion Batteries",
   T. Achiha, T. Nakajima, Y. Ohzawa, M. Koh, A. Yamauchi, M. Kagawa, and H. Aoyama, *J. Electrochem. Soc.*, 156, A483-A488 (2009).

6. "Thermal Stability and Electrochemical Properties of Fluorine-Containing Ethers, Ester and Carbonates as Nonflammable Solvents for Lithium Ion Batteries",
   T. Achiha, T. Nakajima, Y. Ohzawa, M. Koh, A. Yamauchi, M. Kagawa, and H. Aoyama, *J. Electrochem. Soc.*, accepted for publication.

Other publications

1. "Electro-conductive porous ceramics prepared by chemical vapor infiltration of TiN", Y. Ohzawa, X. Cheng, **T. Achiha**, T. Nakajima, and H. Groult, *J. Mater. Sci.*, 43, 2812-2817 (2008).

2. "Electrochemical properties of surface-fluorinated vapor grown carbon fiber for lithium ion battery", T. Nakajima, K. Hashimoto **T. Achiha**, Y, Ohzawa, A. Yoshida, Z, Mazej, B. Žemva, Y.-S Lee, and M. Endo, *Collect. Czech. Chem. Commun.*, 73, 1693-1704 (2008).

3. "Effect of surface fluorination and conductive additives on the electrochemical behavior of lithium titanate ($Li_{4/3}Ti_{5/3}O_4$) for lithium ion battery", T. Nakajima, A. Ueno, **T. Achiha**, Y. Ohzawa, and M. Endo, *J. Fluorine Chem.*, 130, 810-815 (2009).

4. "Effect of Conductive Additives and Surface Fluorination on the Charge/Discharge Characteristics of Lithium Titanate ($Li_{4/3}Ti_{5/3}O_4$) for Lithium Ion Battery", X. Kang, H. Utsunomiya, **T. Achiha**, Y. Ohzawa, T. Nakajima, Z. Mazej, B. Žemva, and M. Endo, *J. Electrochem. Soc.*, accepted for publication.

Presentations at international conferences and symposium

1. "Electrochemical Properties of Surface Fluorinated Graphite in Propylene Carbonate Containing Solvent",
   Takashi Achiha, Seiko Shibata, Tsuyoshi Nakajima, Yoshimi Ozawa, Alain Tressaud, and Etienne Durand,
   Carbon 2008 -International conference on Carbon-, July 13-18, 2008, Nagano, Japan.

2. "Electrochemical Behavior of Non-Flammable Organo-Fluorine Compounds for Lithium Ion Batteries",
   Takashi Achiha, Tsuyoshi Nakajima, Yoshimi Ohzawa, Meiten Koh, Akiyoshi Yamauchi, Michiru Kagawa, and Hirokazu Aoyama
   International conference on Fluorine Chemistry '09 Kyoto, May 20-22, 2009, Kyoto, Japan.

3. "Electrochemical Behavior of Fluorinated Vapor Grown Carbon Fiber"
   Kenichi Hashimoto, **Takashi Achiha**, Yoshimi Ohzawa, Tsuyoshi Nakajima, Akira Yoshida, Zoran Mazej, Boris Žemva, Young-Seak Leed, and Morinobu Endo
   International conference on Fluorine Chemistry '09 Kyoto, May 20-22, 2009, Kyoto, Japan.

4. "Effect of Surface Fluorination on The Charge/discharge Behavior of Lithium Titanate for Lithium Ion Battery"
   Akimi Ueno, **Takashi Achiha**, Yoshimi Ohzawa, and Tsuyoshi Nakajima
   International conference on Fluorine Chemistry '09 Kyoto, May 20-22, 2009, Kyoto, Japan.

5. "Electrochemical Properties of Non-Flammable Organo-Fluorine Compounds for Lithium Ion Batteries"
   Takashi Achiha, Tsuyoshi Nakajima, Yoshimi Ohzawa, Meiten Koh, Akiyoshi Yamauchi, Michiru Kagawa, and Hirokazu Aoyama
   19th International Symposium on Fluorine Chemistry, August 23-28, 2009, Jackson Hole, Wyoming, USA.

Acknowledgements

The present study has been performed in Energy Materials Chemistry Laboratory of Department of Applied Chemistry of Aichi Institute of Technology in the period from 2005 to 2010.

The author sincerely appreciates Professor Tsuyoshi Nakajima who has given the guidance to the present research for his beneficial advices, discussion and consultation.

Sincere thanks are expressed to Professor Yoshimi Ohzawa, Dr. Jianling Li, Dr. Xingun Cheng, Dr. Xiaohong Kang, Mrs Seiko Shibata, Mr. Kenichi Hashimoto and Miss Akimi Ueno for their helpful suggestions and kind assistances to the present work.

The author expresses his hearty thanks to Professor Boris Žemva and Dr. Zoran Mazej (Jožef Stefan Institute, Slovenia), Dr. Alain Tressaud and Dr. Etienne Durand (ICMCB-CNRS, France), Dr. Henri Groult (University of Pierre and Marie Curie, France), Dr. Alexander M. Panich and Dr. A.I. Shames (Ben-Gurion University of the Negev, Israel), Professor Akira Yoshida (Musashi Institute of Technology), Professor Morinobu Endo (Shinshu University), Dr. Meiten Koh, Mr. Akiyoshi Yamauchi, Miss Michiru Kagawa, and Mr. Hirokazu Aoyama (Daikin Industries, Ltd) for their kind collaborations though this work.

The author gratefully acknowledges Professor Yuichi Kobayashi and Professor Masanori Hirano (Department of Applied Chemistry, Aichi Institute of Technology) for their useful advices and encouragement.

The author dearly thanks Dr. Kazuhisa Naga, Mr. Junnosuke Satoh, Mr. Yasuyuki Yamanaka, Mr. Masato Kimura, Mr. Tomohiro Suzuki, Dr. Kazuhiko Matumoto and Mr. Takatsugu Kanatani for their kind advices and friendship.

The author also thanks Mr. Hideki Sakakibara, Mr. Akira Abe, Mr. Hidetoshi Utsunomiya, Mr. Takahiro Kasugai, Mr. Keisuke Isogai, Miss Yoko Hata and Mr. Yuki Matsuda for their kind supports and friendship. Additionally, he thanks all the students of Energy Materials Chemistry Laboratory.

Finally, the author expresses his gratitude to his parents for their continuous support and encouragement.

February 2010

Takashi Achiha